AD

MEMORANDUM REPORT ARBRL-MR-03339

FEASIBILITY STUDY OF SHOCK WAVE MODIFICATION IN THE BRL 2.44 m BLAST SIMULATOR

George A. Coulter
Gerald Bulmash
Charles Kingery

March 1984

US ARMY ARMAMENT RESEARCH AND DEVELOPMENT CENTER
BALLISTIC RESEARCH LABORATORY
ABERDEEN PROVING GROUND, MARYLAND

Destroy this report when it is no longer needed.
Do not return it to the originator.

Additional copies of this report may be obtained from the National Technical Information Service, U. S. Department of Commerce, Springfield, Virginia 22161.

The findings in this report are not to be construed as an official Department of the Army position, unless so designated by other authorized documents.

The use of trade names or manufacturers' names in this report does not constitute indorsement of any commercial product.

REPORT DOCUMENTATION PAGE

READ INSTRUCTIONS BEFORE COMPLETING FORM

1. REPORT NUMBER: MEMORANDUM REPORT ARBRL-MR-03339
2. GOVT ACCESSION NO.:
3. RECIPIENT'S CATALOG NUMBER:

4. TITLE (and Subtitle): FEASIBILITY STUDY OF SHOCK WAVE MODIFICATION IN THE BRL 2.44 m BLAST SIMULATOR
5. TYPE OF REPORT & PERIOD COVERED: Final
6. PERFORMING ORG. REPORT NUMBER:

7. AUTHOR(s): George A. Coulter, Gerald Bulmash, Charles Kingery
8. CONTRACT OR GRANT NUMBER(s):

9. PERFORMING ORGANIZATION NAME AND ADDRESS
US Army Ballistic Research Laboratory, ARDC
ATTN: DRSMC-BLT(A)
Aberdeen Proving Ground, MD 21005
10. PROGRAM ELEMENT, PROJECT, TASK AREA & WORK UNIT NUMBERS: Project 1L162618AH80

11. CONTROLLING OFFICE NAME AND ADDRESS
US Army AMCCOM, ARDC
Ballistic Research Laboratory, ATTN: DRSMC-BLA-S(A)
Aberdeen Proving Ground, MD 21005
12. REPORT DATE: March 1984
13. NUMBER OF PAGES: 94

14. MONITORING AGENCY NAME & ADDRESS (if different from Controlling Office):
15. SECURITY CLASS. (of this report): UNCLASSIFIED
15e. DECLASSIFICATION/DOWNGRADING SCHEDULE:

16. DISTRIBUTION STATEMENT (of this Report)
Approved for public release; distribution unlimited

17. DISTRIBUTION STATEMENT (of the abstract entered in Block 20, if different from Report)

18. SUPPLEMENTARY NOTES

19. KEY WORDS (Continue on reverse side if necessary and identify by block number)

Blast Waves	Hydrocode	Shock Tube
Blast Effects	Model Shock Tube	
BRL 2.44 m Simulator	NASA-Ames Code	
Decaying Wave	Overpressure	
	Rarefaction Wave Eliminator	

20. ABSTRACT (Continue on reverse side if necessary and identify by block number)
Four types of driver sections (short driver, baffled driver, single pipe, and multiple pipe driver) were designed and tested on a 1/48th scale model of the BRL 2.44 m shock tube. Pressures were monitored along the test section with piezoelectric transducers to determine waveshape as a function of drivers. Pressure-time waveforms are compared to computer predictions produced by the NASA-Ames one-dimensional hydrocode. Predictions are given for the performance of the BRL 2.44 m shock tube when suitably modified.

TABLE OF CONTENTS

LIST OF ILLUSTRATIONS

LIST OF ILLUSTRATIONS (CONT)

LIST OF TABLES

I. INTRODUCTION

The general objective of the research reported here is to determine a suitable method for modifying the Ballistic Research Laboratory's (BRL) 2.44 meter shock tube/blast simulator[1,2] to produce an exponentially decaying blast wave. This waveform would complement the long duration flat-topped type produced presently by the shock tube. Possible methods of modifications were to be tried with a 1/48th scale model shock tube. From these results, performance predictions were to be made for the full-size shock tube. Computer code predictions from the NASA Ames one-dimensional hydrocode[3] are also given. Additional comparisons may be found in the appendix.

The study included four possible shock tube driver modifications and one modification to the test section[4] where Gion proposes a large-diameter test section might be added. The four driver modifications include a short driver, a driver with internal baffles, a single pipe driver, and a multiple pipe driver similar to the French shock tube drivers used at the Gramat[5] facility. Each of the listed possible modifications were experimentally tried with the 1/48th scale shock tube model. The hydrocode was also utilized to generate pressure-time profiles for comparison with the experimental data and to predict the performance of the full size 2.44 m shock tube. See the appendix.

---

[1] *Brian P. Bertrand, "BRL Dual Shock Tube Facility," BRL Memorandum Report 2001, Ballistic Research Laboratory, Aberdeen Proving Ground, MD, August 1969 (AD 693264).*

[2] *Brian P. Bertrand, "Proposed Improvement of BRL Dual Shock Tube Facility," BRL Technical Note No. 1733, Ballistic Research Laboratory, Aberdeen Proving Ground, MD, April 1970 (AD 871736).*

[3] *Andrew Mark, "Computational Design of Large Scale Blast Simulators," AIAA 19th Aerospace Sciences Meeting, January 12-15, 1981, St. Louis, Missouri.*

[4] *Edmund J. Gion, "Simulation of Low Level Explosives Blast Loadings at Full Scale by Modifications to BRL Dual Shock Tube Facility," Memorandum Report ARBRL-MR-02853, Ballistic Research Laboratory, Aberdeen Proving Ground, MD, July 1978 (AD A059854).*

[5] *J.R. Crosnier and J.B.G. Monsac, "Large Diameter High Performance Blast Simulator," Seventh MABS, Medicine Hat, Alberta, Canada, 13-17 July 1981.*

II. TEST PROCEDURE

This section describes details of the 1/48th scale shock tube model, the various modifications to it, and the associated electronic recording used.

A. 1/48th Scale Shock Tube Model

A standard calibration shock tube had been redesigned previously[6] to a 1/48th scale model of the BRL 2.44 m shock tube. Figures 1 and 2 show sketches of the full size and the model shock tubes, respectively.

The shock tube model (and the full-size one) were operated in an air-air mode with a rarefaction wave eliminator (RWE) in place at the end of the test section. Each of the modifications was tried on the scale shock tube model over a side-on shock overpressure range of 25 kPa (3.6 psi) to 125 kPa (18 psi). A variety of mylar diaphragms was used with a bursting range sufficient for driver pressures to give blast waves in this desired range. This range included the most useful range of expected future tests at the BRL 2.44 m shock tube.

The transducer Stations 1-4, Figure 2, were located from the diaphragms so as to agree with the scaled-down distances from the full-size shock tube as shown on Figure 1. The transducers and associated electronics are described in the next section.

B. Instrumentation

A schematic of the data acquisition-reduction system is given in Figure 3. Quartz piezoelectric transducers were used in the shock tube test section to monitor the blast wave shape and interaction with the rarefaction wave eliminator. The results from the transducers were used to evaluate each modification of the driver section.

The transducers were coupled through a power supply and data amplifiers to a digitizing oscilloscope. On-site comparisons of the results were made directly from the hard copies of the pressure-time records. Final data processing was completed with the computer, printer, and plotter. Tables of data and plots of pressure-time records for the various test stations are included for comparison of results obtained from each driver.

C. Types of Shock Tube Drivers

Four representative types of shock tube drivers are shown in Figures 4A to 4D. The upper three drivers are designed to cause a rarefaction wave to catch up to the shock front at the desired test station. A peaked shock

---

[6] *George A. Coulter, Gerald Bulmash, and Charles N. Kingery, "Experimental and Computational Modeling of Rarefaction Wave Eliminators Suitable for the BRL 2.44 m Shock Tube," Technical Report ARBRL-TR-02503, Ballistic Research Laboratory, Aberdeen Proving Ground, MD, June 1983 (AD A131894).*

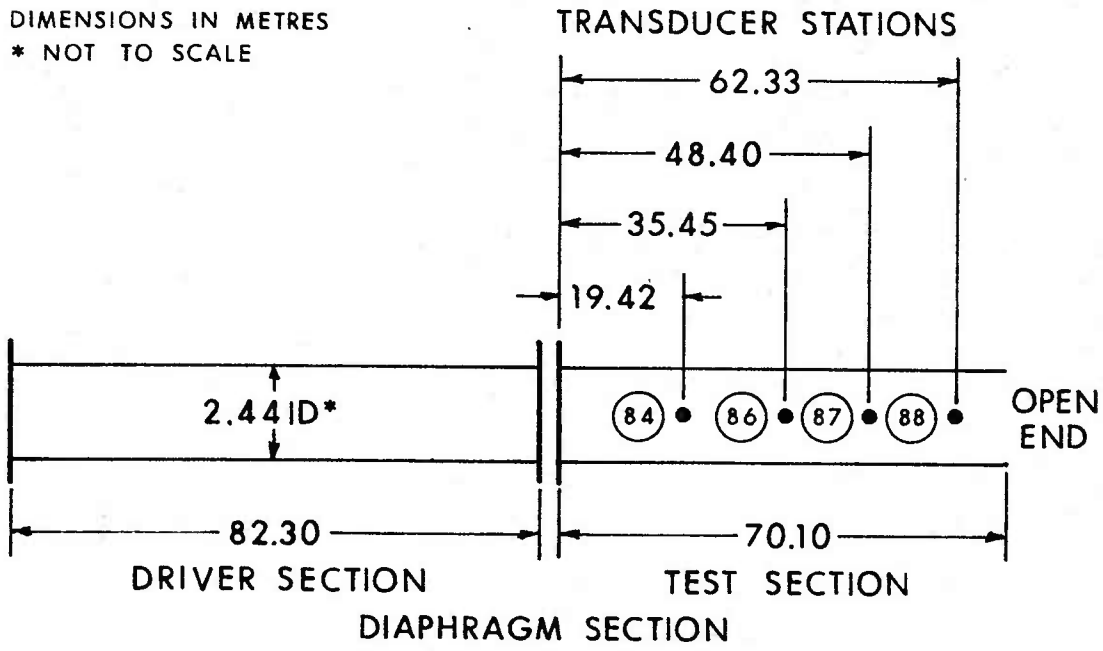

Figure 1. Sketch of BRL 2.44 m Shock Tube.

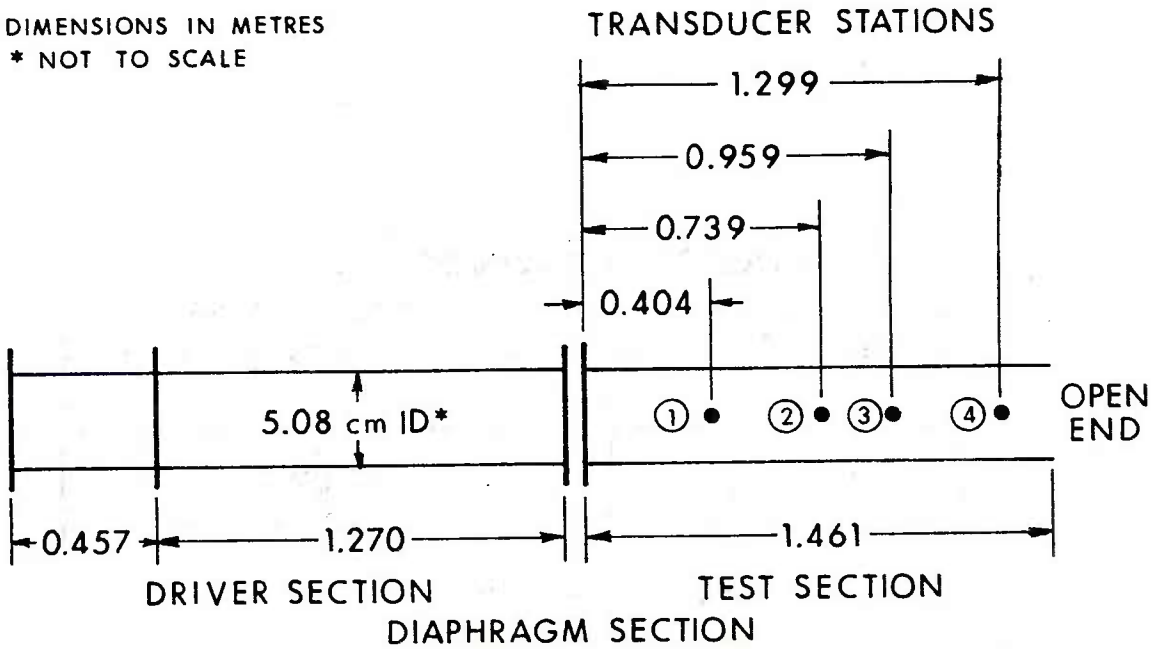

A. Sketch of Shock Tube Models.

Figure 2. 1/48th Scale Shock Tube Model

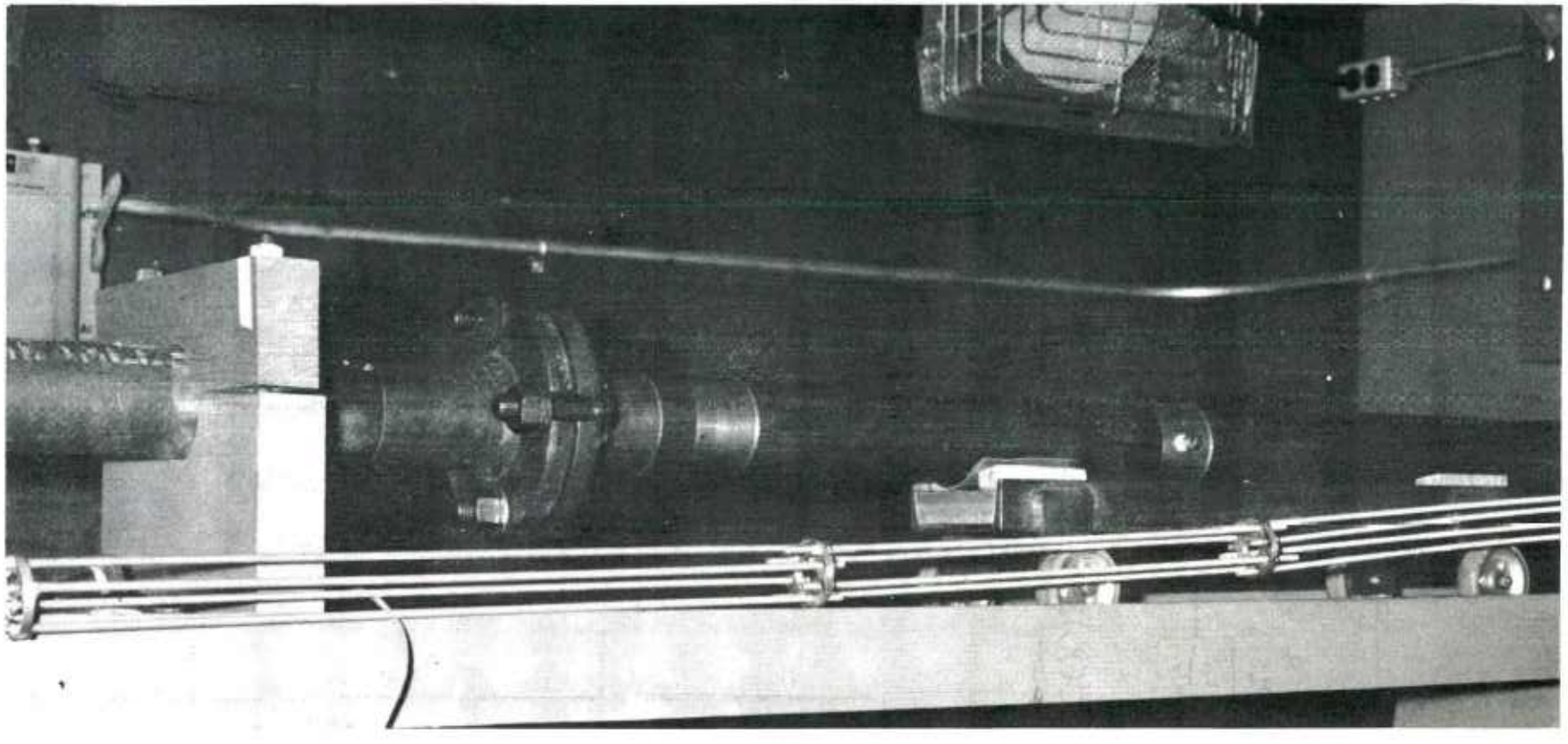

B. Photograph of Driver Section/Baffles

Figure 2. 1/48th Scale Shock Tube Model (Cont.)

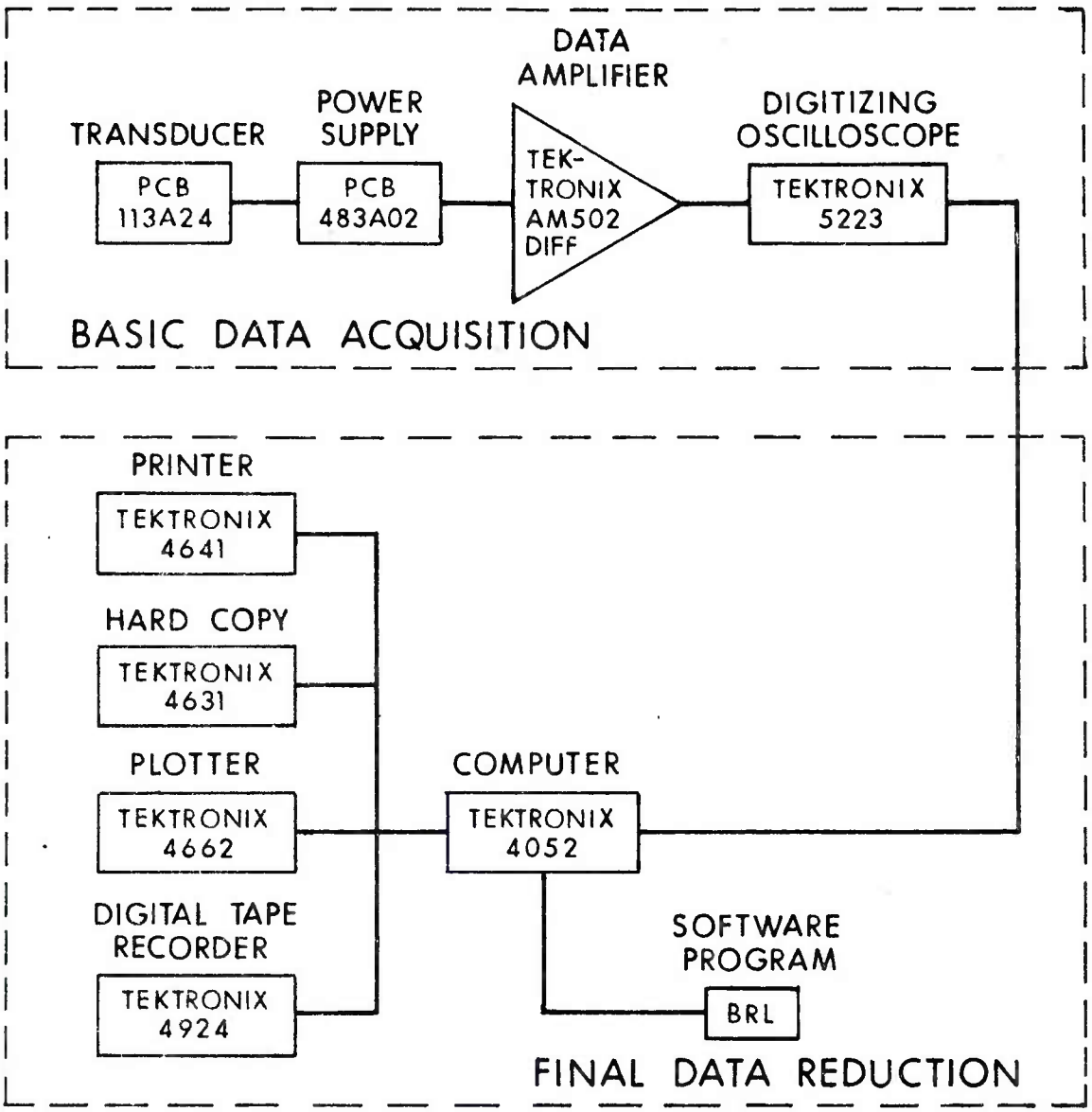

Figure 3. Schematic of Data Acquisition-Reduction System

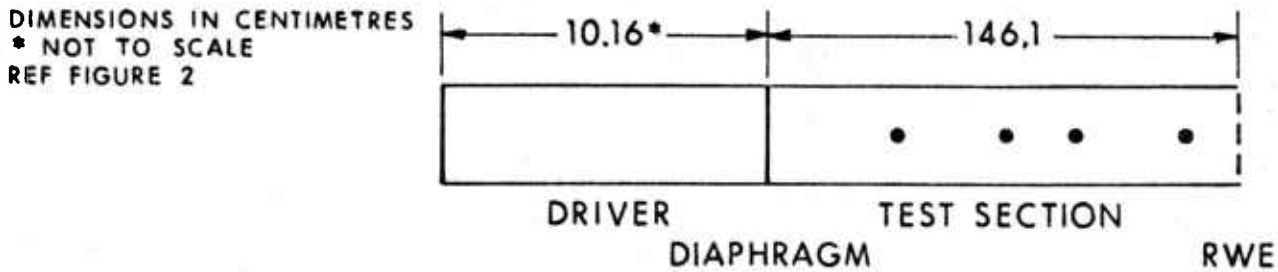

A. Short Driver

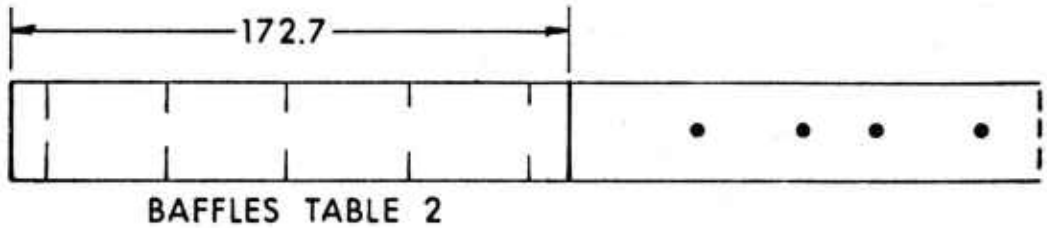

B. Driver with Baffles

Figure 4. Driver Modifications to 1/48th Scale Model Shock Tube

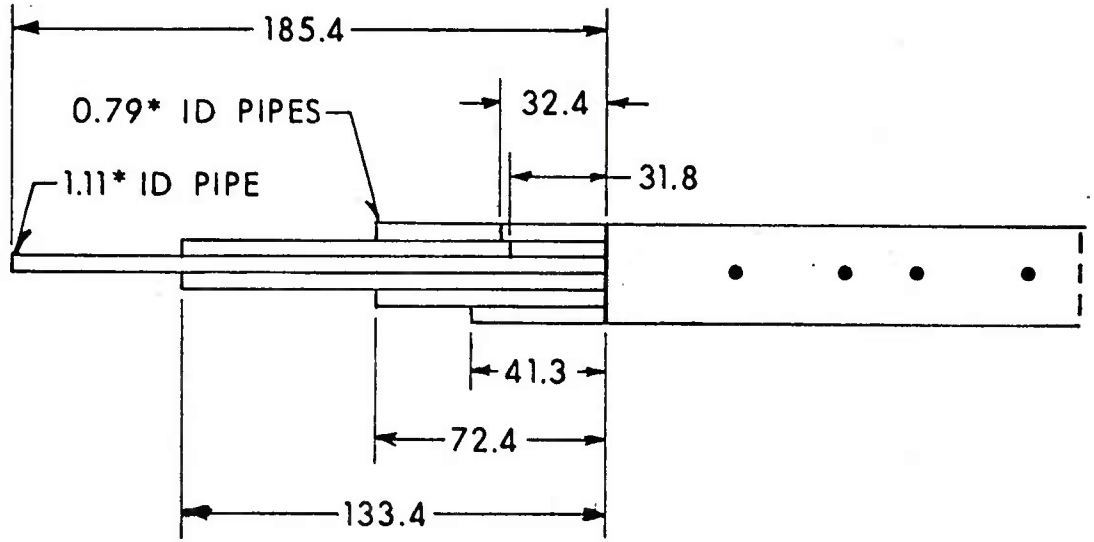

C. Multiple Pipe Driver

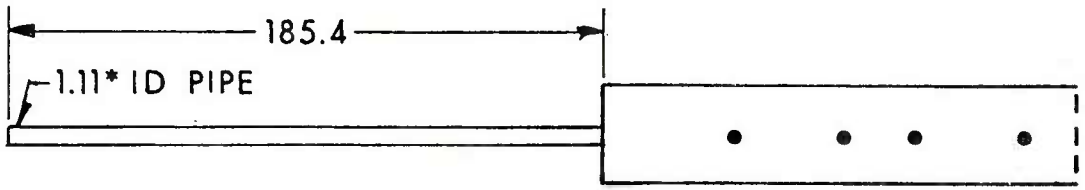

D. Small Diameter Driver

Figure 4. Driver Modifications to 1/48th Scale Model Shock Tube (Continued)

wave will occur due to rarefaction catch-up after this point.[7,8] Reference 7 shows this distance to be fifteen to sixteen driver lengths. The fourth driver shown in Figure 4-D is much smaller in diameter than the test section of the shock tube; therefore, a peaked wave front will occur shortly after expansion into the larger test section. See Reference 4.

The next section gives results for the four types of shock tube drivers.

III. EXPERIMENTAL RESULTS

The results are summarized in the data tables and with pressure-time records to illustrate the variations in waveforms caused by the different shock tube drivers.

A. Data Tables

The pertinent shot parameters, types of shock tube drivers tested, and input shock pressure levels used are listed in Table 1. The shots are grouped by the type of driver used.

The rarefaction wave elimination (RWE) standoff distance suitable for a peaked, decaying waveform necessary to eliminate the end rarefaction and to extend the test time (positive duration of the shock wave) is presented also. The RWE used in these tests had a fixed open area of 2.54 cm by 3.49 cm (8.86 cm^2). This area plus the area represented by the standoff distance are combined to give an effective open area. The effective open area divided by the cross-section area of the shock tube gives the vented area ratio. The vented area ratio is a function of peak overpressure which ranges from 23 to 124 kPa.

B. Driver Configurations

The pressure-time records are presented for the various driver configurations.

1. Long Straight Driver. The first series of records shown in Figure 5 illustrates the pressure time waveforms as a function of transducer station at one shock overpressure level. This is the standard flat-top wave form available from the shock tube in its present configuration (Figure 2).

---

[7] *C. W. Lampson, "Résumé of the Theory of Plane Shock and Adiabatic Waves with Applications to the Theory of the Shock Tube," BRL Technical Note 139, Ballistic Research Laboratories, Aberdeen Proving Ground, MD, March 1950 (AD 629328).*

[8] *I. I. Glass, "Shock Tubes Part I: Theory and Performance of Simple Shock Tubes," UTIA Review No. 12, Part I, Institute of Aerophysics, University of Toronto, Toronto, Canada, May 1958.*

Table 1. SHOT PARAMETERS

Shot No.	Station No.	Shock Overpressure kPa	Positive Duration ms	Standoff Distance cm	Vented Area Ratio	Type Driver	Comments
2-82-31	2	58.0	16.2	0.30	0.579	Long Driver	
31	3	60.0	17.4				
12	4	60.0	16.2	0.90	0.559		
2-83-88	3	58.5	2.5	0.15	0.517	4 inch diameter	
88	4	56.5	1.8				
89	3	93.5	3.1	0.49	0.791		
89	4	86.0	2.2				
2-83-62	3	56.0	29.2	0.30	0.579	Long driver, five baffles.	Case 1-A
62	4	54.0	30.0				
2-83-85	3	60.0	29.0	0.30	0.579	Long driver, four baffles.	Case 1-B
85	4	59.0	30.0				
2-83-64	3	60.0	27.7	0.30	0.579	Long driver, three baffles.	Case 1-C
64	4	57.0	27.7				
2-83-65	3	60.0	27.0	0.30	0.579	Long driver, three baffles.	Case 1-D
65	4	57.0	27.0				
2-83-68	3	60.0	26.0	0.35	0.599	Long driver, three baffles.	Case 1-E
68	4	58.0	27.7				
2-83-70	3	61.0	26.0	0.35	0.599	Long driver, three baffles.	Case 1-F
70	4	59.0	27.7				
2-83-74	3	42.5	24.7	0.15	0.517	Long driver, three baffles.	Case 1-E
74	4	41.0	27.4				
77	3 stag	52.5	25.9				
84	4 stag	50.5	27.4				
2-83-71	3	62.3	26.7	0.30	0.579		
71	4	58.5	29.0				
78	3 stag	77.0	29.0	0.35	0.599		
83	4 stag	71.5	29.0				

Table 1. SHOT PARAMETERS (Cont.)

Shot No.	Station No.	Shock Overpressure kPa	Positive Duration ms	Standoff Distance cm	Vented Area Ratio	Type Driver	Comments
2-83-72	3	95.0	37.6	0.49	0.729	Long Driver, three baffles	Case 1-E
72	4	90.0	35.0				
79	3 stag	131.0	35.5				
82	4 stag	123.0	37.0				
2-83-73	3	127.0	45.0	0.79	0.853		
73	4	120.0	45.0				
80	3 stag	174.0	40.1				
81	4 stag	162.0	42.0				
2-83-4	1	41.5	6.2	0.30	0.579	Single pipe driver	Case 3
4	2	34.0	4.3				
3	3	27.5	3.1				
3	4	23.5	1.2				
2-83-8	1	60.0	12.6	0.0	0.457	Multiple pipe driver	Case 2
8	2	46.0	12.6				
12	3	41.5	11.7				
12	4	38.5	12.0				

Notes:

1. Cross-section area of 1/48th scale model shock tube is 20.27 cm^2.
2. Cross-section open area in the 1/48 scale model RWE is 8.86 cm^2, was used on all tests except Shot 2-82-12.
3. Range of ambient temperature was 20^{o} C to 24^{o} C.
4. Range of ambient pressure was 101 kPa to 102 kPa.

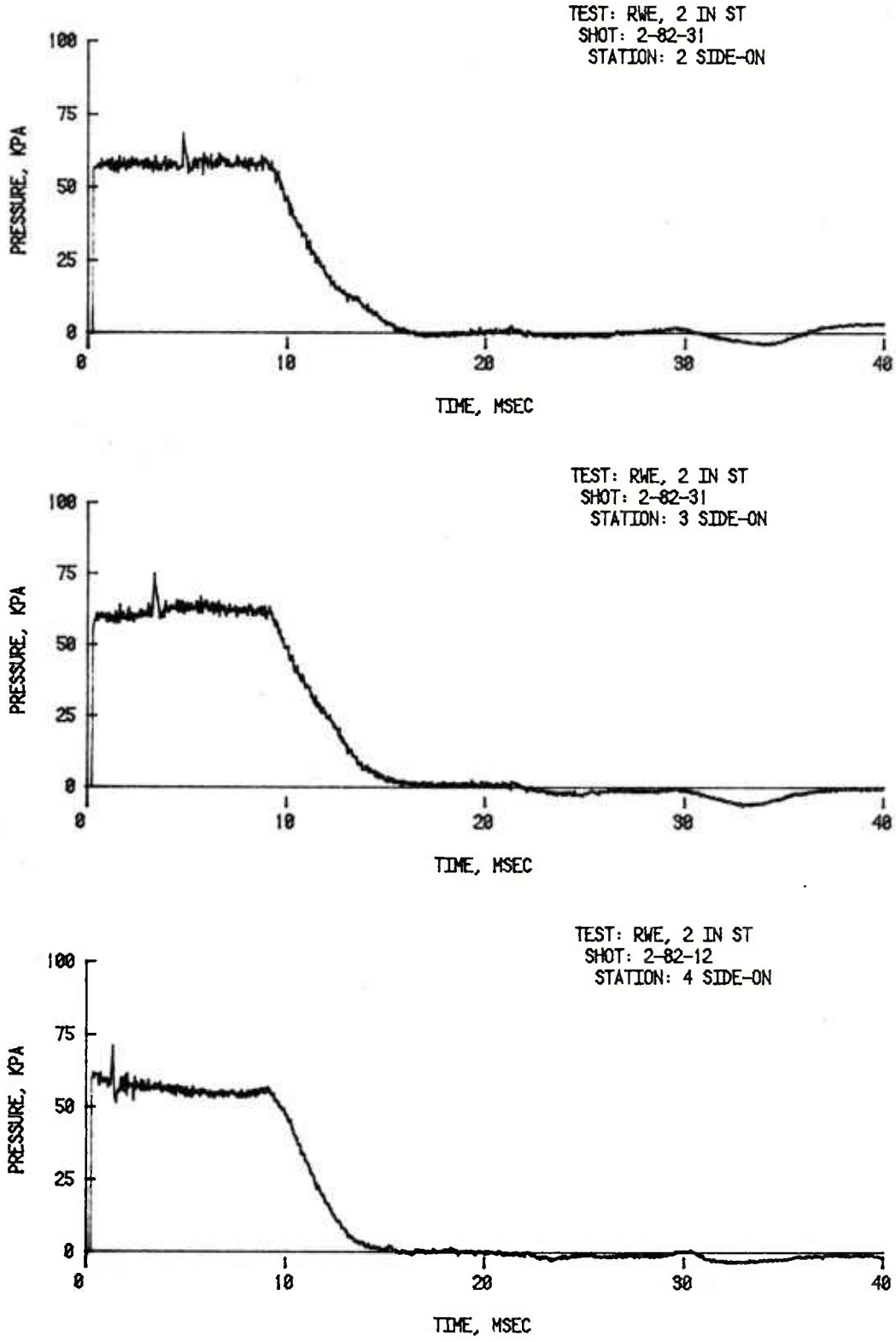

Figure 5. Pressure-Time Records for Long Straight Driver

By multiplying the time scale by 48, the result will apply to the RWE 2.44 metre shock tube shown in Figure 1.

2. Short Straight Driver. The records shown in Figure 6 are from a short driver (10.16 cm) as shown in Figure 4-A above. The length was chosen (References 7 and 8) so as to allow the rarefaction from the end of the closed driver to overtake the shock front at the desired test station. Test Station 3 was chosen (Station 87 in the 2.44 mm shock tube) since it is of the most interest. Even though a peaked decaying shock wave was formed with the short driver, the total duration is short - about 2-3 ms.

3. Baffles in Long Driver. When the baffles were selected for placement in the driver there were two variables: one, the amount of open area and two, the location within the driver. Therefore, the method of threaded rods with lock nuts (Figure 2-B) was used for ease in varying the separation distance between the baffles. The details of the number, opening, and locations are presented in Table 2. These same baffle parameters are presented graphically in Figures 7, 8, and 9.

The decaying wave achieved with five baffles (Case 1-A) is presented in Figure 10A. The baffle location and percent openings are presented in Figure 7. The five baffles produced an acceptable decaying shock wave. The predicted duration for a similar shock wave in the 2.44 metre tube would be 1.44 seconds.

The number of baffles was decreased to four (Case 1-B). The percent opening, and location are shown in Figure 8, and the overpressure versus time at Stations 3 and 4 is presented in Figure 10B. There is no significant difference noticed between the five-baffle and four-baffle cases.

The three-baffle tests are designated Cases 1-C, 1-D, 1-E, and 1-F. The percentage openings and locations are listed in Table 2 and plotted in Figure 9. The overpressure versus time at Stations 3 and 4 for Case 1-C and 1-D are plotted in Figure 10-C. The baffles were rearranged as noted for Cases 1-E and 1-F and the records are shown in Figure 10-D. From these tests it was determined that an optimum spacing, in terms of the most smoothly decaying shock wave, was considered to be Case 1-E.

A number of tests at different pressure levels was fired with three baffles spaced as noted for Case 1-E. Stagnation pressure, side-on pressure, and their differences (called Q) for Stations 3 and 4 are shown in Figure 11 according to pressure level and transducer station.

4. Single and Multiple Pipe Driver. The configuration for the single pipe driver (Case 3) is shown in Figure 4-D and listed in Table 1. The overpressure versus time recorded at the four stations is presented in Figure 12-A. Because of the expansion from a single pipe of small diameter into a larger pipe the overpressure versus time recorded at Station 1 shows a sharp decay behind the shock front. The peak overpressure also decays with distance down the tube. The single pipe does not produce an acceptable wave shape for a nuclear blast simulation.

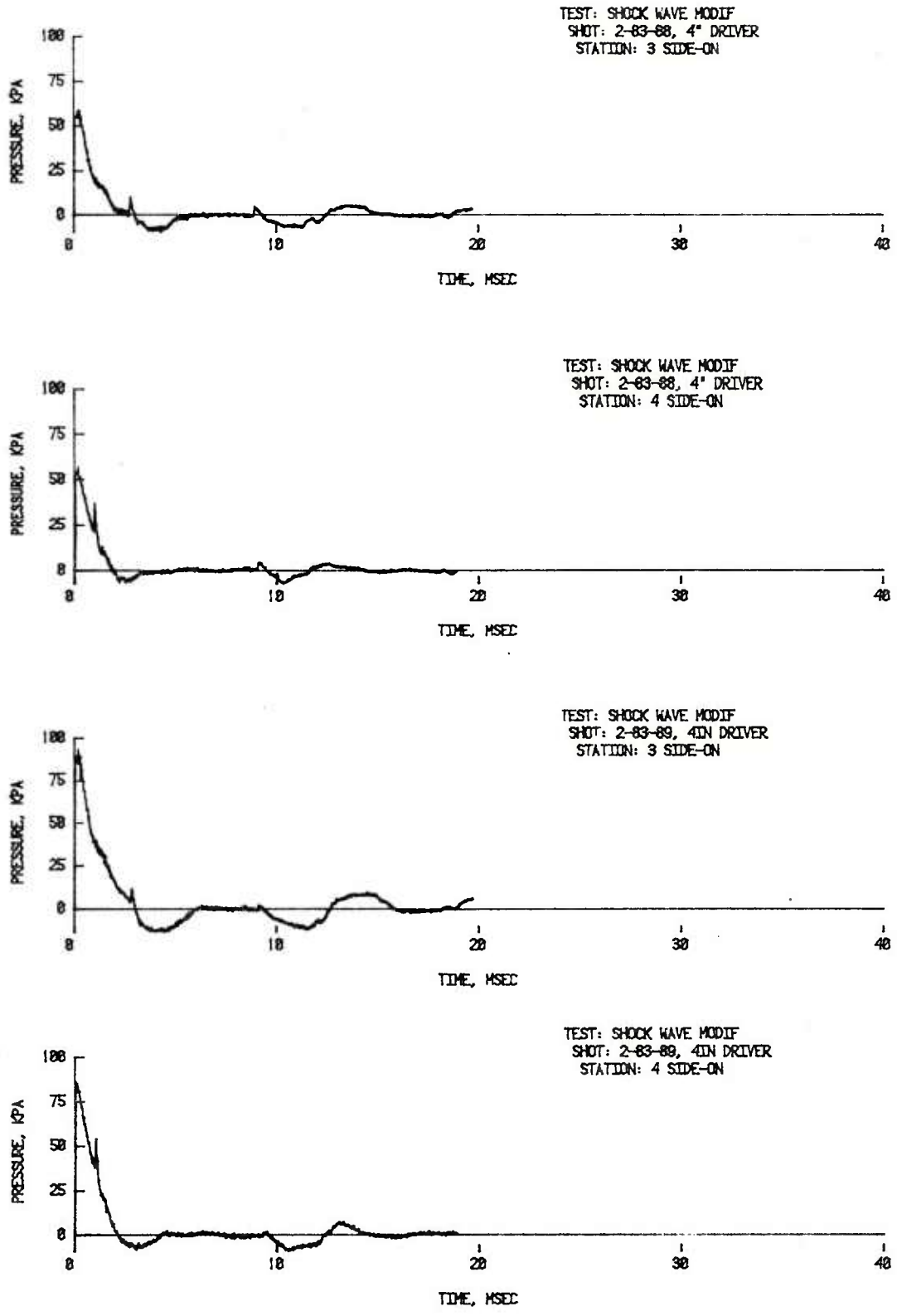

Figure 6. Pressure-Time Records for Short Straight Driver

Table 2. BAFFLE PARAMETERS

No.of Baffles	Position from Closed End of Driver cm	Position from Closed End of Driver in.	Baffle Ratio Open	Baffle Thickness	Case
5	20.32	8.0	0.050	All baffles	1-A
	58.42	23.0	0.105	were 0.635 cm	
	103.89	40.9	0.275	(1/4 in.)	
	144.27	56.8	0.491		
	161.80	63.7	0.680		
4	58.42	23.0	0.105		1-B
	103.89	40.9	0.275		
	144.27	56.8	0.491		
	161.80	63.7	0.681		
3	58.42	23.0	0.105		1-C
	103.89	40.9	0.275		
	162.05	63.8	0.560		
3	58.42	23.0	0.105		1-D
	103.89	40.9	0.275		
	162.05	63.8	0.680		
3	82.55	32.5	0.180		1-E
	142.24	56.0	0.491		
	160.02	63.0	0.680		
3	58.43	23.0	0.105		1-F
	142.24	56.0	0.491		
	160.27	63.1	0.680		

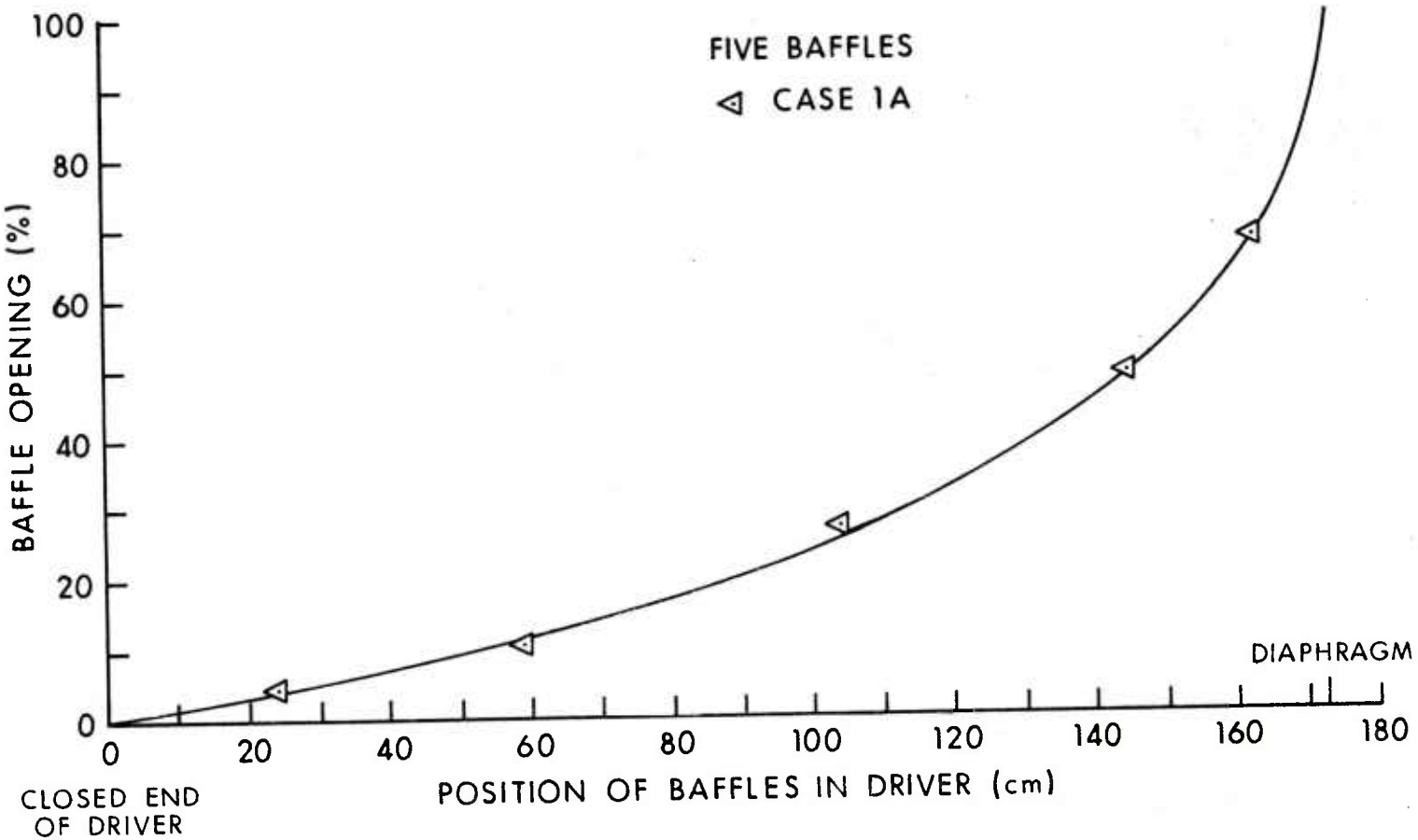

Figure 7. Five Baffles Placed Along Driver Section

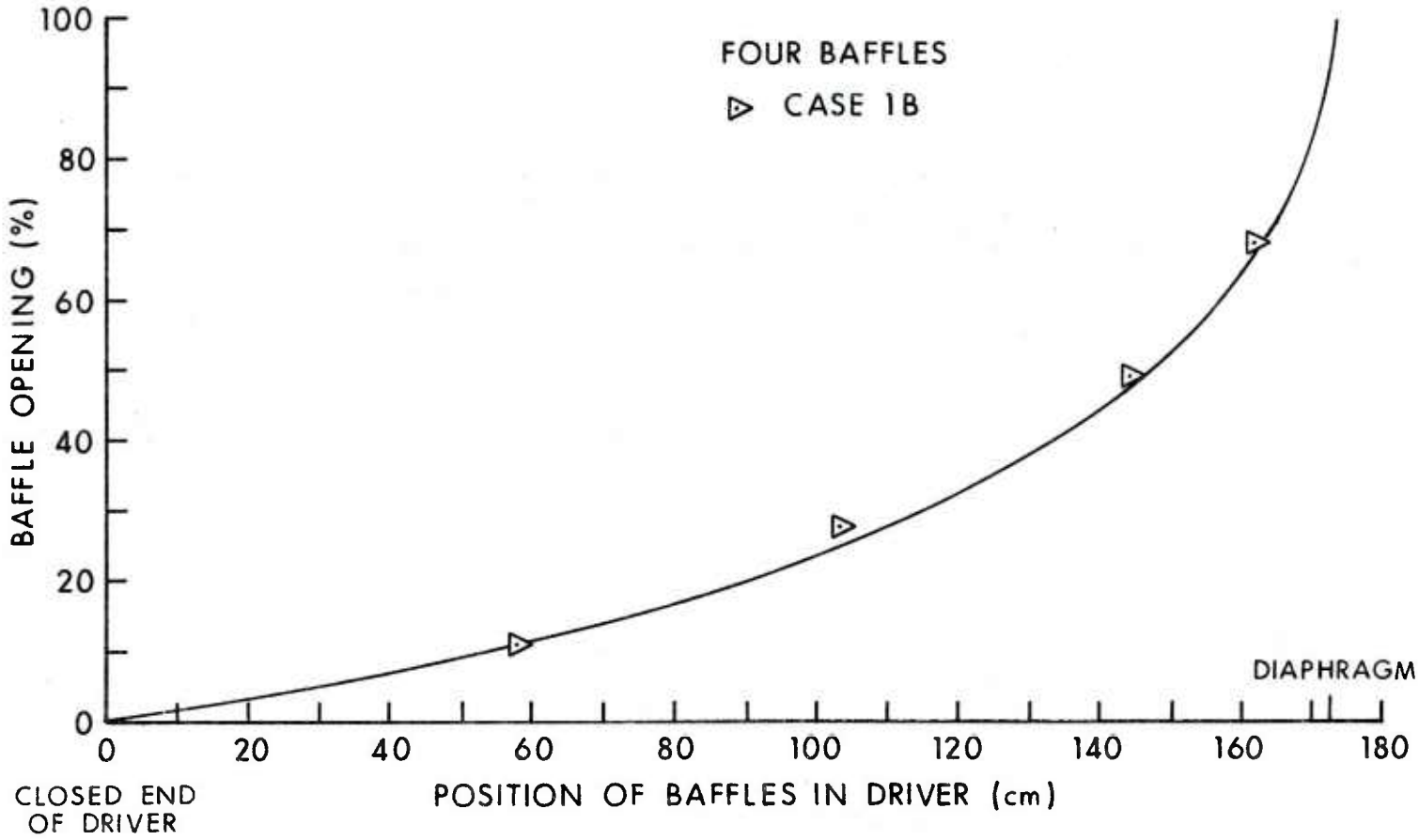

Figure 8. Four Baffles Placed Along Driver Section

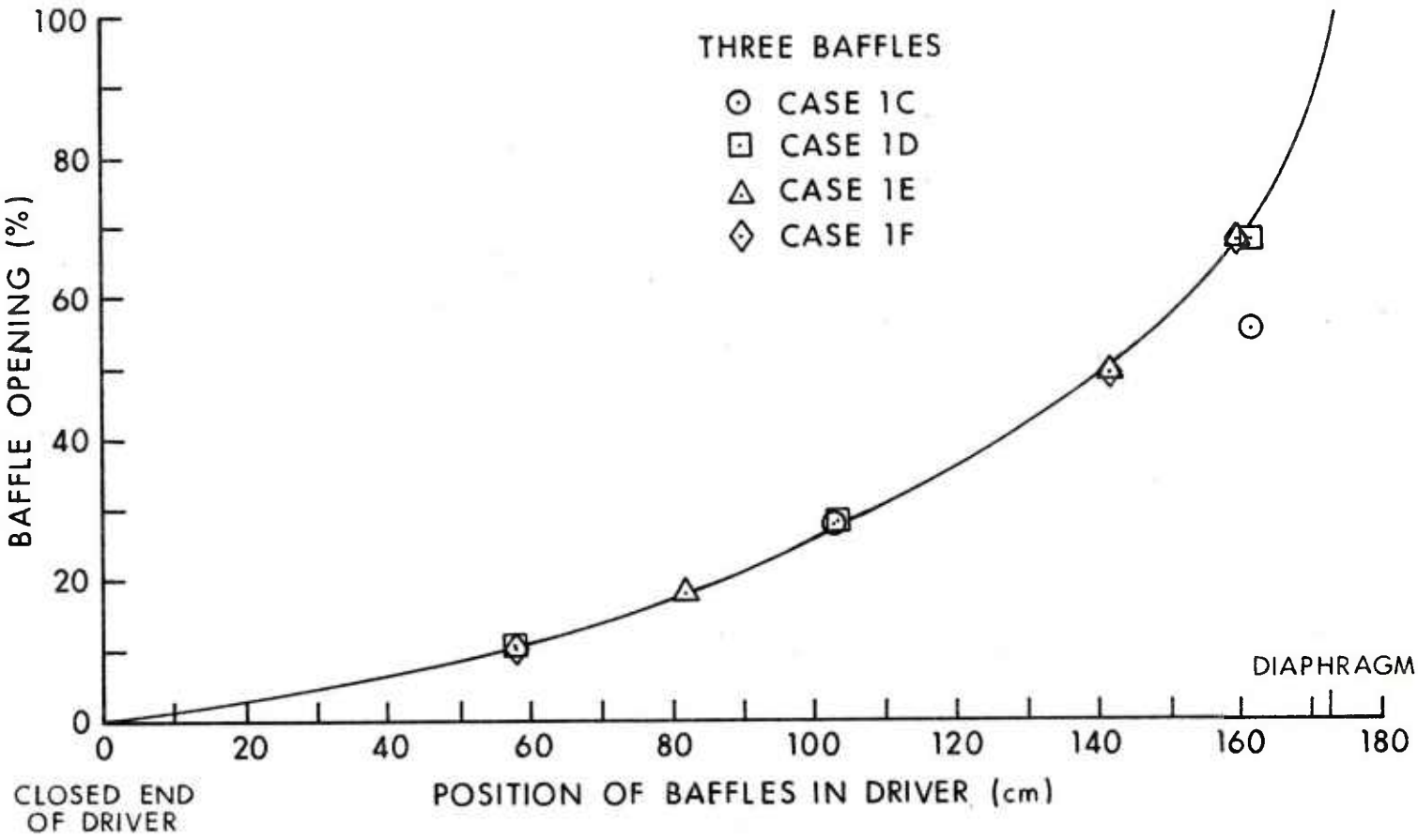

Figure 9. Three Baffles Placed at Various Locations Along Driver Section

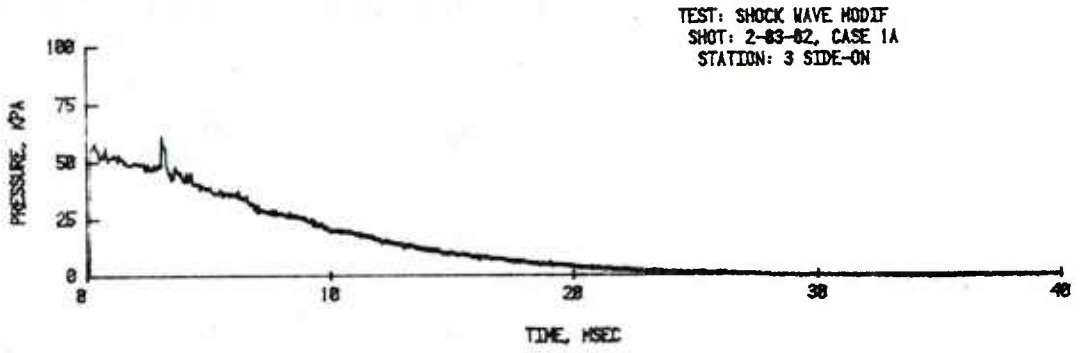

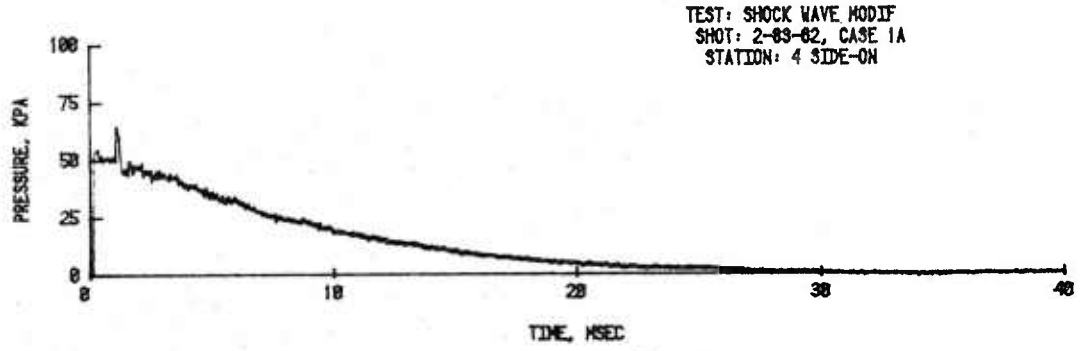

A. Five Baffles

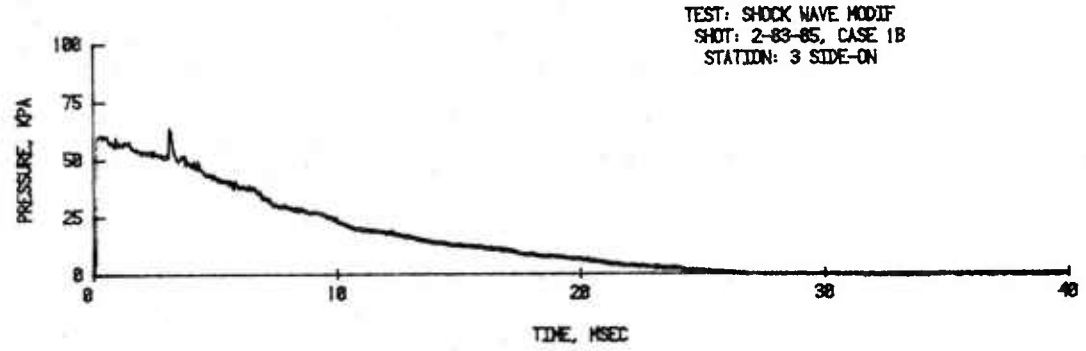

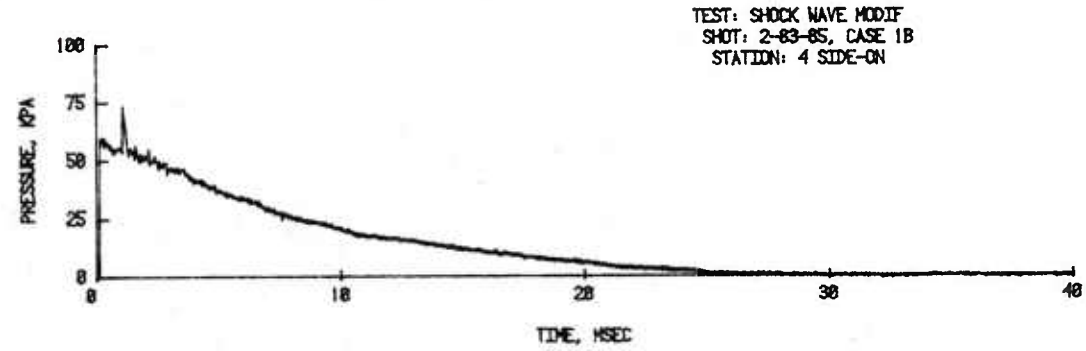

B. Four Baffles

Figure 10. Pressure-Time Records with Baffles in Long Driver

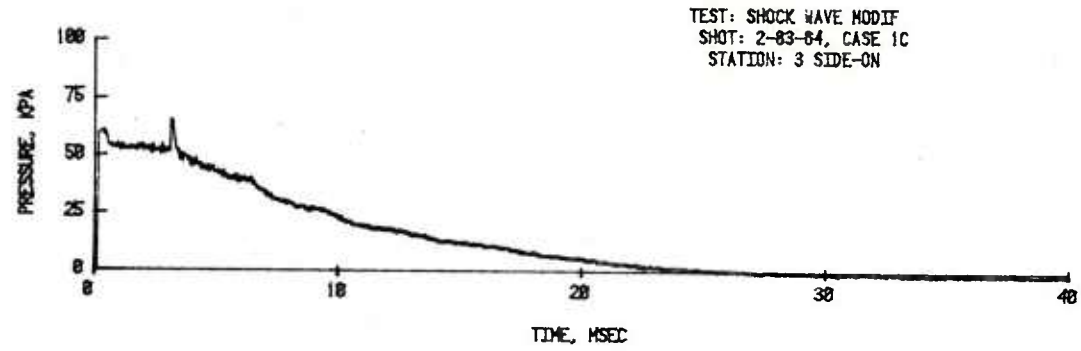

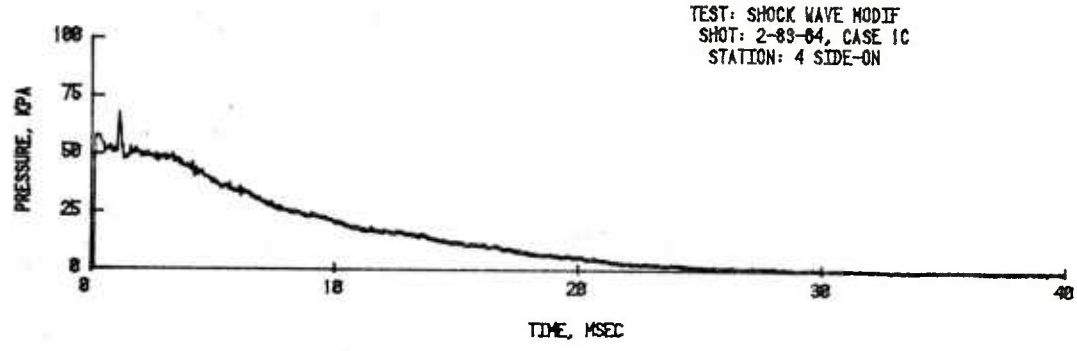

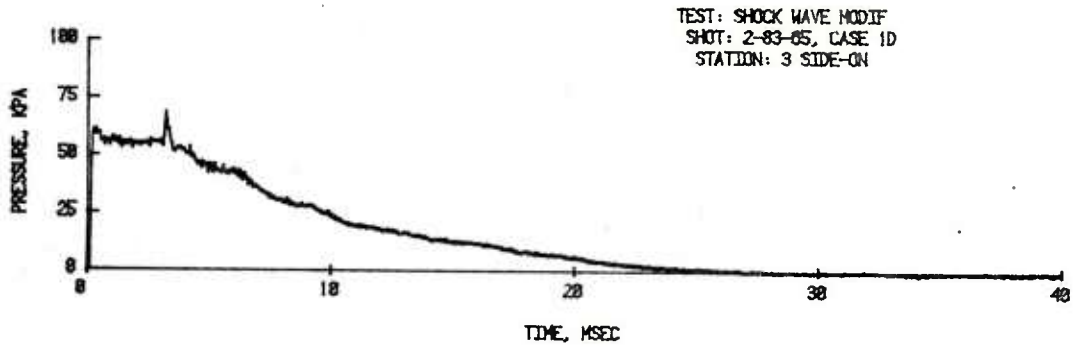

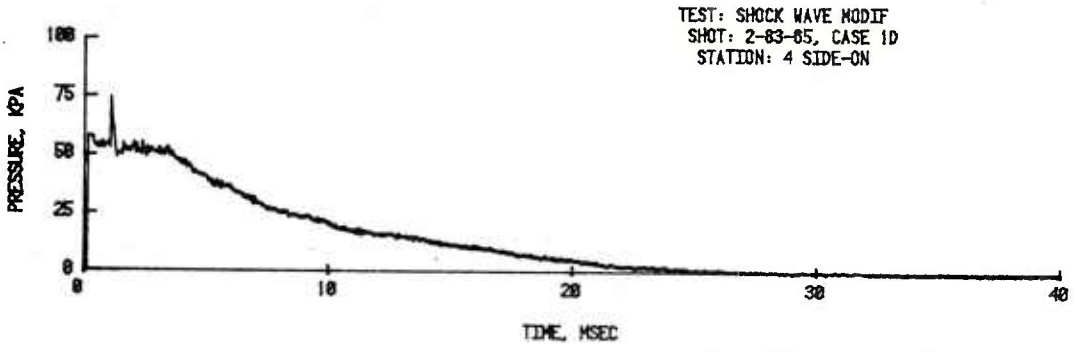

C. Three Baffles

Figure 10. Pressure-Time Records with Baffles in Long Driver (Cont.)

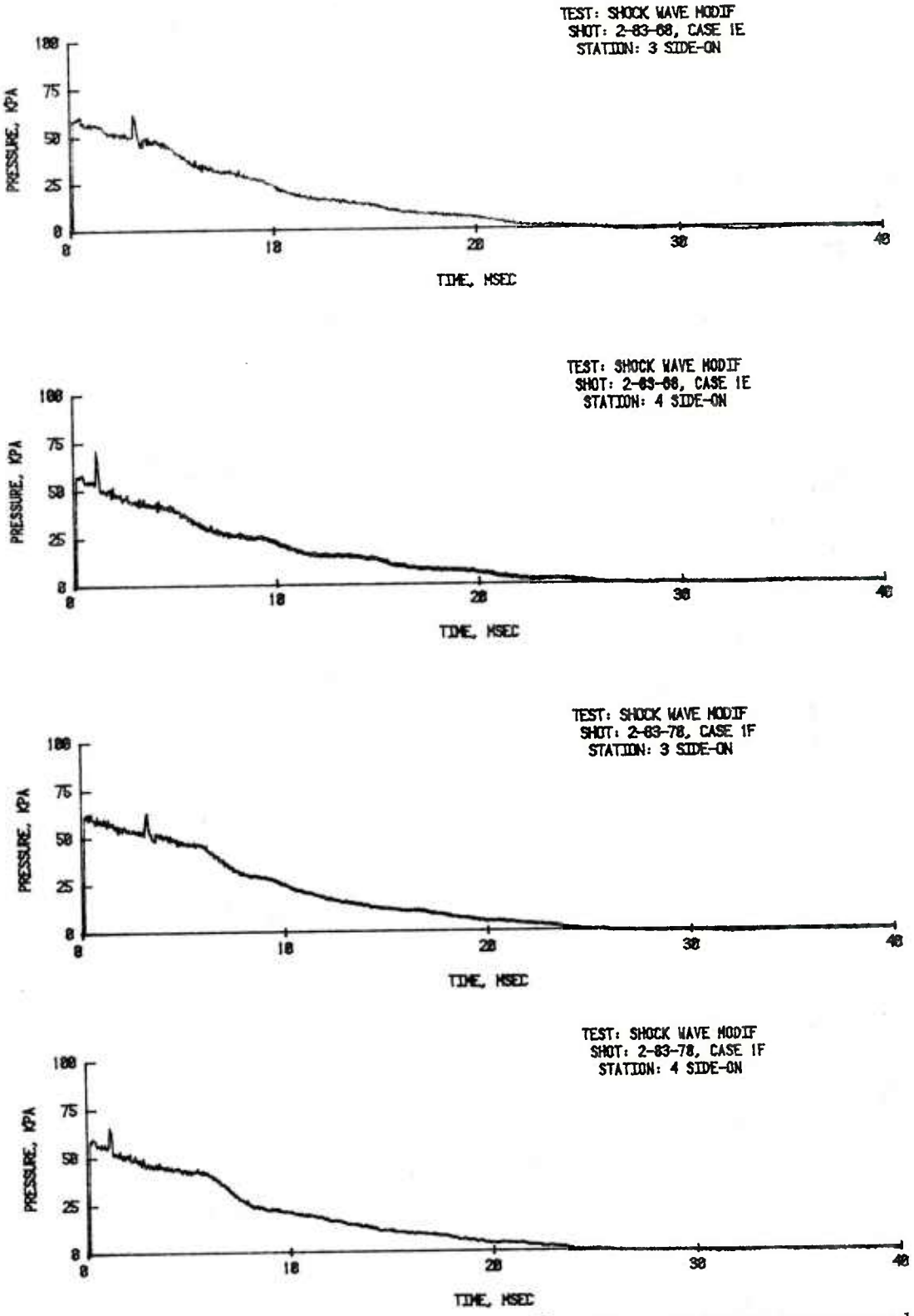

D. Three Baffles Rearranged

Figure 10. Pressure-Time Records with Baffles in Long Driver (Cont.)

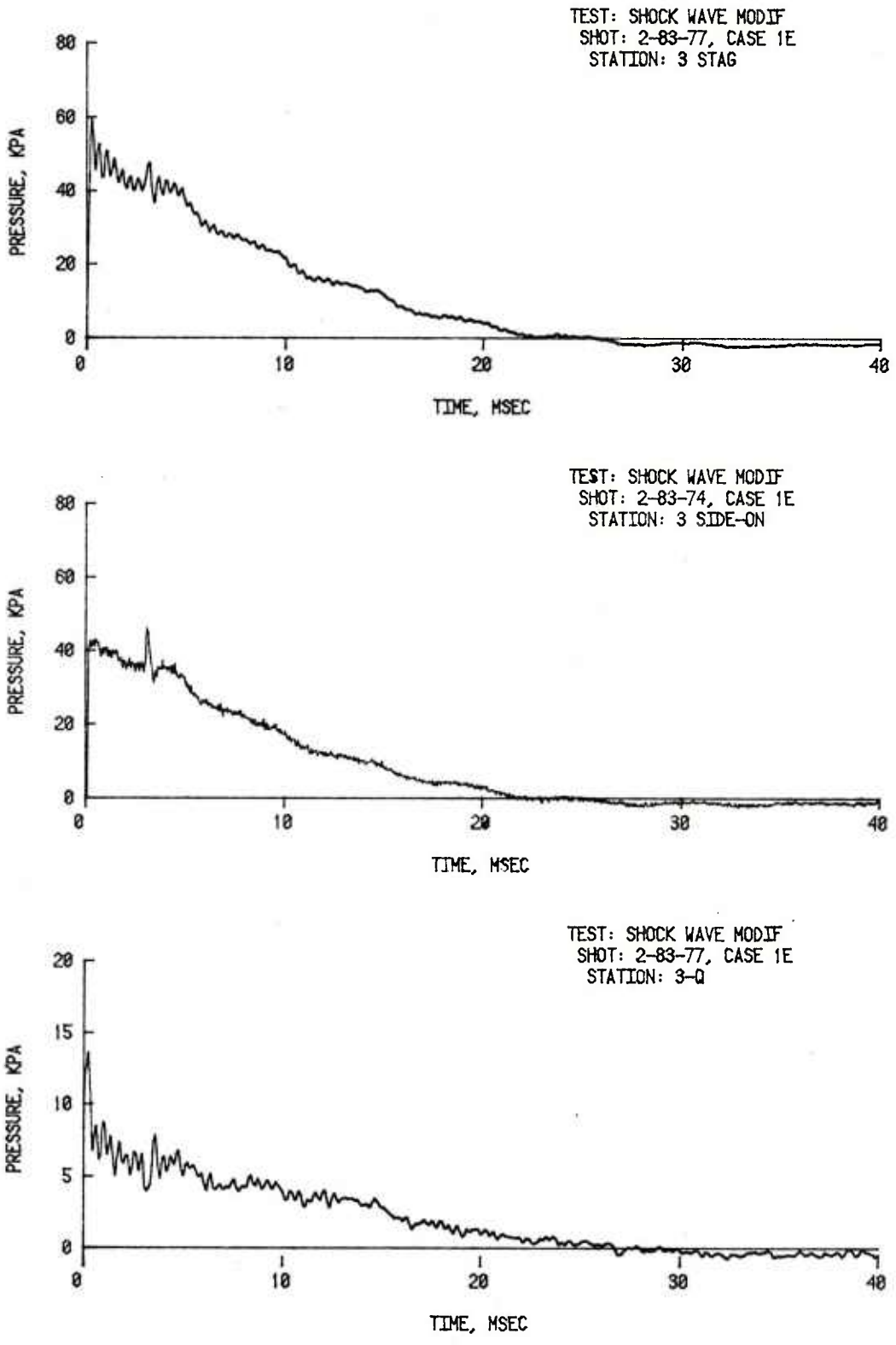

Figure 11. Pressure-Time Records with Three Baffles in Long Driver

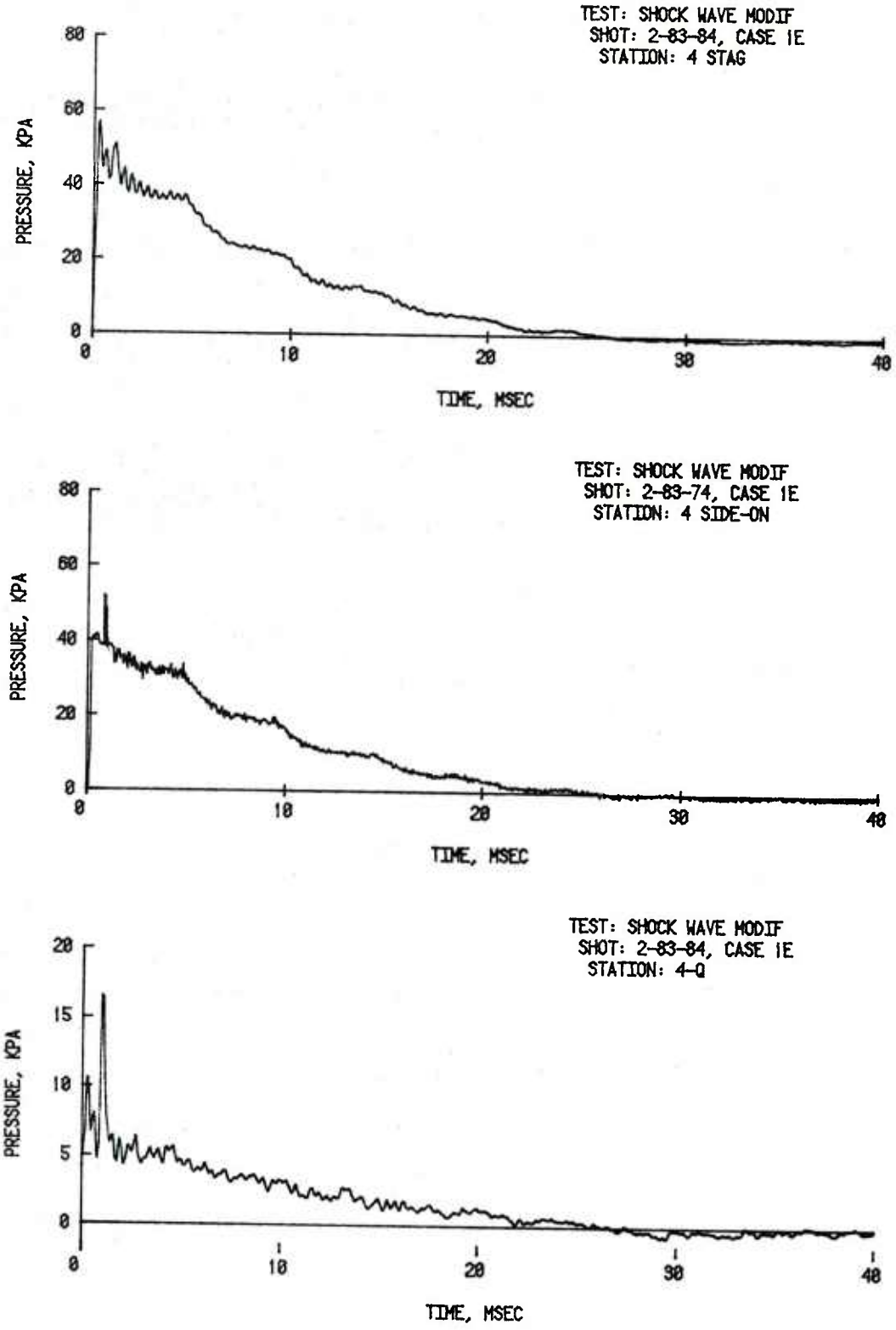

Figure 11. Pressure-Time Records with Three Baffles in Long Driver (Cont.)

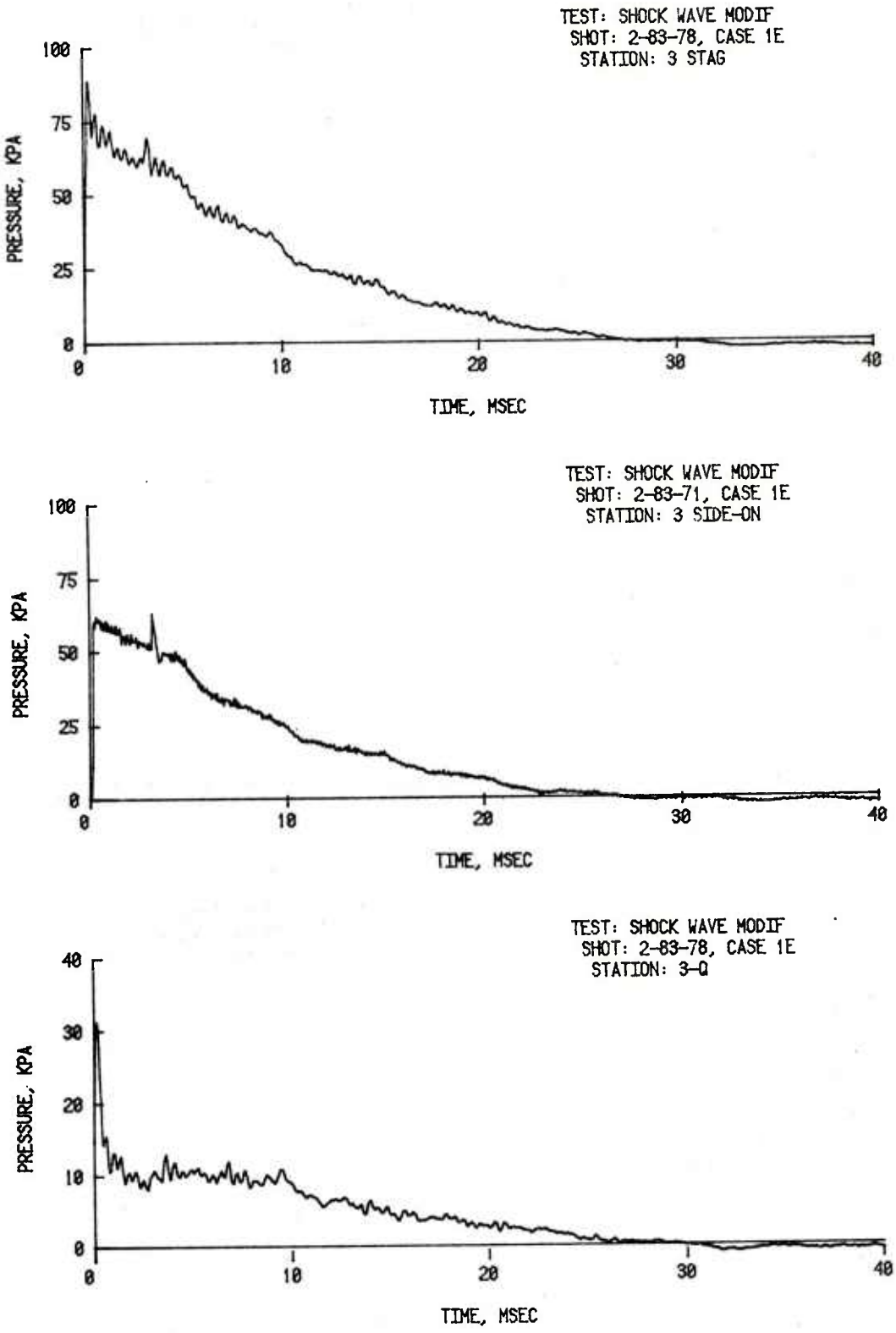

Figure 11. Pressure-Time Records with Three Baffles in Long Driver (Cont.)

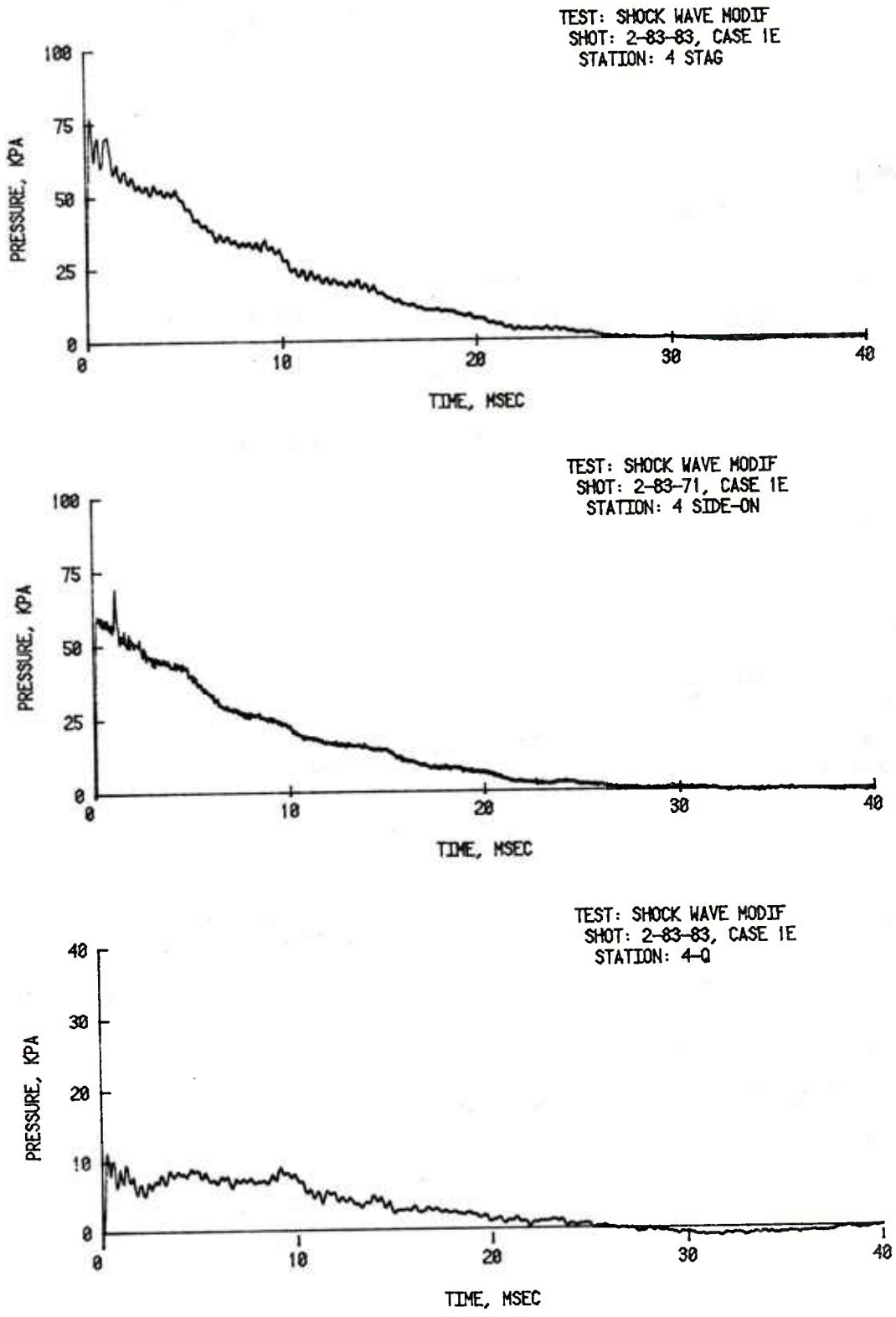

Figure 11. Pressure-Time Records with Three Baffles in Long Driver (Cont.)

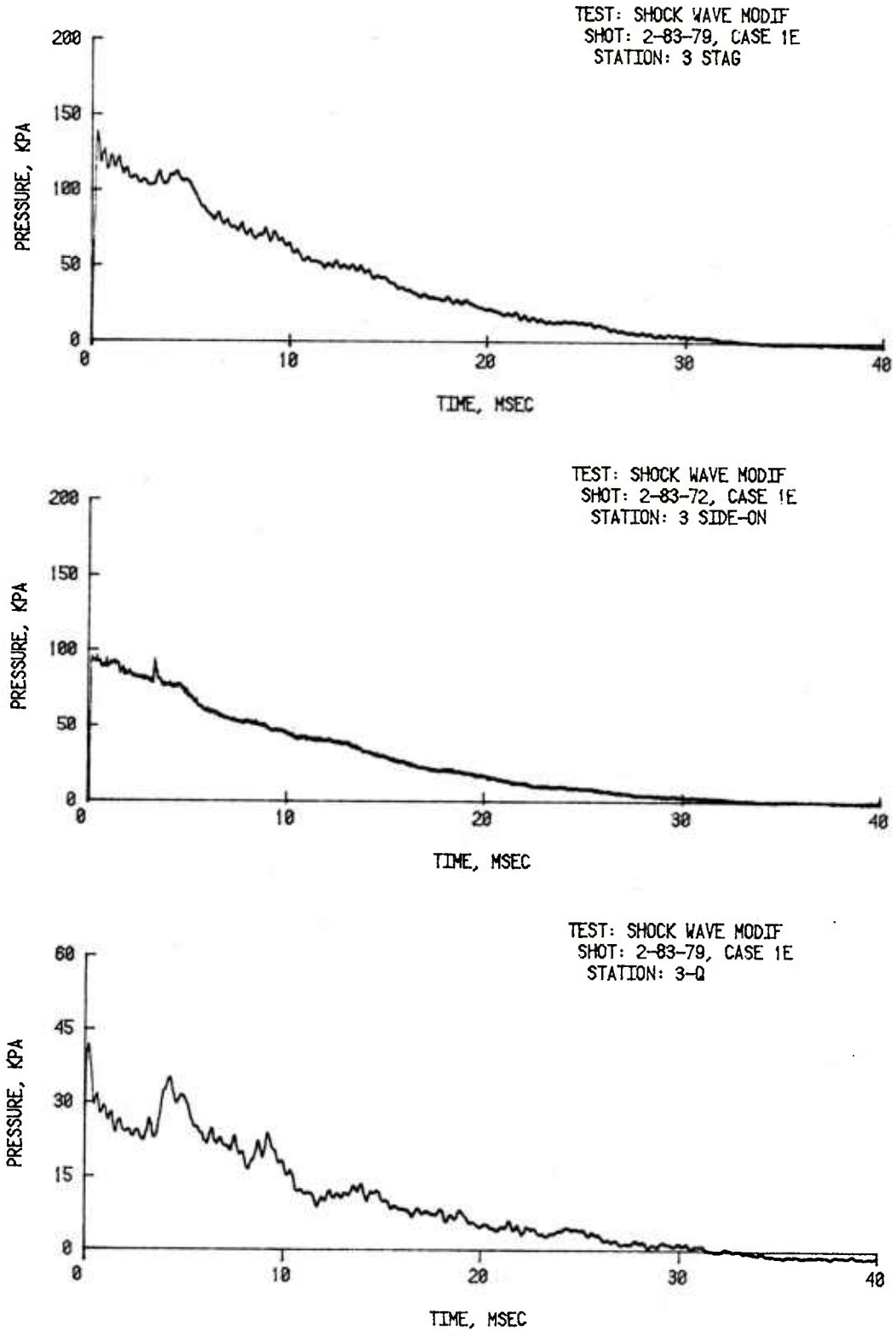

Figure 11. Pressure Time Records with Three Baffles in Long Driver (Cont.)

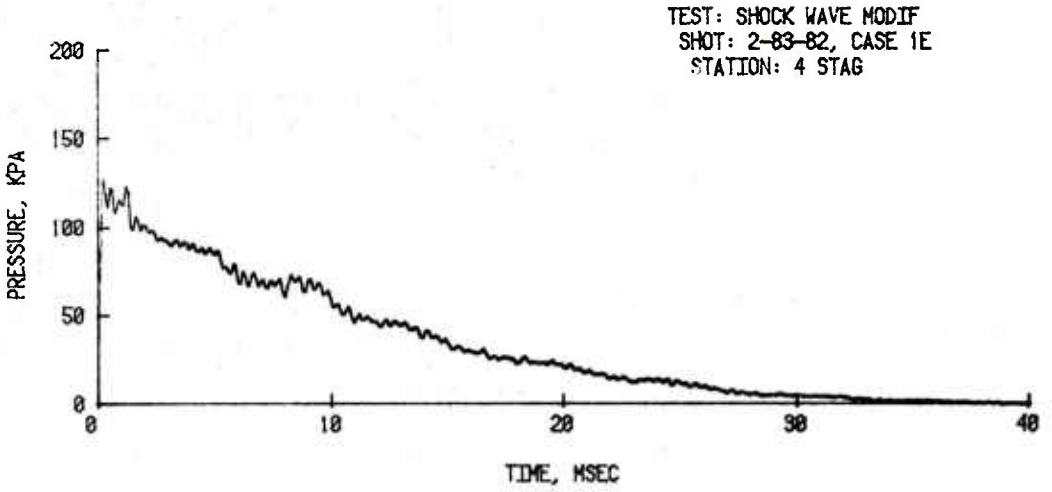

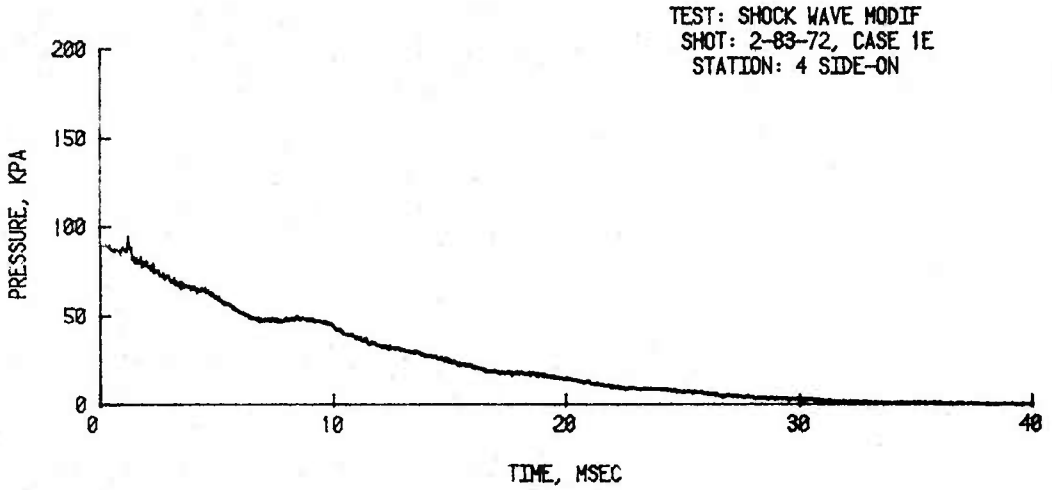

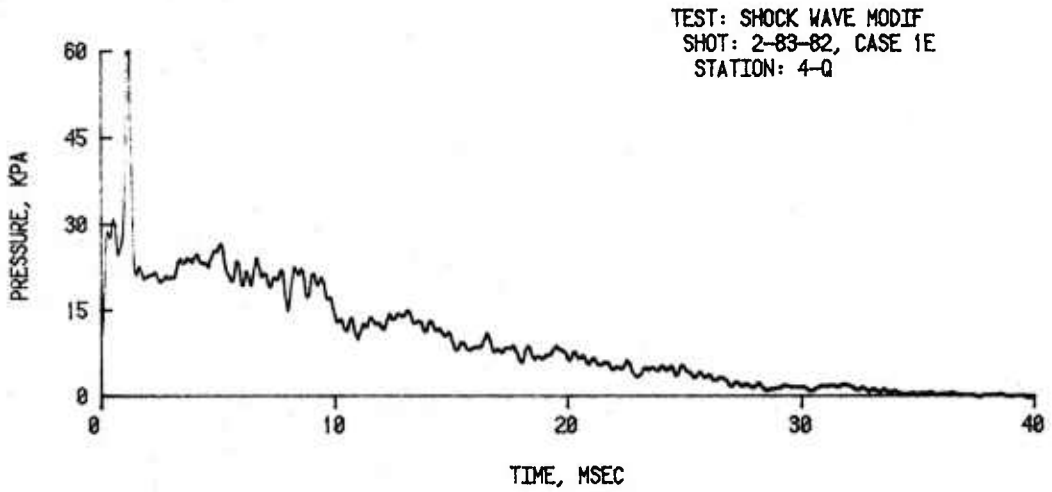

Figure 11. Pressure-Time Records with Three Baffles in Long Driver (Cont.)

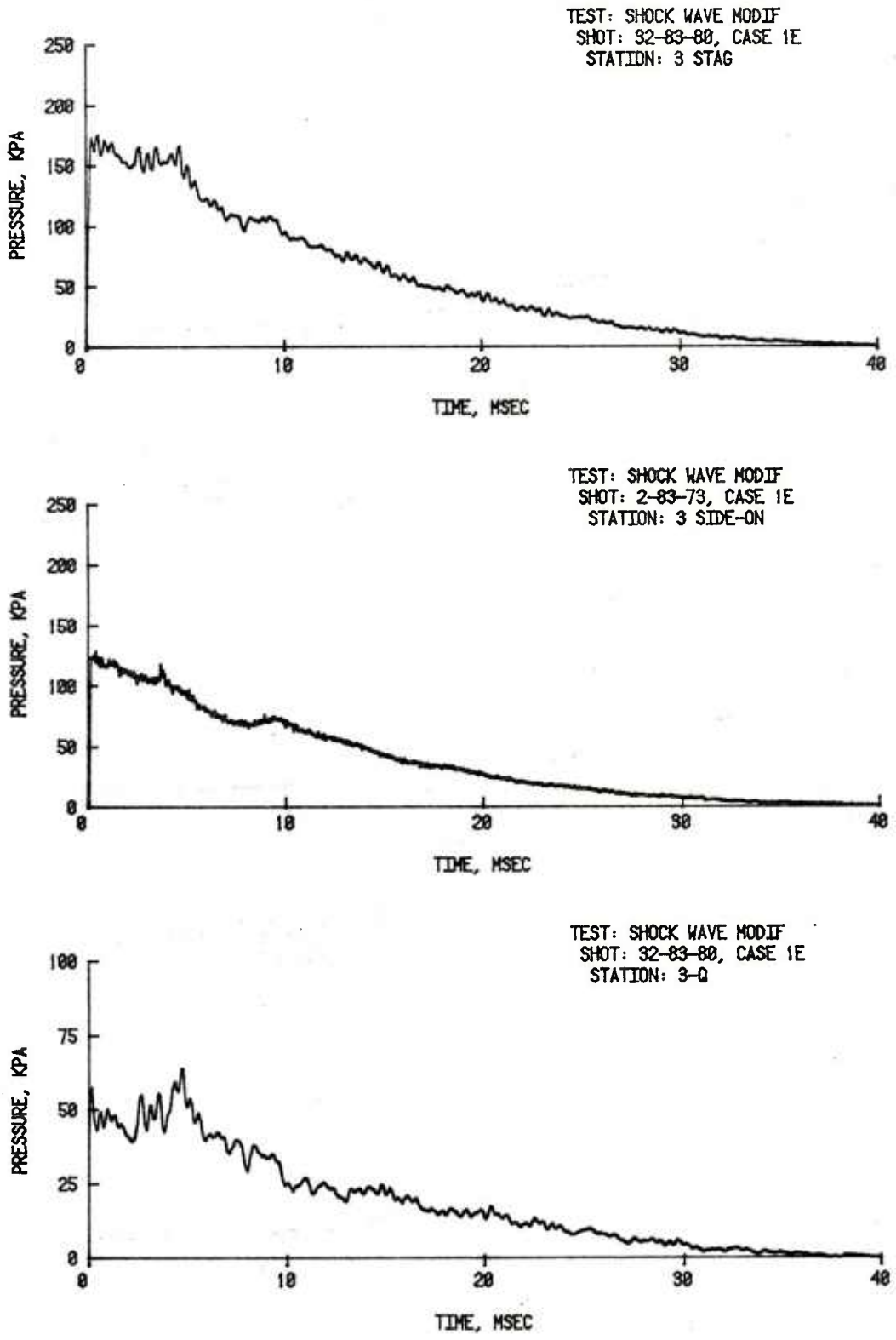

Figure 11. Pressure-Time Records with Three Baffles in Long Driver (Cont.)

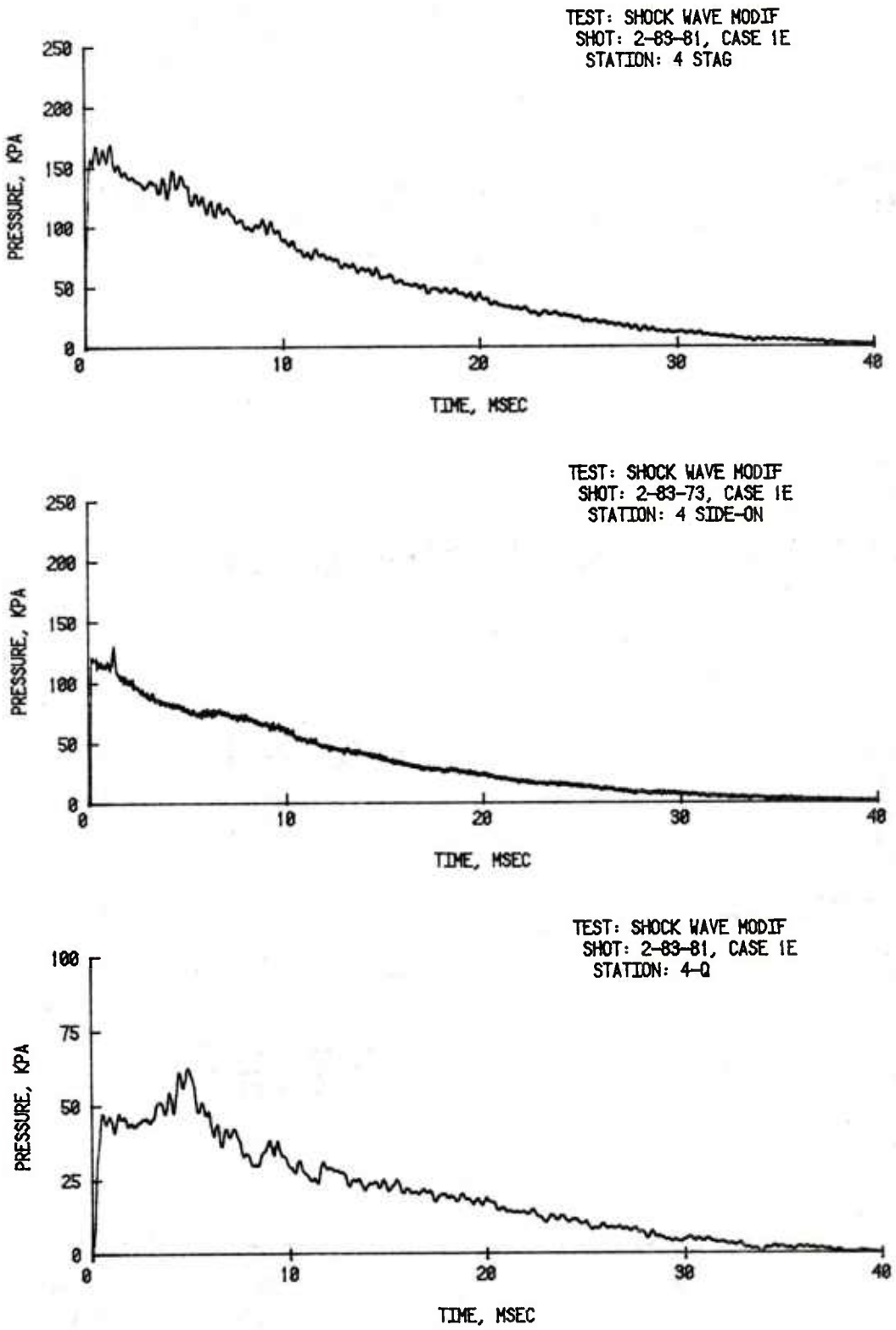

Figure 11. Pressure-Time Records with Three Baffles in Long Driver (Cont.)

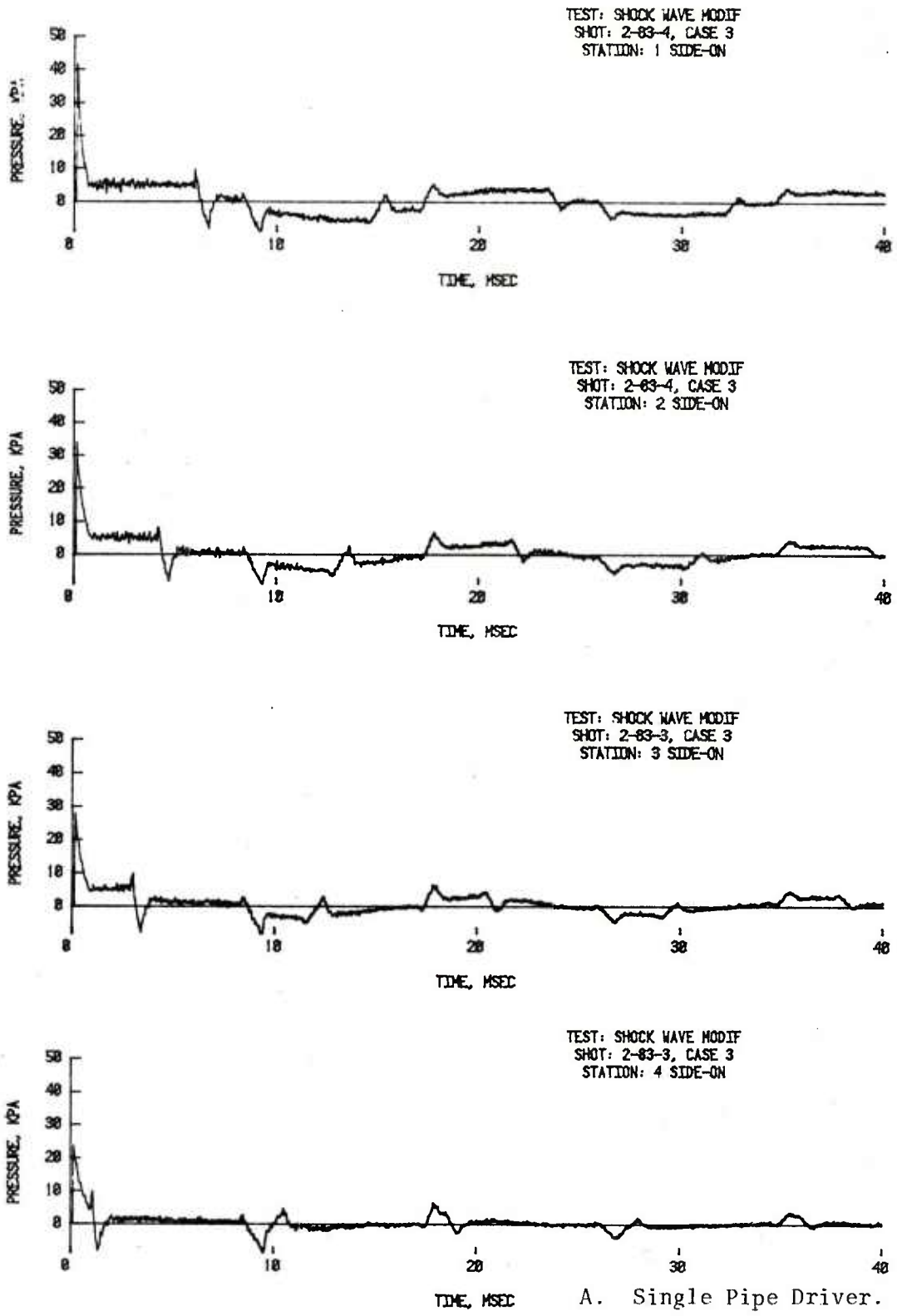

A. Single Pipe Driver.

Figure 12. Pressure-Time Records with Single and Multiple Pipe Drivers

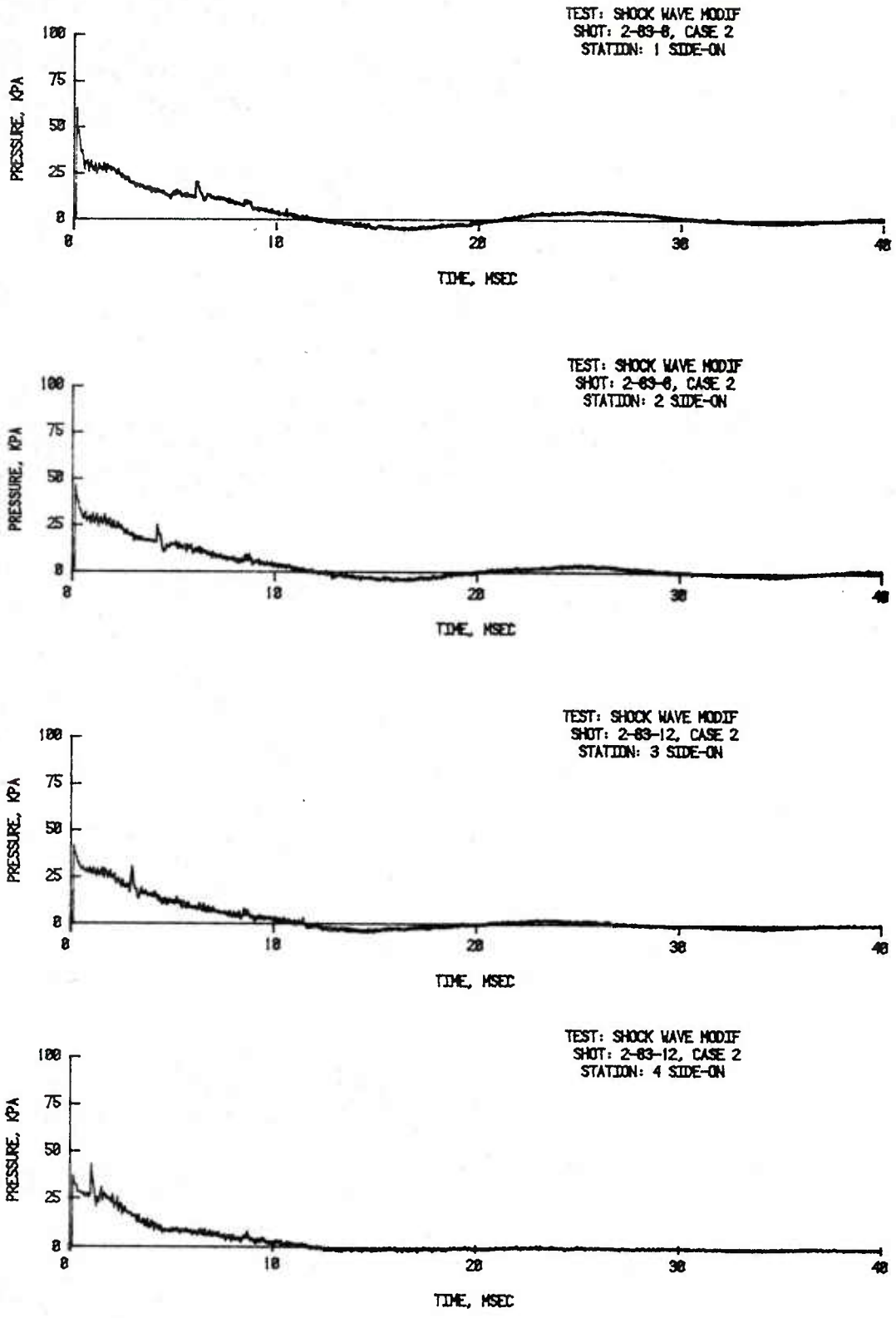

B. Multiple Pipe Driver.

Figure 12. Pressure-Time Records with Single and Multiple Pipe Drivers (Cont.)

The multiple pipe drivers, Case 2, as shown in Figure 4-C and Table 1 produced a uniformly decaying peaked shock wave. The wave shapes recorded at the four test stations are shown in Figures 12-B. Here again there is an expansion from the compression chamber to the test chamber when the diaphragm is broken and a peaked wave is recorded at Station 1. When compared to the baffled straight driver, the multiple tube driver produces a blast wave lower in peak overpressure and with about one half the positive duration.

IV. ANALYSIS

A discussion of rarefaction catch-up is given to illustrate how this technique may be used to produce a decaying shock wave starting with a step shock wave. Results obtained from the 1/48th scale shock tube model using this method are scaled up to predict results for the BRL 2.44 m shock tube. The equivalent weight of high explosive (TNT) needed to produce similar free-field waveforms are then calculated.

A. Rarefaction Catch-Up

Lampson in Reference 7 has shown that given a long enough test section, the reflected rarefaction from the closed end of the shock tube driver will overtake the shock front. From that point on, the shock wave will have a peak and a decaying waveform. The resulting waveform more nearly simulates the free-field blast from a nuclear weapon than does a flat-top wave.

Equation 1 gives the distance x in the test section, measured from the shock tube diaphragm, at which the reflected rarefaction wave reaches the cool gas boundary.

$$x = \left(\frac{5L_D(Y-1)}{\sqrt{7(1+6Y)}}\right)\left(\frac{2\sqrt{7(1+6Y)} + 4(Y-1)}{\sqrt{7(1+6Y)} - (Y-1)}\right), \quad \text{for air,} \tag{1}$$

where L_D is the shock tube driver length and Y is the absolute shock pressure ratio. Equation 2 gives the additional distance x_1 for the rarefaction to travel through the hot gas to reach the shock front.

$$x_1 = x\left(\frac{6+Y(5\ (Y-1) + \sqrt{7Y\ (6+Y)})}{5(Y-1)(\sqrt{7Y\ (6+Y)} - (6+Y)}\right), \tag{2}$$

where x is the distance from Equation 1 and Y is again the absolute shock pressure ratio. The total distance L_R from the diaphragm at which the rarefaction overtakes the shock wave is given by the sum of the results from Equations 1 and 2.

$$L_R = x + x_1 = x\left(1 + \frac{(6+Y)\left(\sqrt{7Y(6+Y)} + 5(Y-1)\right)}{5(Y-1)\left(\sqrt{7Y(6+Y)} - (6+Y)\right)}\right). \quad (3)$$

Set $$A = \frac{x}{L_D} \quad \text{and} \quad (4)$$

$$B = 1 + \frac{(6+Y)\left(\sqrt{7Y(6+Y)} + 5(Y-1)\right)}{5(Y-1)\left(\sqrt{7Y(6+Y)} - (6+Y)\right)}, \quad (5)$$

so that $$\frac{L_R}{L_D} = AB. \quad (6)$$

This ratio is tabulated in Table 3 and graphed in Figure 13. The ratio is very dependent upon shock pressure at the lower range pressures. It is necessary to choose carefully the first baffle location in the driver for the smallest anticipated pressure level. Otherwise, the rarefaction will not catch up to shock front to produce the desired peak decaying waveform.

A wave diagram [9] showing the travel of the rarefaction wave from the closed end of a uniform diameter shock tube with a rarefaction wave eliminator in place is shown in Figure 14-A; also see Figure 5.

Assuming the same shock input conditions, a wave diagram has been constructed with three baffles in the compression chamber. This is shown in Figure 14-B. Also see Figure 10-D, Case 1-E for the recorded overpressure versus time. The baffles and the rarefaction wave eliminator work together to enhance the shock wave's positive duration.

---

[9] *H. Reichenbach, "Simulierung Langdauernder Druckatösse," Wissenchaftlicher Bericht Nr. 10/64, Ernst-Mach-Institut, October 1964.*

Table 3. PARAMETERS FOR RAREFACTION CATCH-UP

Y	P_s, kPa	A	B	L_R/L_D
1.10	10.14	0.1428	382.4	54.6
1.15	15.20	0.2141	183.0	39.2
1.20	20.27	0.2854	110.5	31.6
1.25	25.34	0.3567	75.77	27.0
1.30	30.41	0.4278	56.22	24.1
1.35	35.47	0.4989	44.03	22.0
1.40	40.54	0.5698	35.87	20.4
1.45	45.61	0.6407	30.09	19.3
1.50	50.68	0.7116	25.83	18.4
1.55	55.74	0.7823	22.59	17.7
1.60	60.81	0.8530	20.05	17.1
1.55	65.88	0.9236	18.02	16.6
1.70	70.95	0.9942	16.36	16.3
1.75	76.01	1.065	14.99	15.0
1.80	81.08	1.135	13.84	15.7
1.90	91.22	1.276	12.02	15.3
2.00	101.35	1.466	10.65	15.1
2.10	111.49	1.557	9.596	14.9
2.20	121.62	1.698	8.756	14.9
2.30	131.76	1.834	8.074	14.8
2.40	141.89	1.979	7.511	14.9
2.50	152.02	2.120	7.039	14.9
2.60	162.16	2.260	6.638	15.0
2.70	172.30	2.401	6.293	15.1
2.80	182.43	2.543	5.994	15.2
2.90	192.56	2.684	5.733	15.4
3.00	202.70	2.826	5.502	15.5

Note: Ambient pressure is taken as 101.35 kPa.

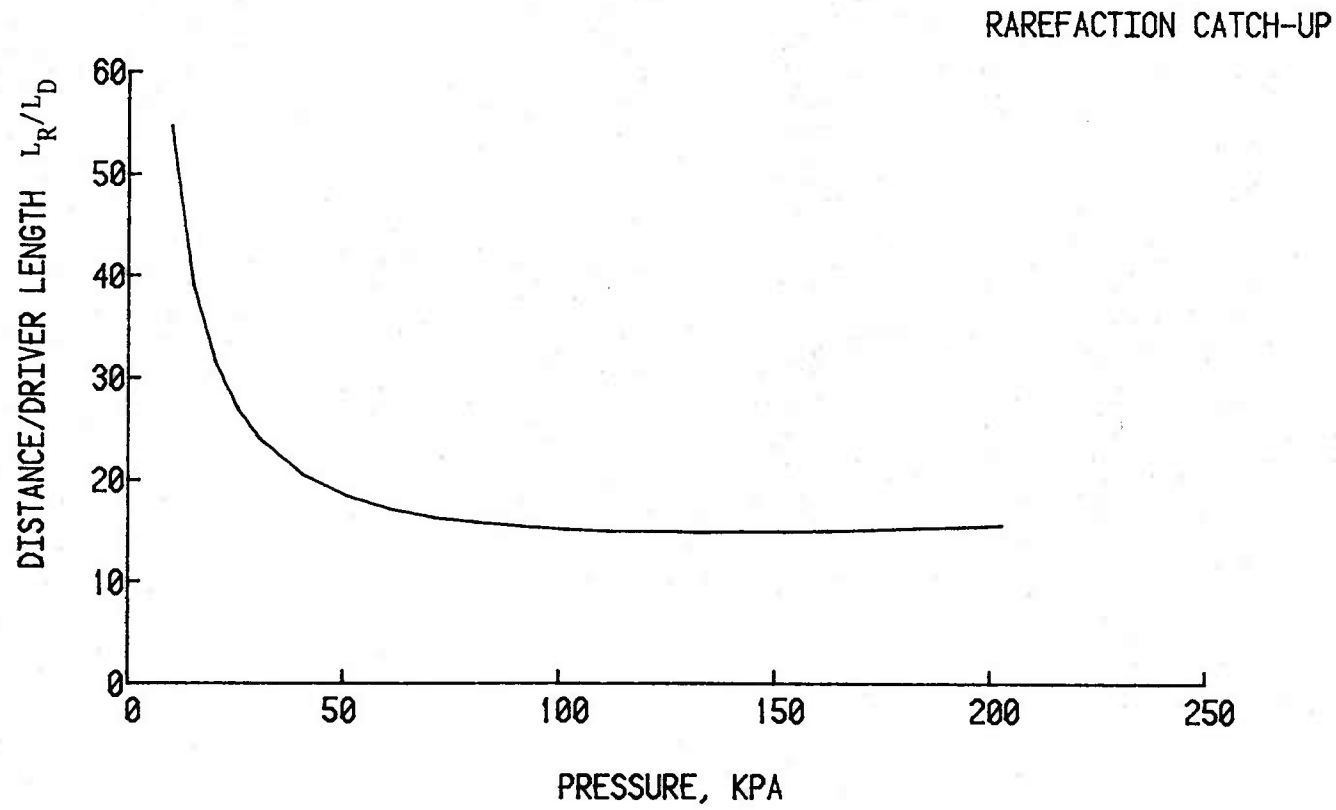

Figure 13. Rarefaction Catch-up as a Function of Shock Overpressure

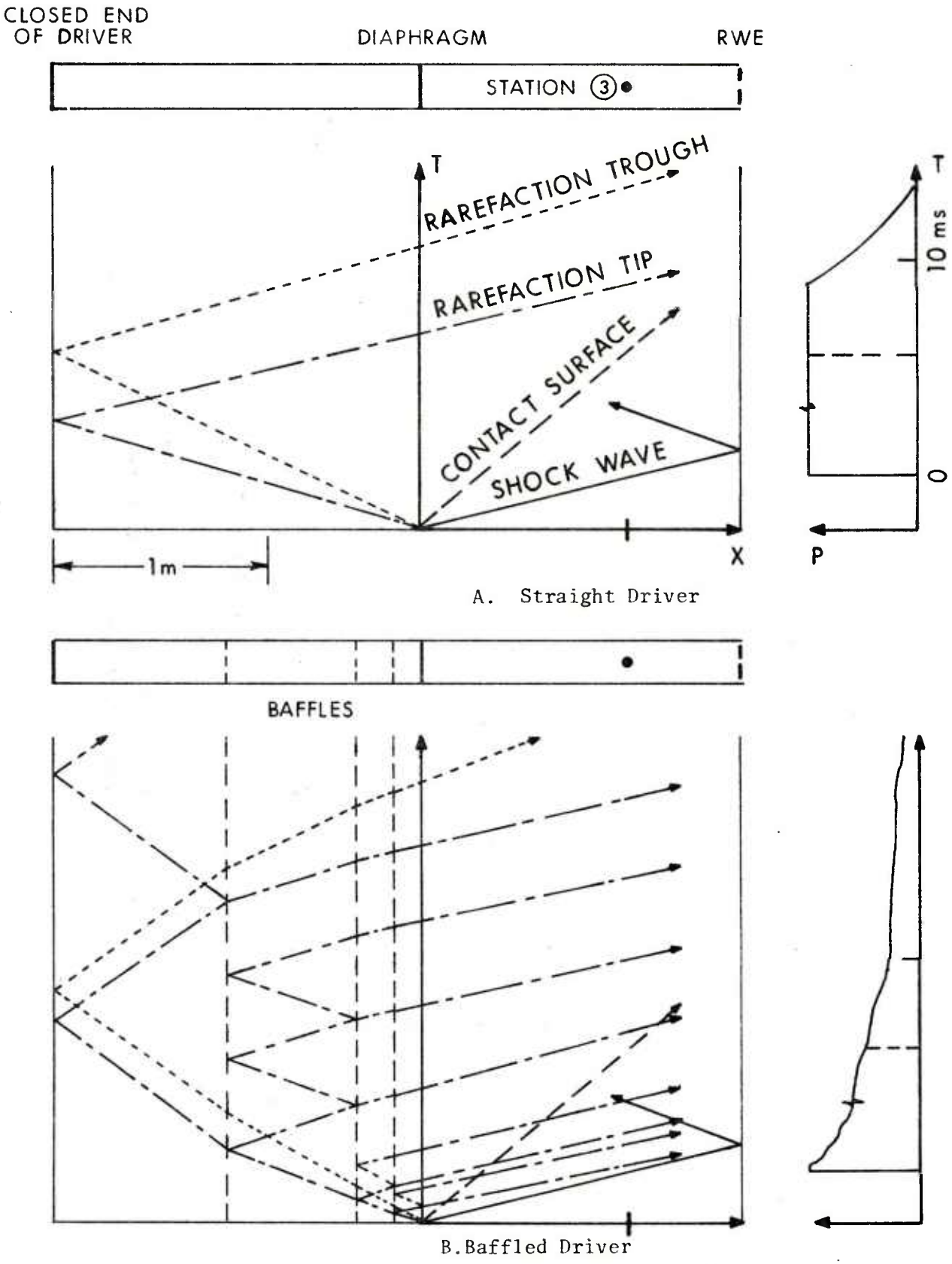

Figure 14. Wave Diagrams for Shock Overpressure of 60 kPa

B. Application of 1/48th Scale Model Results to Full-Size BRL 2.44 m Shock Tube with RWE

The experimental results for the RWE vented area ratios and driver configurations for the 1/48th scale model were scaled up (48 times) to the BRL 2.44 m shock tube. Assuming a vented RWE for the full size shock tube with an opening of 2.043 m^2, the standoff distances, W, may be calculated from Equations 7 through 11.

$$R \equiv \frac{A_V}{A_T} , \tag{7}$$

where A_V is the effective vented area, A_T is the total area of shock tube (4.699 m^2), and R is defined to be the vented area ratio. See Table 4 and Figure 15 for values of the vented area ratio.

$$A_V = A_{SV} + A_{Hole} , \tag{8}$$

where the vented area is the sum of the side vent area, A_{SV}, and the hole area, A_{Hole}.

$$A_{SV} = (\pi DW - A_{Bolts}), \tag{9}$$

where the side vented area for a circular test section is the total circular spacing, πDW, less the obstructed bolt area, $A_{Bolts} = 21(0.0476)W$. Combining Equations 7-9 and rearranging, the result in Equation 10:

$$W = \frac{A_T R - A_{Hole} + A_{Bolts}}{\pi D} \tag{10}$$

Substituting in the values $A_T = 4.699\ m^2$, $A_{Hole} = 2.043\ m^2$, $A_{Bolts} = 21\ (0.0476)\ W,\ m^2$ (for 21 bolts), and D = 2.44 m:

$$W = 0.075R - -.306,\ m. \tag{11}$$

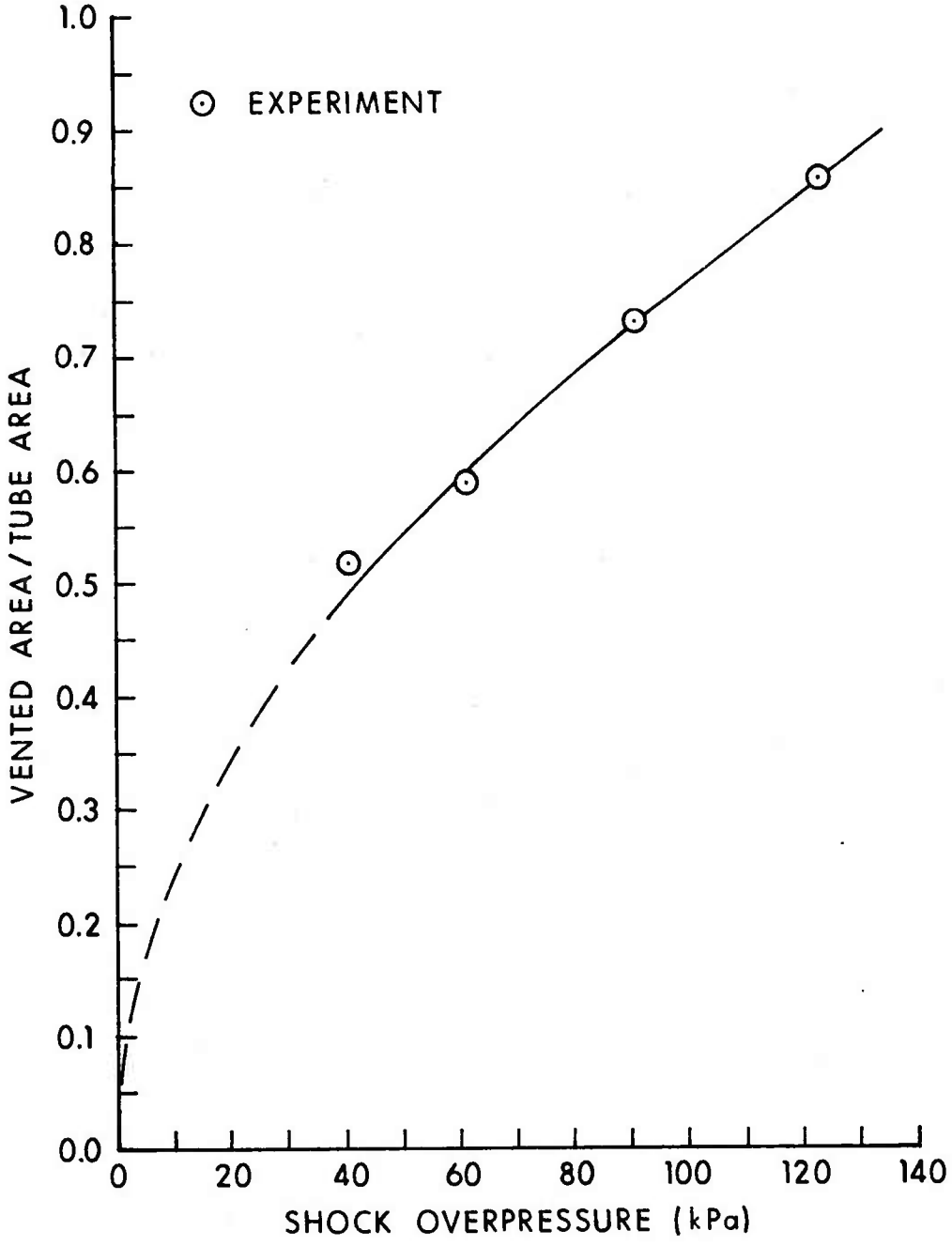

Figure 15. Vented Area Ratio of RWE as a Function of Shock Overpressure

Table 4. VENTED AREA RATIO OF RWE VERSUS INPUT SHOCK OVERPRESSURE

Input Overpressure, kPa	Vented Area / Total Area
42	0.517
61	0.579
93	0.729
124	0.853

Table 5 and Figure 16 summarize the calculations for RWE standoff distance, W, for the BRL 2.44 shock tube when used to produce decaying shock waves.

Scaling up the 1/48th scale model results as indicated gave the predicted pressure-time waveforms shown in Figure 17 at Stations 87 and 88 for four pressure levels. The upper traces show the predicted stagnation overpressure to be expected, the middle traces show the predicted side-on overpressure, and the bottom traces are the results of subtracting side-on from stagnation ($P_{stag} - P_s$), the compressible dynamic pressure.

The next section gives equivalent yields of TNT needed to produce free-field blast waves corresponding to those predicted for the BRL 2.44 m shock tube if modified as suggested to produce decaying waves.

C. Equivalent Yield for Similar Free-Field Blast Waves

Cube root scaling[10] allows the blast parameters from one high-explosive yield of TNT to be found for another yield. For the same atmospheric test conditions, the scaling relationships are given by Equation 12 where the scaling is from charge (1) to charge (2).

$$\frac{D_2}{D_1} = \frac{TA_2}{TA_1} = \frac{t_2}{t_1} = \frac{I_2}{I_1} = \left(\frac{W_2}{W_1}\right)^{1/3} \qquad (12)$$

where D, TA, t, I, and W are the station distance, time of arrival, positive duration, positive impulse, and charge mass of the explosive. Subscript (1) parameter values are taken from Reference 11 and are listed in Table 6 for Examples 1-4.

[10] *Samuel Gladstone and Philip J. Dolan - Editors, "The Effects of Nuclear Weapons," Dept. of Army Pamphlet No. 50-3, Hq, Dept. of Army, March 1977.*

[11] *"Structures to Resist the Effects of Accidental Explosions," TM 5-1300, Dept. of Army, June 1969.*

Table 5. STANDOFF DISTANCE VERSUS INPUT SHOCK OVERPRESSURE-VENTED PLATE RWE

Input Overpressure kPa	psi	Vented Area Ratio	Standoff Distance[a] cm	in.	Hole in RWE Plate m^2	ft^2
40	5.80	0.49	3.9	1.54	2.044	22.0
45	6.53	0.46	6.1	2.40		
50	7.25	0.54	7.5	2.95		
60	8.70	0.59	11.0	4.33		
70	10.15	0.63	13.8	5.43		
80	11.60	0.68	17.3	6.81		
90	13.05	0.72	20.2	7.95		
100	14.50	0.76	23.0	9.06		
110	15.95	0.80	25.8	10.16		
120	17.40	0.84	28.6	11.26		
130	18.85	0.88	31.4	12.36		
140	20.31	0.92	34.3	13.50		
Area of RWE has to be decreased for inputs below 40 kPa.						
5	0.73	0.17	0	0	0.794	8.55
10	1.45	0.25	0	0	1.167	12.56
20	2.90	0.34	0	0	1.587	17.08
30	4.35	0.42	0	0	1.961	21.2

[a]Standoff distance was calculated from the vented area ratio based on shock tube internal diameter. Exposed bolts/spacers were subtracted from the side-vented area. Twenty-one bolt spacers were assumed to be 4.76 cm diameter. Area of shock tube is 4.67 m^2 (50.265 ft^2).

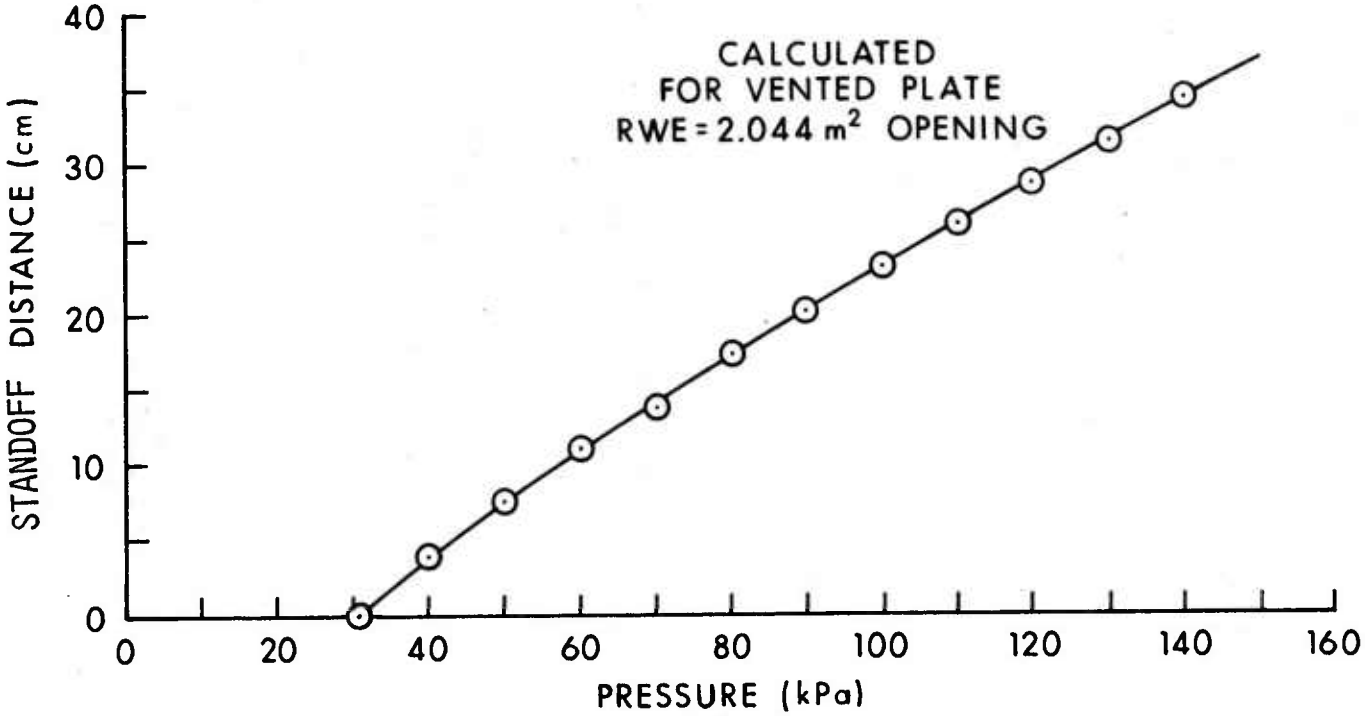

Figure 16. Predicted Standoff Distance for RWE on BRL 2.44 m Shock Tube Modified to Produce Decaying Waves

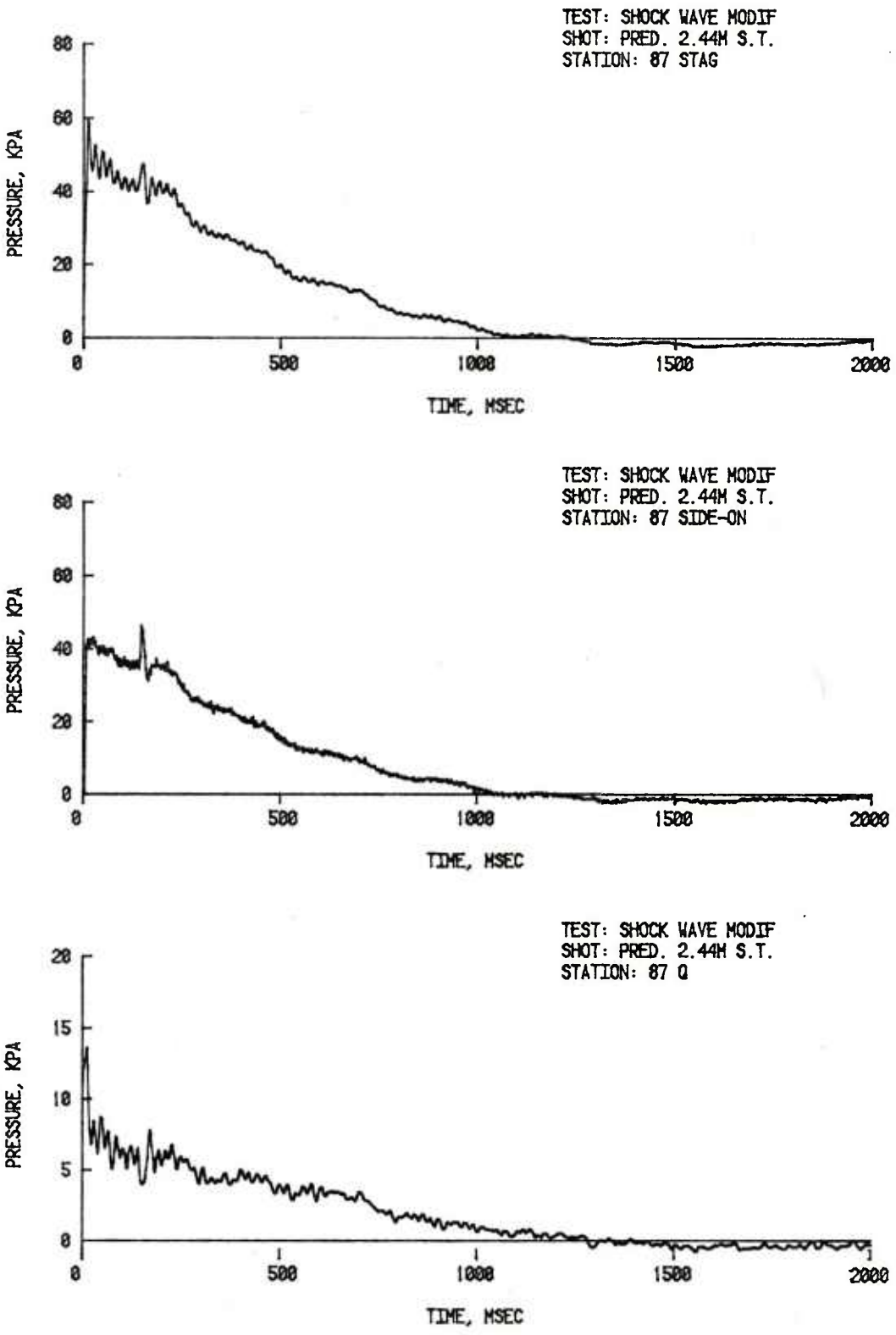

Figure 17. Predicted Results for BRL 2.44 m Shock Tube

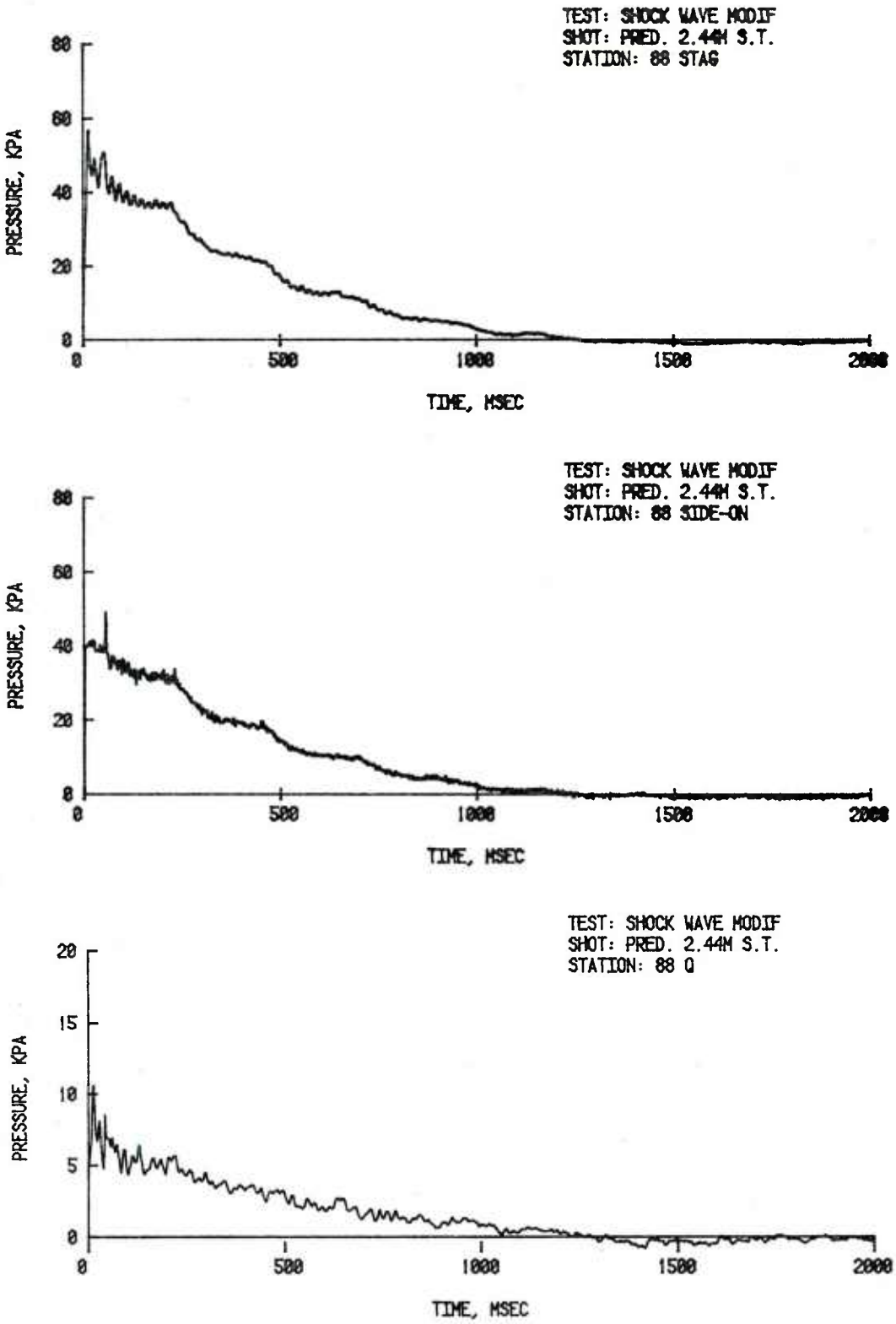

Figure 17. Predicted Results for BRL 2.44 m Shock Tube (Cont.)

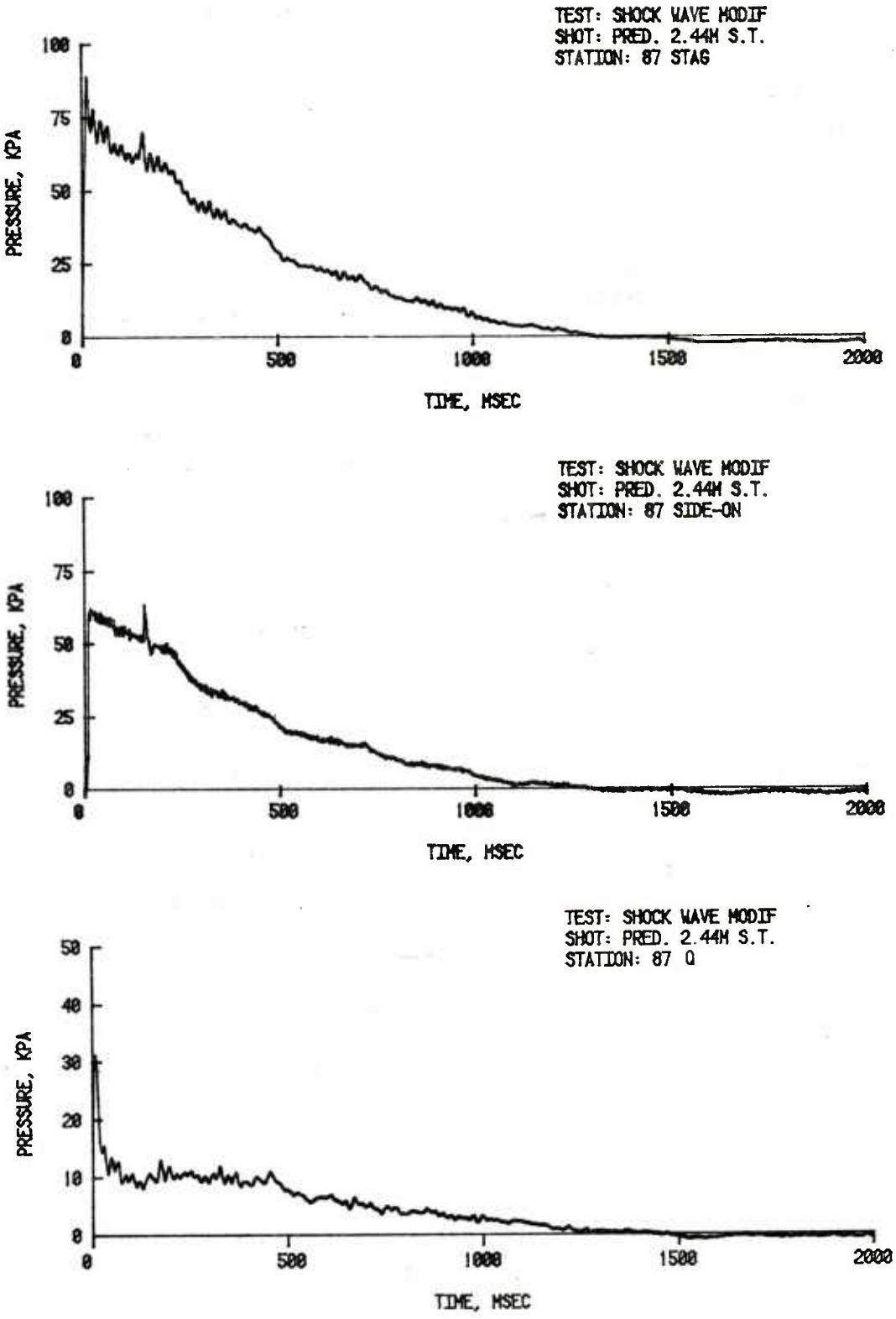

Figure 17. Predicted Results for BRL 2.44 m Shock Tube (Cont.)

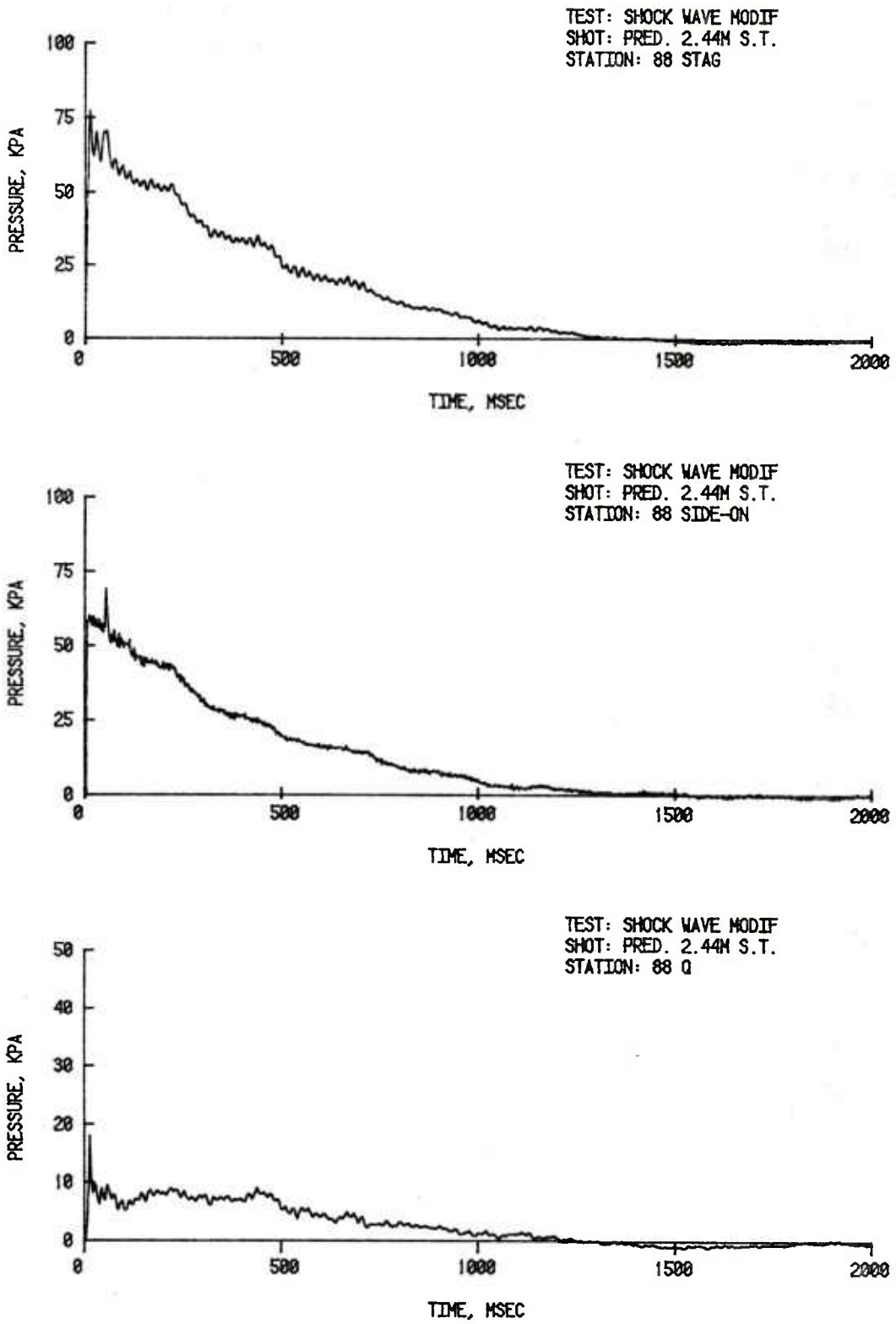

Figure 17. Predicted Results for BRL 2.44 m Shock Tube (Cont.)

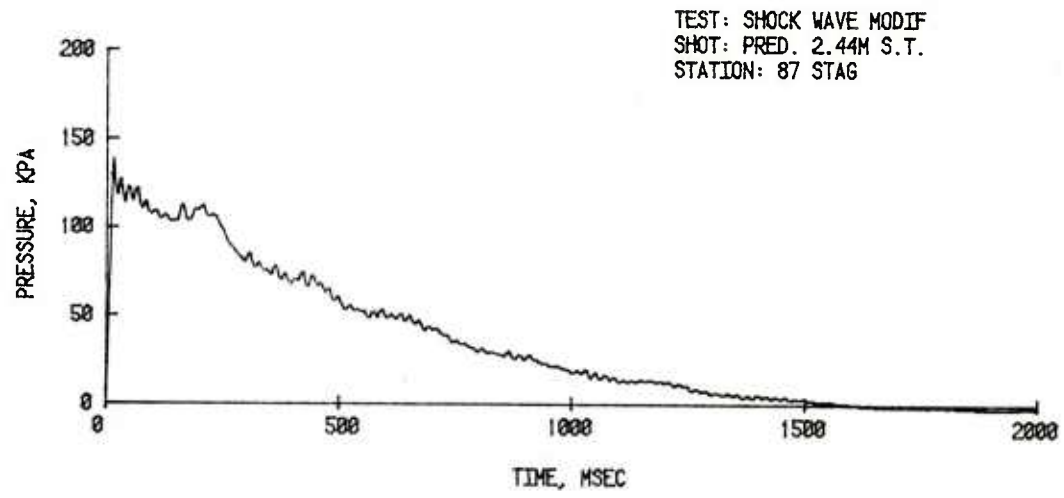

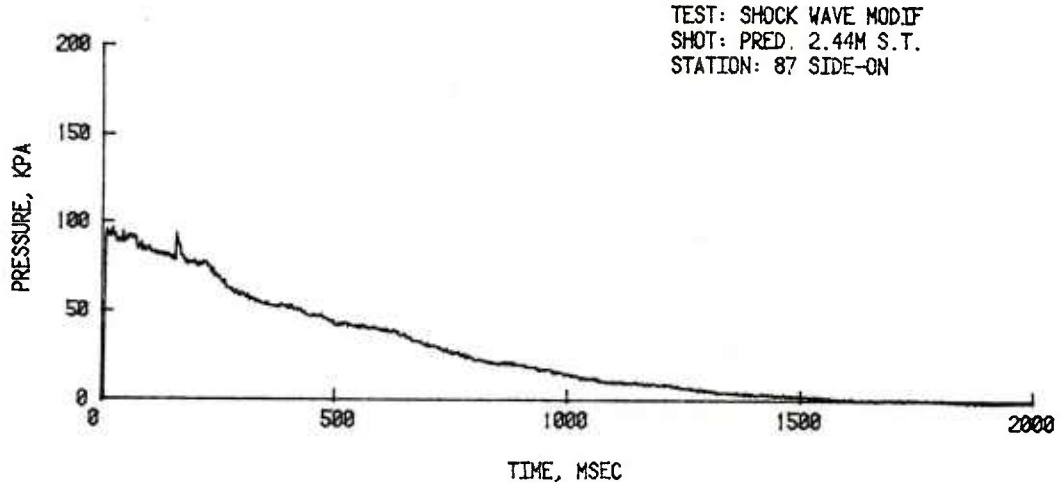

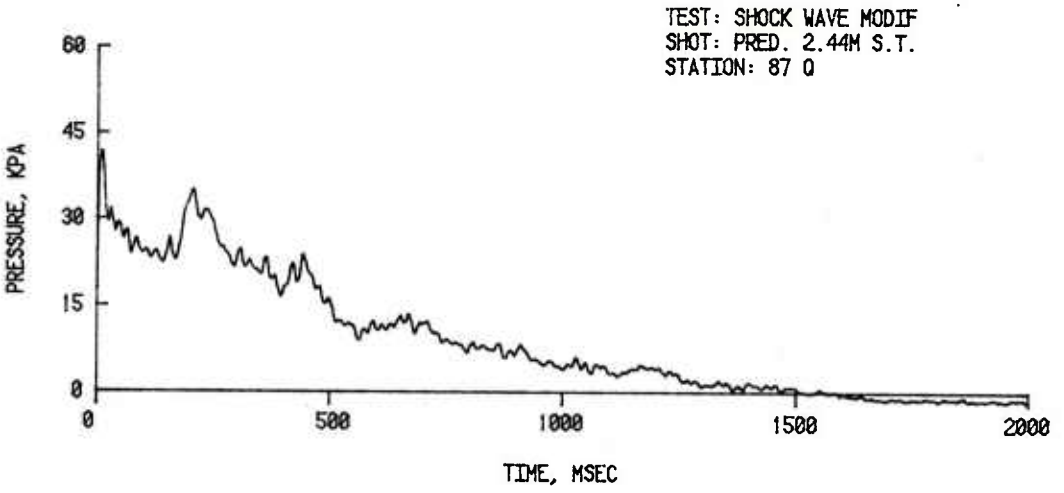

Figure 17. Predicted Results for BRL 2.44 m Shock Tube (Cont.)

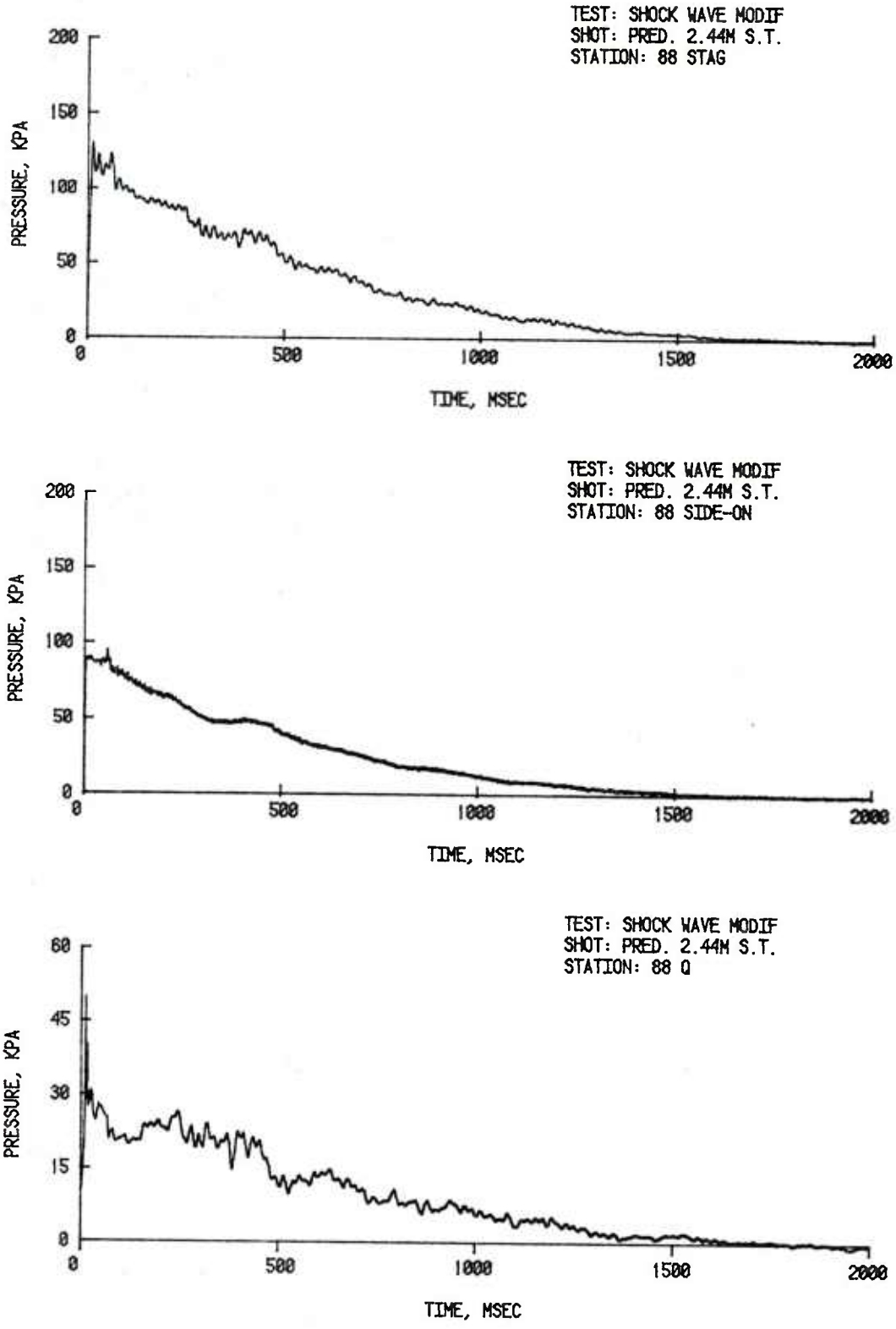

Figure 17. Predicted Results for BRL 2.44 m Shock Tube (Cont.)

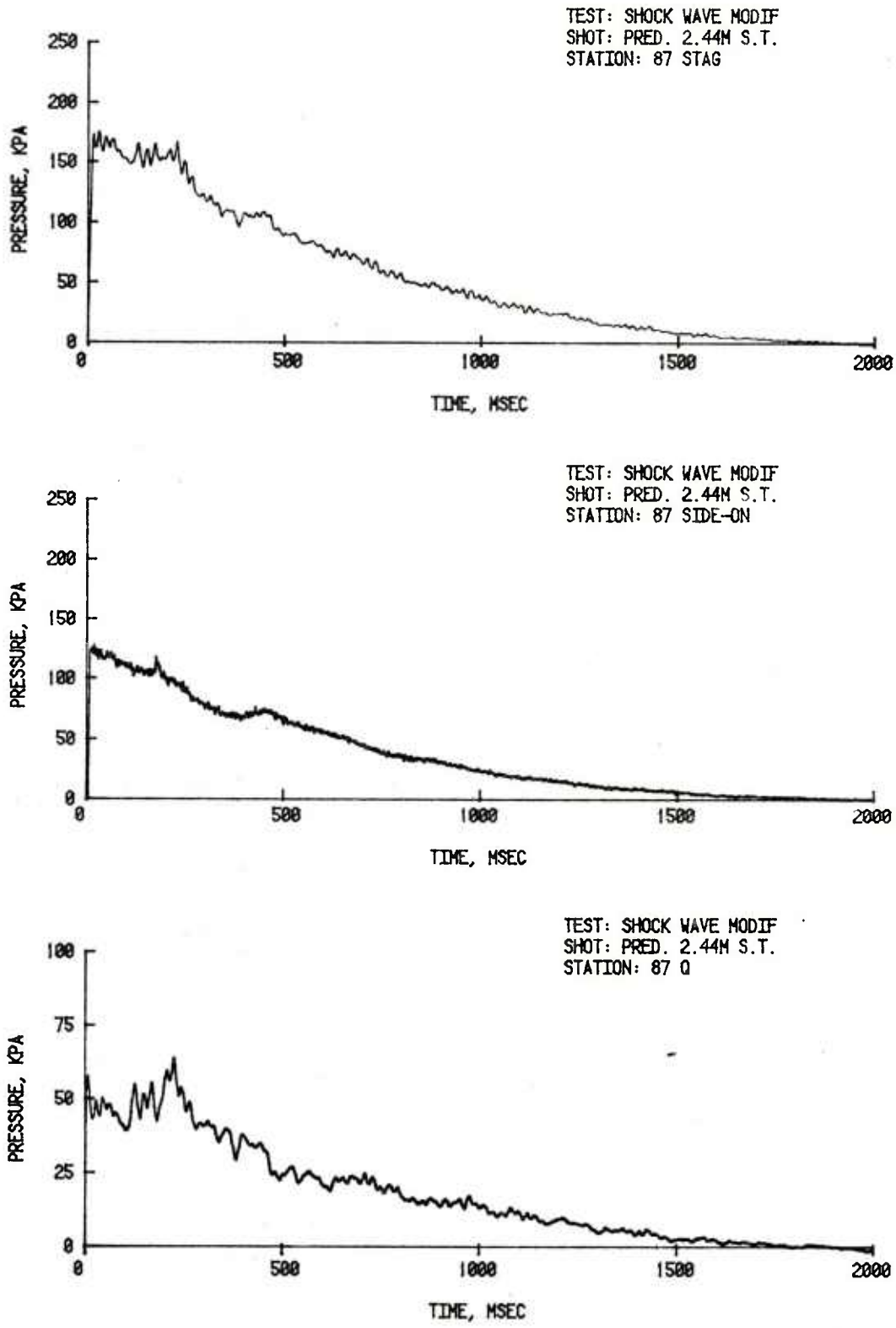

Figure 17. Predicted Results for BRL 2.44 m Shock Tube (Cont.)

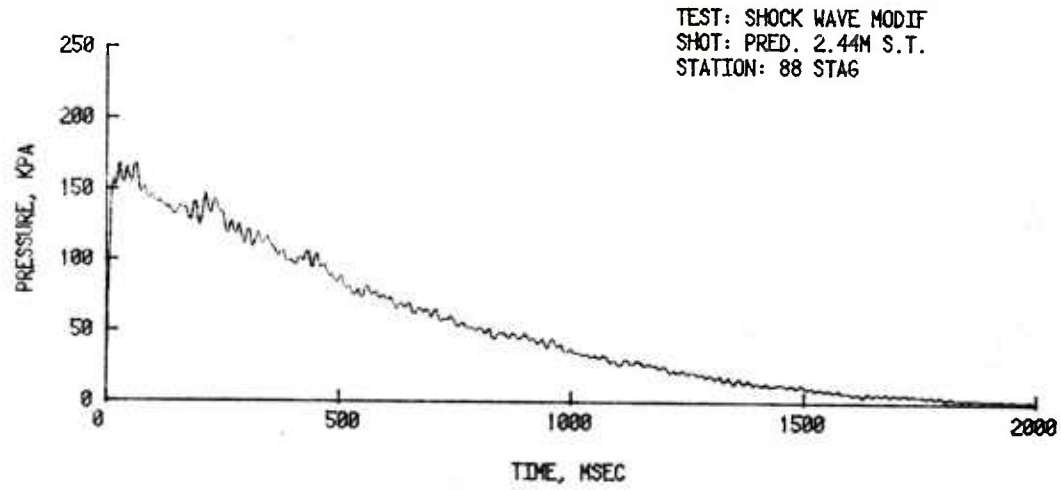

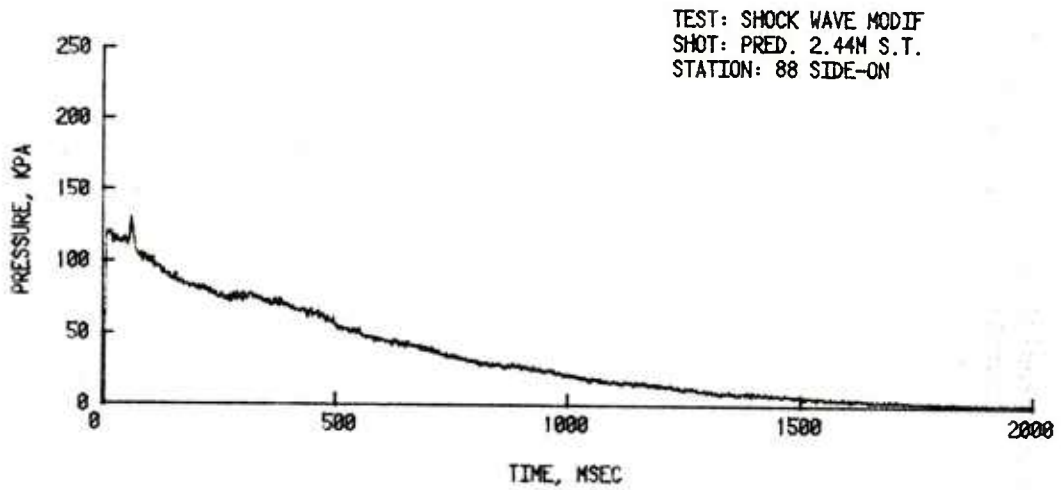

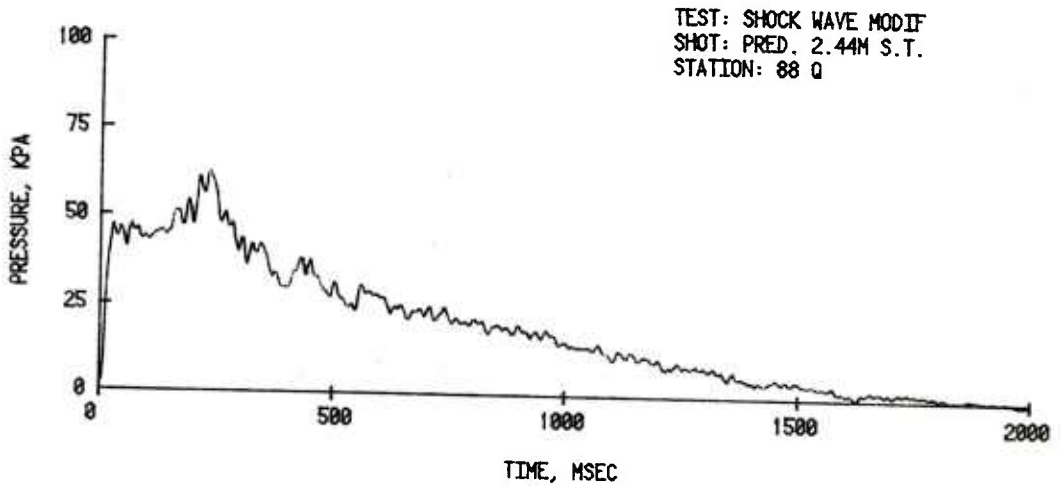

Figure 17. Predicted Results for BRL 2.44 m Shock Tube (Cont.)

Table 6. FREE-AIR BLAST PARAMETERS FOR TNT EQUIVALENT

Example	Peak Overpressure kPa	Station Distance m	Arrival Time ms	Positive Duration ms	Positive Impulse kPa-ms	Ambient Pressure kPa	Ambient Temperature ^{o}K	Charge Mass-TNT kg (Nuclear equiv.)
Scaled Charges								
1	42.5	4.20	6.98	3.14	47.5	101.35	288.0	1.0[a]
2	62.3	3.45	5.04	2.88	57.0	101.35	288.0	1.0
3	95.0	2.82	3.60	2.57	68.3	101.35	288.0	1.0
4	127.0	2.45	2.81	2.31	77.2	101.35	288.0	1.0
2.44 m Shock Tube								
1	42.5	1586	2636	1185.6[b]	17935	101.35	288.0	53.83 million (118.6 KT)[c]
2	62.3	1535	2243	1281.6	25365	101.35	288.0	88.12 million (194.3 KT)
3	95.0	1980	2528	1804.8	47963	101.35	288.0	346.3 million (763.6 KT)
4	127.0	2291	2628	2160.0	72187	101.35	288.0	817.6 million (1.80 MT)

[a]Scaling was from standard conditions of an atmosphere of 101.35 kPa at a temperature of 288^{o}K.

[b]Values for positive blast duration in the 2.44 m shock tube were obtained by multiplying by 48 the values measured in the 5.8 cm model shock tube at Station 3.

[c] About one-half of a nuclear weapon's yield goes into blast.

The equivalent charge mass to be found may be obtained by rewriting a portion of Equation 12 as Equation 13.

$$W_2 = W_1 \left(\frac{t_2}{t_1} \right)^3 \qquad (13)$$

where W_2 is the equivalent mass of TNT needed to reproduce a blast wave with the same side-on overpressure and duration, t_2. Table 6 lists these values for each example of predicted shots for the BRL 2.44 m shock tube. The values used for t_1 are listed for Examples 1-4 and correspond to average side-on pressure values obtained during the 1/48th scaled shock tube model tests (Table 1).

After equivalent values of W_2 are calculated (last column of Table 6) the remaining parameters of distance, arrived time, and positive impulse may be calculated by use of Equation 12 above. For example, for free-air, a blast wave equal in pressure to 62.3 kPa and positive duration of 1281.6 ms from the second shock tube example would be produced by an equivalent yield of 88.12 million kg of TNT. The desired pressure would occur at a distance of 1535 m from the charge center of detonation. The blast wave would arrive 2243 ms after detonation with the required positive impulse of 25365 kPa-ms.

Table 6 summarizes the calculations for the four examples from the BRL 2.44 m shock tube predictions.

D. Comparison of Experimental and Computational Results

The hydrocode predictions described in the appendix were used to compare with the experimental results as well as to check the limits of a 1-D code when applied to a 2-D problem.

1. Long Straight Driver. The comparison of the experimental results and the computer output for a long straight tube with an RWE is presented in Figure 18-A. This is a 1-D problem and the correlation is excellent. The only deviation noted is the undershoot of the hydrocode calculation going into a negative pressure where the experimental record remains above the base line.

2. Short Straight Driver. The short straight driver produced a decaying wave but the duration was much too short for application to target loading and response. The comparison of the hydrocode calculations and an experimental record are presented in Figure 18-B. This is a 1-D problem and the correlation is quite good.

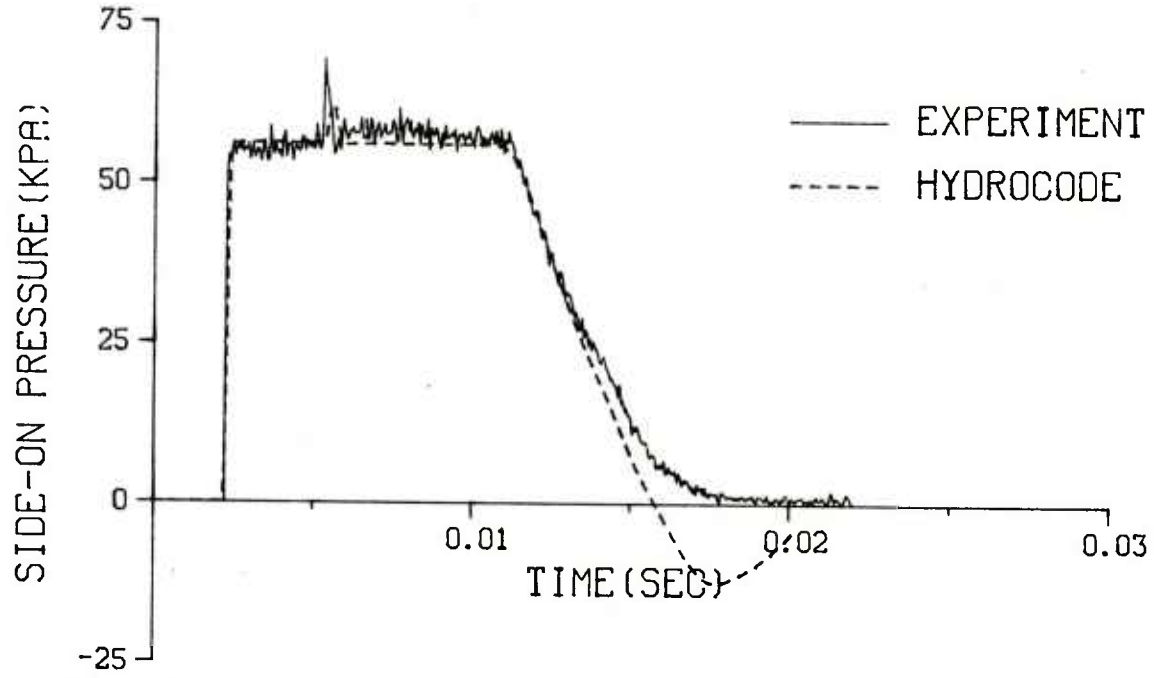

A. Long Straight Driver

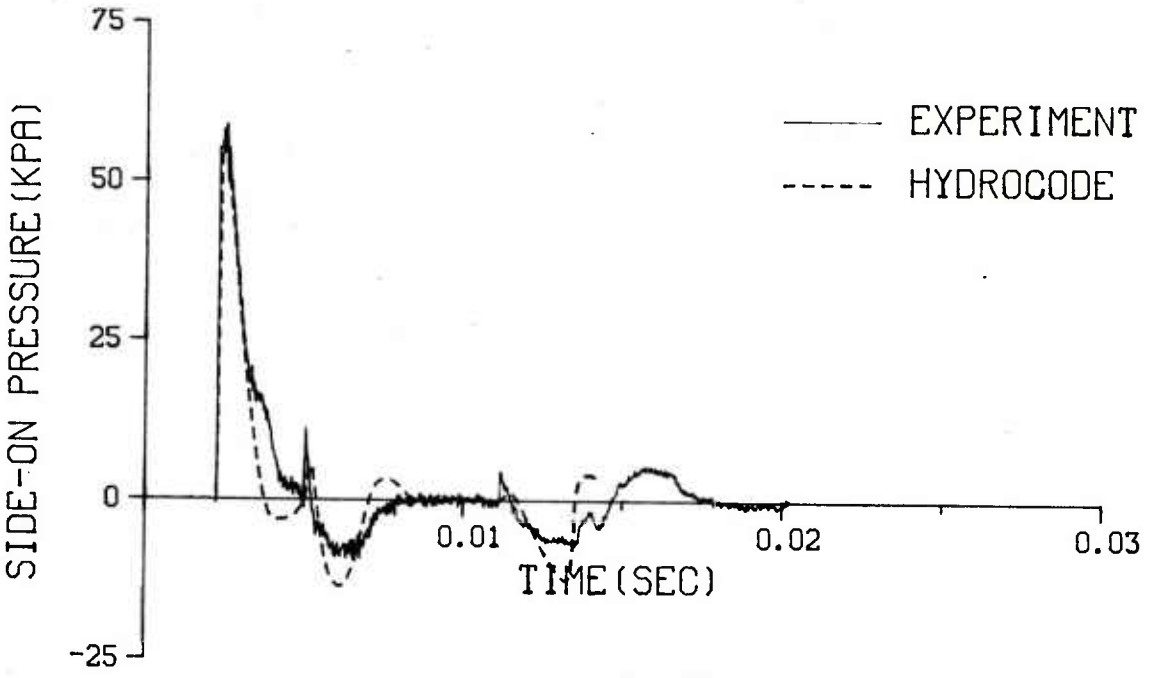

B. Short Straight Driver

Figure 18. Comparison of Experimental and Computational Results

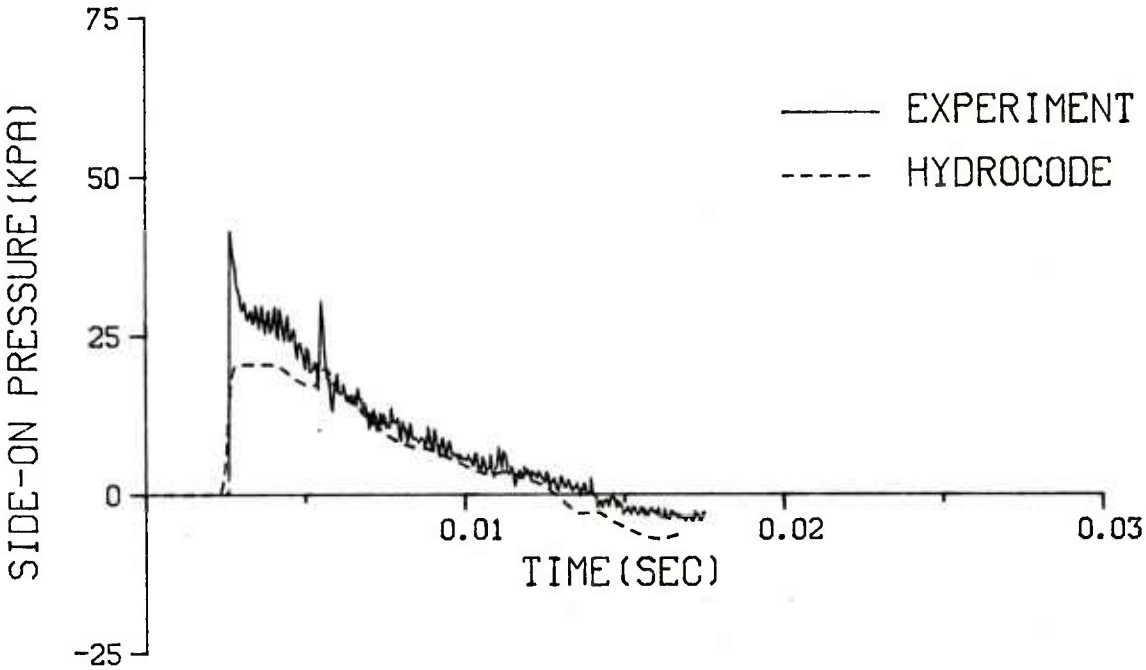

C. Multiple Pipe Driver

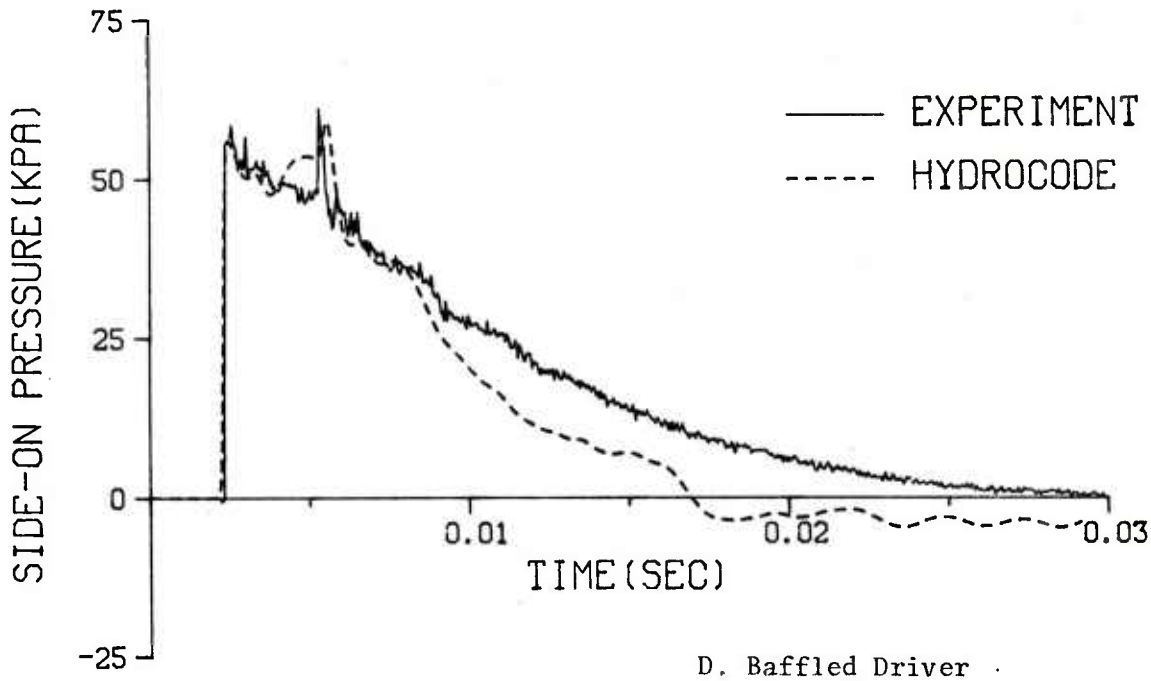

D. Baffled Driver

Figure 18. Comparison of Experimental and Computational Results (Cont)

3. Multiple Pipe Driver. The multiple pipe driver is another valid method for producing a decaying shock wave in the test section of the shock tube. Experimental and computational results are compared in Figure 18-C. The compression chamber volume is 1/8th the volume of the long straight driver and there is a significant expansion from the compression chamber into the test section. The test section area is approximately 4.5 times the multiple pipe total area. This expansion creates a pressure-time record with a sharp decay behind the shock front. The smaller compression chamber volume causes a shorter duration and less impulse than a long straight pipe driver. The expansion of the wave into the test section and the following interactions are a 2-D problem and it can be seen in Figure 18-C that the comparison of the experimental results and the hydrocode calculations does not compare well.

4. Baffles in the Driver. A third method for producing a decaying wave is the placement of baffles in the driver section. This is a 2-D problem for the computer program and it can be seen in the comparison presented in Figure 18-D that the comparison between the experimental results and the 1-D computer output does not present an accurate agreement. This difference is discussed in greater detail in the appendix.

V. SUMMARY AND CONCLUSIONS

Four types of shock tube drivers were designed to produce a decaying shock wave in the test section of a shock tube. The driver designs were built and tested on a 1/48th scale model of the BRL 2.44 m shock tube. The tests included parameter changes in input shock overpressure and standoff distances of the rarefaction wave eliminator (RWE) at the end of the test section. Pressure-time records were obtained at scaled distances along the test section corresponding to the test stations in the BRL 2.44 m shock tube. Standoff distances were calculated for the full-sized RWE to be used.

Pressure-time records were compared from the four drivers: short driver, baffled driver, small diameter driver, and multiple pipe driver. The tests showed the baffled driver produced the least attenuated and smoothest decaying wave. This driver method was chosen in order to make predictions for the 2.44 m BRL shock tube. Typical expected pressure-time records were presented for side-on overpressure, stagnation, and their difference, compressible Q (stagnation - side-on pressure).

Equivalent yields of TNT necessary to produce similar free-field blast waves were calculated for four example cases. Yields were found to vary from 53.83 million kg (118.6 KT nuclear) to 817.6 million kg (1.8 MT nuclear) over the pressure range predicted.

The NASA-Ames one-dimensional hydrocode was used to simulate the scaled shock tube experiments. The results of these comparisons are shown in the text and more completely in the appendix.

REFERENCES

1. Brian P. Bertrand, "BRL Dual Shock Tube Facility," BRL MR 2001, Ballistic Research Laboratory, Aberdeen Proving Ground, MD, August 1969 (AD 693264).

2. Brian P. Bertrand, "Proposed Improvement of BRL Dual Shock Tube Facility," BRL Technical Note No. 1733, Ballistic Research Laboratory, Aberdeen Proving Ground, MD, April 1970 (AD 871736).

3. Andrew Mark, "Computational Design of Large Scale Blast Simulators," AIAA 19th Aerospace Sciences Meeting, January 12-15, 1981, St. Louis, Missouri.

4. Edmund J. Gion, "Simulation of Low Level Explosives Blast Loadings at Full Scale by Modifications to BRL Dual Shock Tube Facility," Memorandum Report ARBRL-MR-02853, Ballistic Research Laboratory, Aberdeen Proving Ground, MD, July 1978 (AD A059854).

5. J. R. Crosnier and J. B. G. Monsac, "Large Diameter High Performance Blast Simulator," Seventh MABS, Medicine Hat, Alberta, Canada, 13-17 July 1981.

6. George A. Coulter, Gerald Bulmash, and Charles N. Kingery, "Experimental and Computational Modeling of Rarefaction Wave Eliminators Suitable for the BRL 2.44 m Shock Tube," Technical Report ARBRL-TR-02503, Ballistic Research Laboratory, Aberdeen Proving Ground, MD, June 1983 (AD A131894).

7. C. W. Lampson, "Résumé of the Theory of Plane Shock and Adiabatic Waves with Applications to the Theory of the Shock Tube," BRL Technical Note 139, Ballistic Research Laboratories, Aberdeen Proving Ground, MD, March 1950 (AD 629328).

8. I. I. Glass, "Shock Tubes Part I: Theory and Performance of Simple Shock Tubes," UTIA Review No. 12, Part I, Institute of Aerophysics, University of Toronto, Toronto, Canada, May 1958.

9. H. Reichenbach, "Simulierung Langdauernder Druckatösse," Wissenchaftlicher Bericht Nr. 10/64, Ernst-Mach-Institut, October 1964.

10. Samuel Gladstone and Philip J. Dolan - Editors, "The Effects of Nuclear Weapons," Dept. of Army Pamphlet No. 50-3, Hq, Dept. of Army, March 1977.

11. "Structures to Resist the Effects of Accidental Explosions," TM 5-1300, Dept. of Army, June 1969.

APPENDIX A

HYDROCODE PREDICTIONS

TABLE OF CONTENTS

LIST OF ILLUSTRATIONS

I. INTRODUCTION

The Ballistic Research Laboratory 2.44 meter shock tube[A-1] located on Spesutie Island is used to test the blast loading on and response of materiel and scale models. In the standard test configuration, the shock tube produces a flattop wave. The actual free-field blast loading that a military target is exposed to may be of longer duration and is an exponentially decaying wave.

II. OBJECTIVE

This study provides recommendations for serviceable modifications to the 2.44 meter shock tube facility so that it produces blast loading that better simulates an actual free-field blast event. Results from the 5.08 cm shock tube are presented in the main body of this report. This appendix discusses the computational simulation of decaying waves in the 2.44 metre shock tube. Modeling the decaying wave problem is a more pragmatic approach than attempting to modify the 2.44 meter facility directly.

III. METHOD

A. NASA-Ames One-Dimensional Hydrocode

With a mainframe computer it is possible to simulate complicated fluid flow by using a mathematical algorithm based on either the Lagrangian or Eulerian fluid mechanics model. Detailed information describing field variables may be obtained at any spacial and temporal location. Essentially, this is the computational equivalent of a fluid dynamics experiment.[A-2]

The NASA-Ames hydrodynamic code[A-3] employed in this study is a one-dimensional, adiabatic, inviscid, Eulerian computer algorithm written by Dr. Andrew Mark and modified by Mr. Klaus Opalka of the Ballistic Research Laboratory.

A-1 *Brian P. Bertrand, "BRL Dual Shock Tube Facility," BRL M-2001, August 1969 (AD 693264).*

A-2 *Patrick J. Roache, Computational Fluid Mechanics, Hermosa Publishers, Albuquerque, N.M., 1972, pp 1-13, 204-286.*

A-3 *Andrew Mark, "Computational Design of Large Scale Blast Simulators," AIAA 19th Aerospace Sciences Meeting, January 12-15, 1981, St. Louis, MO.*

The ideal gas equation of state (Equation A-1) and the Euler equations for conservation of mass, momentum, and energy per unit volume (Equation A-2) are applied to a variable area shock tube. See Figure A-1. The Euler equations are solved in differential form for density, total energy, a one-dimensional component of flow velocity, and pressure using finite difference formulations attributed to Beam and Warming.[A-4]

The initial conditions are normalized, and the independent variables (x,t) are transformed into a computational grid. The governing equations are solved implicitly at one-dimensional spacial grid points (x) as a function of time.

B. Baffles

Multiple area contractions in the compression chamber are the mechanism for producing decaying waves in the 2.44 meter shock tube. These baffles affect the shock wave profile in several ways.

The baffles serve as reflection surfaces for the rarefaction wave originating at the diaphragm when the diaphragm bursts. Reflected rarefaction waves travel downstream, overtake the shock wave, and decrease the pressure. Furthermore, a pressure drop occurs across each baffle. As the flow passes through an area constriction, the pressure decreases and the flow velocity increases. Downstream from each baffle the flow is markedly two-dimensional; strong vortices form. The kinetic energy of the vortex formation is slowly released as internal energy when the vortices move downstream and dissipate. Although the flow velocity increases in the area constriction, the net mass flow decreases. Therefore, the duration of the shock wave is increased. The baffles produce a long duration decaying wave.

Whereas the experimental baffles are thin plates having one rounded orifice to regulate the flow, the computational baffles are parabolic area contractions that occupy a significant finite length in the computational shock tube. Three to six baffles with different open area rations are placed in the driver section.

C. Rarefaction Wave Eliminator

A rarefaction wave eliminator, placed at the shock tube open end, partially reflects the shock wave alleviating the magnitude and effect of the open end rarefaction wave.[A-5] Thus, the premature decay of the shock wave, which is not a free-field phenomenon, is eliminated resulting in a longer duration shock wave. The RWE also decreases the abnormally high flow velocity that is caused by the shock wave leaving the tube.

A-4 *R. M. Beam and R. F. Warming, "An Implicit Factored Scheme for the Compressible Navier Stokes Equations," AIAA Journal, Volume 16, No. 4, April 1978, pp 393-402.*

A-5 *George A. Coulter, Gerald Bulmash, and Charles N. Kingery, "Experimental and Computational Modeling of Rarefaction Wave Eliminators Suitable for the BRL 2.44 m Shock Tube," Technical Report ARBRL-TR-02503, Ballistic Research Laboratory, Aberdeen Proving Ground, MD, June 1983 (AD A131894).*

$$P = (\gamma - 1)\ (\ e - 1/2\ \rho u^2)\ , \qquad \text{(A-1)}$$

$$\frac{\partial}{\partial t}(\rho A) + \frac{\partial}{\partial x}(\rho u A) = 0 \qquad \text{(A-2a)}$$

$$\frac{\partial}{\partial t}(\rho u A) + \frac{\partial}{\partial x}\left[(\rho u^2 + p)A\right] - p\frac{\partial A}{\partial x} = 0, \qquad \text{(A-2b)}$$

and

$$\frac{\partial}{\partial t}(eA) + \frac{\partial}{\partial x}\left[\ uA(e + p)\ \right] = 0, \qquad \text{(A-2c)}$$

where p = pressure, γ is the ratio of specific heats,

e = total energy, ρ = density, u = flow velocity,

A = tube cross-sectional area, t = time, and

x = distance.

The NASA-Ames hydrocode models an RWE that is a flat circular plate having the same diameter as the shock tube. The RWE has one circular hole of time invariant cross-sectional area that allows for outflow. The cross-sectional area is varied with each run depending on the driver pressure. Reference A-5 discusses vented area ratios.

D. Input Parameters

The area contractions and rarefaction wave eliminator must occupy physical length in the computational shock tube. Otherwise, a spacial grid point would be dual valued, which is a computational impossibility. More importantly, the computational scheme is sensitive to the number of spacial grid points within the length of an area change. A large number of grid points is needed to define a continuous area change and provide valid numerical results. Reference A-5 shows that computational results approach an asymptotic value if seven or more grid points are placed within the length occupied by an area change.

The distribution and total number of grid points are established as computer input parameters. The spacial computational grid may be equidistantly partitioned along the tube length or clustered about a specific location. Thus, a proportionally large number of grid points may be placed where a cross-sectional area change occurs.

However, in this study, where there are up to seven area changes, a grid clustering function was not feasible because clustering about one area contraction attenuates the grid at other area contractions. Therefore, a large number of grid points (602) was used in the spacial grid. Area contractions were input having a physical length of 1.5% for an increasing or decreasing segment, that is, 1.5% for the RWE and 3.0% for each parabolic area contraction. This arrangement provided nine grid points within an increasing or decreasing segment.

E. Pipes

Experimentally, another method to produce decaying waves was also tried. Placing a number of pipes of different lengths in the driver produced a decaying wave. These pipes reduced the compression chamber volume and provided for expansion of the shock wave when the flow left the pipes at the diaphragm. Also, the ends of the pipes provided a reflecting surface for upstream traveling waves. This method seems a bit contrived and awkward to implement, but is included in this report for completeness.

Pipes in the driver were simulated computationally by changing the French-type driver that the NASA-Ames one-dimensional code models. The NASA-Ames driver has a four phase steplike increase in cross-sectional area ratio, a convergent section, throat, and divergent section. By eliminating the convergent section, throat and divergent section, it was possible to simulate the cross-sectional area reductions of pipes by using the four-phase step increase.

DIMENSIONS ARE NORMALIZED

(% Tube length)

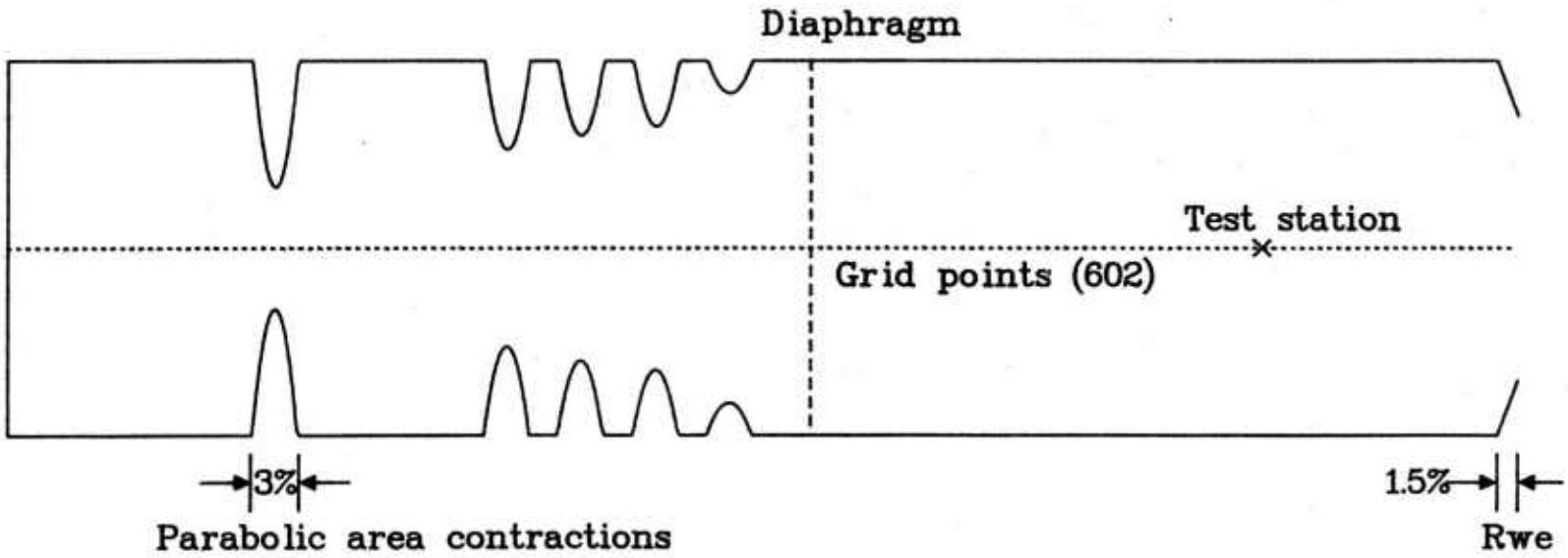

Figure A-1. Schematic of the Computational Shock Tube.

IV. RESULTS

Computational results apply to both the 5.08 cm and 2.44 m shock tubes. These dimensions are normalized by the hydrodynamic code. Since the 5.05 cm tube is a 1/48th scale model of the 2.44 m tube, the normalized dimensions apply to both shock tubes. For the 2.44 m tube arrival time and shock duration are 48 times those values for the 5.08 cm tube. Results are presented for Station 3 of the 5.08 cm shock tube which corresponds to Station 87 in the 2.44 m tube. Station 87 is the primary test station. Time is measured from when the diaphragm ruptures.

The compression chamber pressure ratio was 2.520 for the straight tube and baffle cases. It was increased to 2.939 for the pipe cases to compensate for the reduced volume.

A. 5.08 cm Shock Tube in the Standard Configuration

Figure A-2-A shows the pressure-time record at Station 3 in the 5.08 cm shock tube with the driver in the standard test configuration. Neither baffles nor a rarefaction wave eliminator (RWE) is present. Maximum side-on pressure is sustained until the open end rarefaction wave mitigates the pressure. Subsequently, a rarefaction wave from the closed end of the tube, occurring at about 11 ms, reduces the pressure to well below ambient. This waveform, with the 5.08 cm shock tube in its standard test configuration, may be used as a reference for comparing other waveforms in the 5.08 cm and 2.44 m tubes.

Figure A-2-B displays the pressure history with a rarefaction wave eliminator in use. The RWE nullifies the effects of the open end rarefaction. The duration of the flattop wave is increased by 150%.

B. Simulation of the 5.08 cm Shock Tube Experiment

The main body of this report demonstrates that smoothly decaying, long duration waves can be produced in the 5.08 cm model of the 2.44 m shock tube. Experimentally, beneficial results are achieved with six, five, or four baffles in the driver and to a lesser degree satisfactory results are obtained with three baffles. Figures A-3-A and A-3-B display the computer simulations of the experimental results for the five and four baffle cases, respectively.

Initially, the computer simulations show decay which can be correlated with two baffles close to the diaphragm. The decay is caused by rarefaction waves reflected from these baffles. Subsequently, there is an increase in pressure in the computational case where as experimentally the decay continues. Note that the RWE does extend the duration of the wave when compared to Figure A-2-A where an RWE was not used. However, when compared with Figure A-2-B, evidently there is no significant increase in the duration because of the baffles. Experimentally, there is a significant increase in duration when baffles are used when compared to the case without baffles.

Comparing A-3-A with A-3-B shows that the baffle farthest from the diaphragm in A-3-A does not appreciably affect the waveform.

C. Computationally Modeled Smoothly Decaying Waves

Evidently, in order to maintain a decaying wave, another baffle close to the diaphragm is required to act as a reflecting surface for the rarefaction wave originating from the diaphragm. Figure A-4-A shows the one-dimensional code may be used to produce a decaying wave when five baffles are used. Figure A-4-B shows four baffles will produce an acceptably decaying wave. If another baffle is removed, reducing the total number to three baffles, the results resemble the experimental simulations displayed on Figure A-5-A where a problem existed because there were too few baffles near the diaphragm.

D. Pipes

Figure A-5-A shows the effects of a step-like increase in cross-sectional area ratio on the driver. When the diaphragm bursts, compressed gas is allowed to expand, which reduces the pressure. Subsequently, the open end rarefaction wave causes the pressure to decay below ambient pressure.

Figure A-5-B shows a pipe-like simulation with an RWE. This pressure-time history shows smooth decay. There is an increase in pressure at about 9 msec because of reflections from the ends of the steps. The wave that is reflected here originated as a compression wave travelling upstream from the RWE.

Positive phase impulse and peak pressure are less than the baffle cases because the driver volume is much less in the pipe simulation. This was partially compensated for by increasing the compression chamber ratio to 2.939.

V. ANALYSIS

Figure A-6 is a direct comparison of the experimental and computational results for the five baffle cases, which vividly shows the disparities stated below.

What is occurring in the 5.08 cm shock tube experiment that the one-dimensional hydrodynamic code does not simulate? It is necessary to answer this question to determine three things: 1) why the positive phase duration in the experiment is significantly longer than in the computer simulation, 2) why the baffle arrangement provides smooth decay experimentally, and 3) why there is an increase in presssure for the computational model; this increase in pressure occurs after the effects of the two baffles closest to the diaphragm are experienced (at 5 msec).

An irrecoverable drop in pressure or head loss occurs across each baffle. As stated in the "Method" Section, within the constricted volume the flow velocity increases and the pressure decreases. The net mass flow is reduced; this elongates the duration. Downstream from each baffle vortices form. The flow is distinctly two-dimensional with respect to the shock tube axis. Kinetic energy in the vortex formations is slowly dissipated as internal energy. Downstream from each baffle the pressure does not return to its original value.

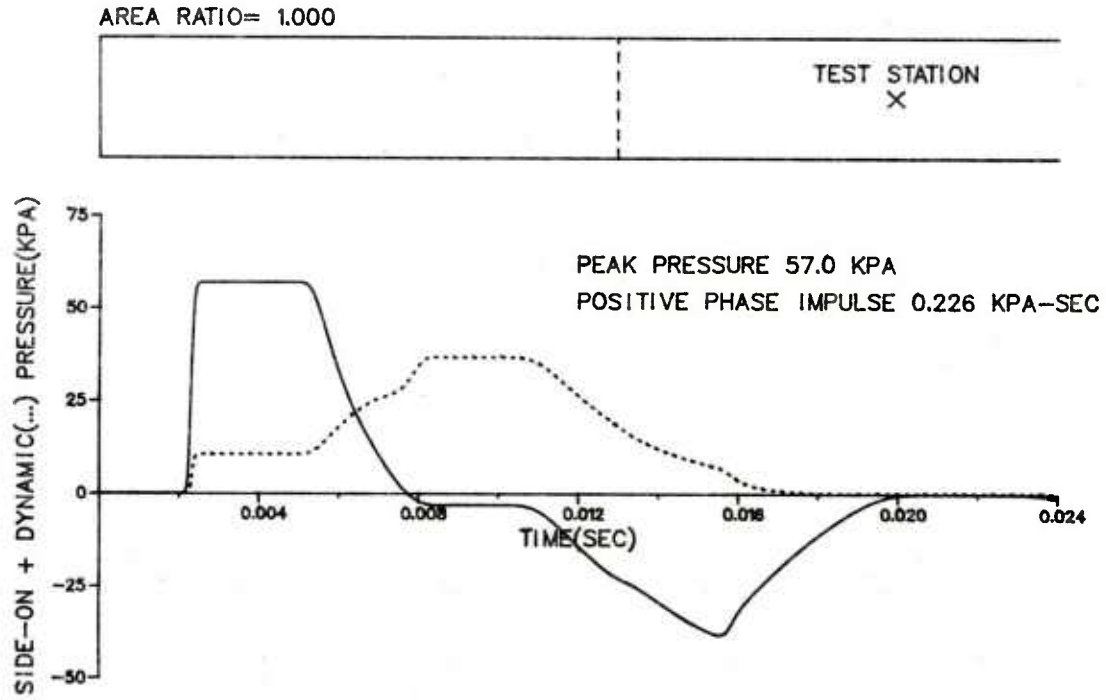

A. Without RWE.

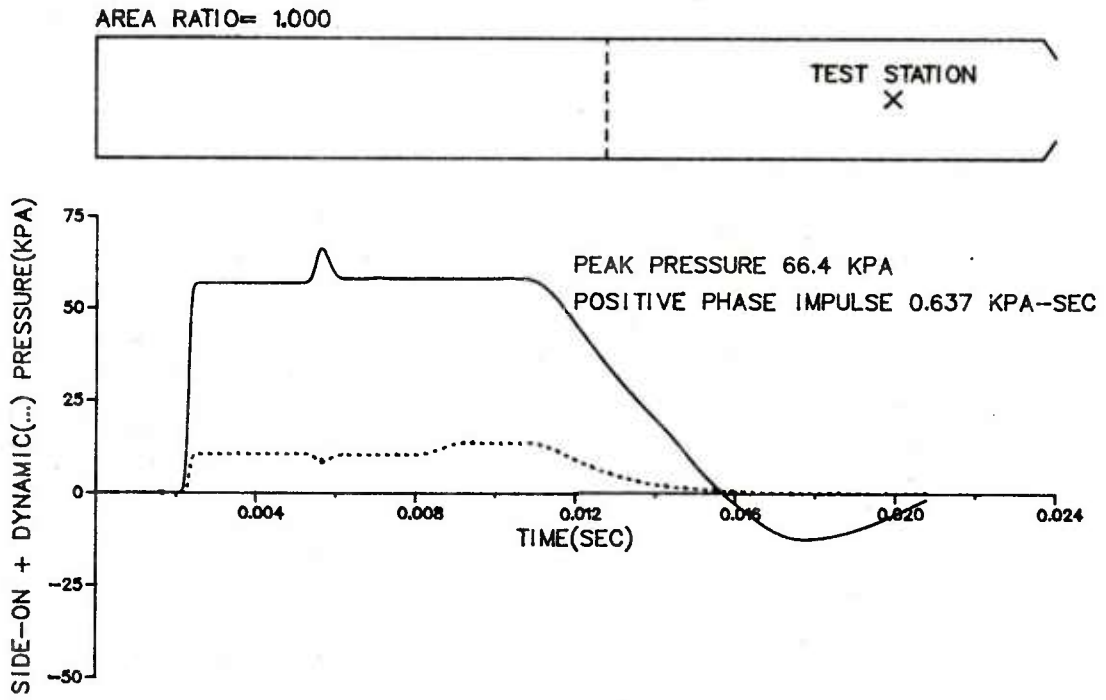

B. With RWE.

Figure A-2. Pressure-Time Records for a Straight Shock Tube without an RWE and with an RWE

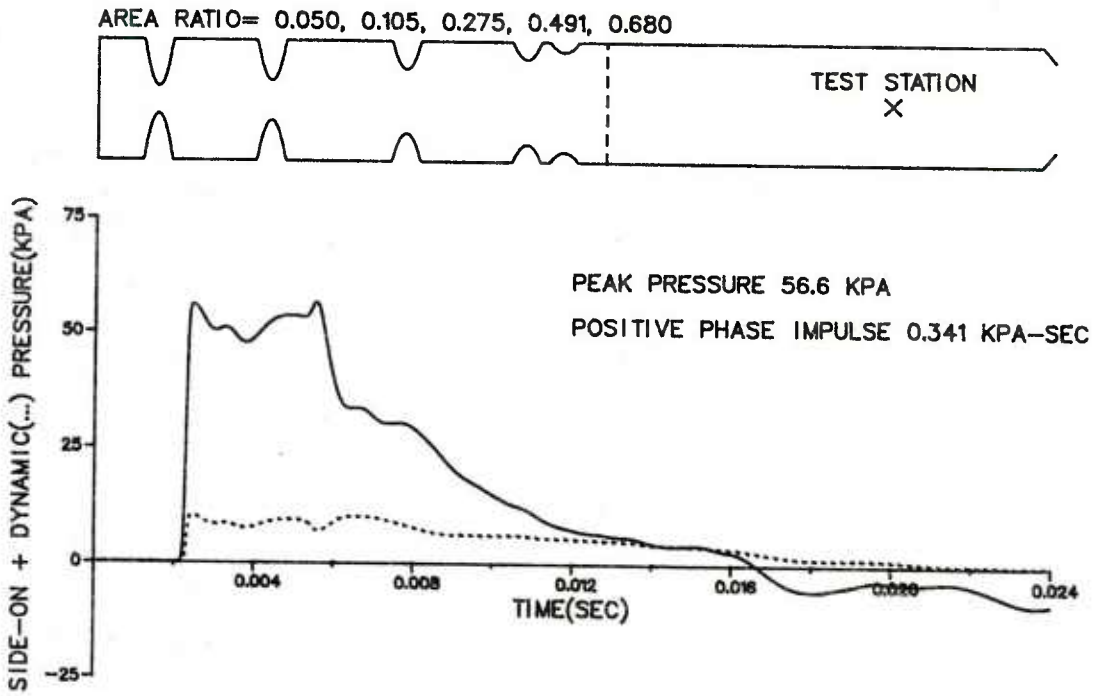

A. Five baffles.

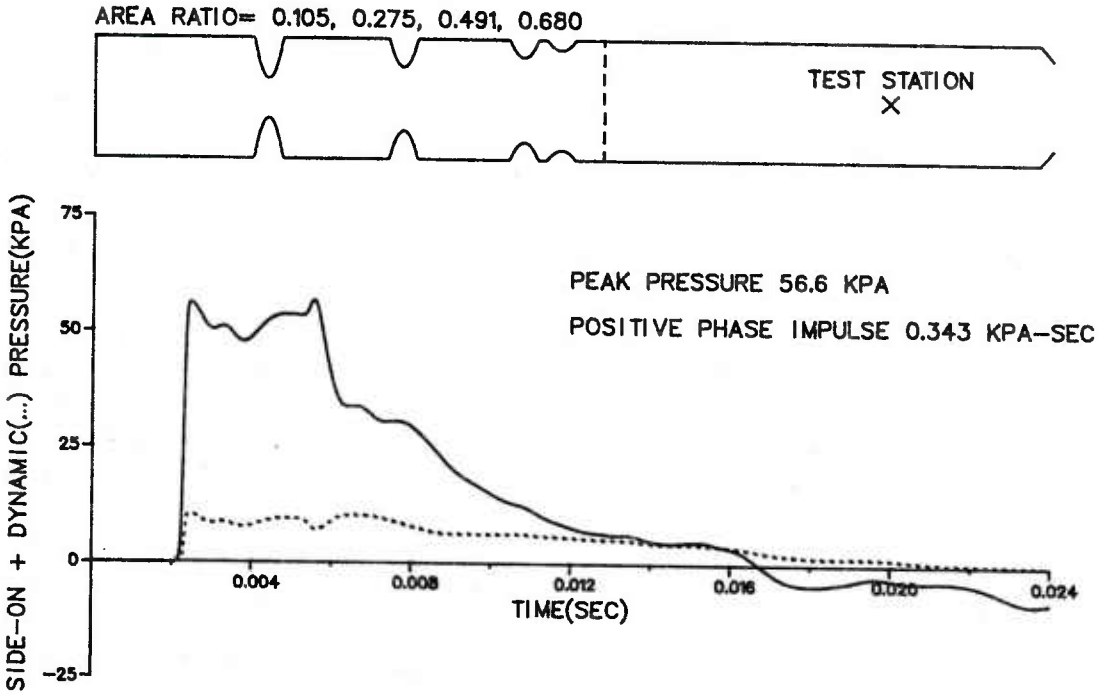

B. Four baffles.

Figure A-3. Simulation of the 5.08 cm Shock Tube Experiment with Five Baffles and Four Baffles

The one-dimensional hydrocode does not expressly simulate head losses. The one-dimensional code solves for the variables at the spatial grid points at a given time step and returns artificially high pressure values which are used to solve at the next time step. The large increase in pressure, seen on the computer simulation, following the effects of the baffles near the diaphragm is because the hydrocode does not consider head losses.

Gottlieb[A-6] has shown in a computer simulation of the BRL 2.44 m shock tube facility, for a specific baffle arrangement, head losses associated with the baffles are an important mechanism for producing long duration smooth decay.

The one-dimensional code yields a smoothly decaying wave (Figure A-4) with an extra baffle as an additional reflecting surface for rarefaction waves. This baffle compensates for the required head losses.

The one-dimensional code does not consider boundary layer frictional effects. The rarefaction wave eliminator study (Reference A-5), which compares the 5.08 cm shock tube without baffles and the one-dimensional code, showed the durations and wave profiles were quite similar although the one-dimensional code is inviscid. Of course, boundary layer effects could be intensified in the baffle region. This would serve to further reduce the effective area constrictions in the experimental tube which would increase the head losses.

VI. CONCLUSIONS

The one-dimensional hydrocode corroborates the experimental results. Both methods produced smoothly decaying waves by placing area constrictions in the standard length driver which demonstrates that the 2.44 m shock tube facility may be readily modified to produce decaying waves. This is of primary importance to the specific study.

This particular application of the one-dimensional code, with numerous severe area contractions and associated strong two-dimensional flow components, tested one-dimensional modeling limitations and provided feedback to enhance the one-dimensional code. Inclusion of head losses (currently under development)* will provide a more powerful one-dimensional modeling technique to further increase the value of an already viable hydrodynamic code.

A-6 *James Joseph Gottlieb and Tsutomu Saito, "Use of Perforated Plates in the Driver of the BRL 8-Foot Shock Tube To Produce Simulated Blast Waves with Decaying Overpressure Signatures," Final Progress Report, April 7, 1983, University of Toronto Institute for Aerospace Studies, Downsview, Canada.*

**Private Communications with Andrew Mark and Dixie Hisley, BRL, April 1983.*

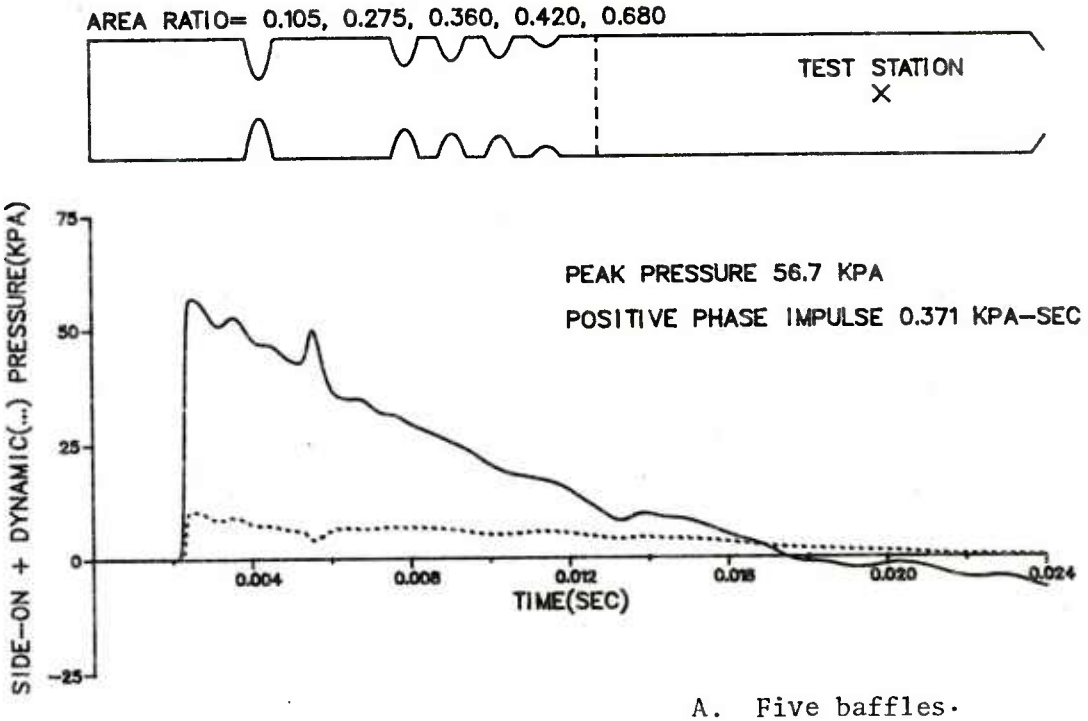

A. Five baffles.

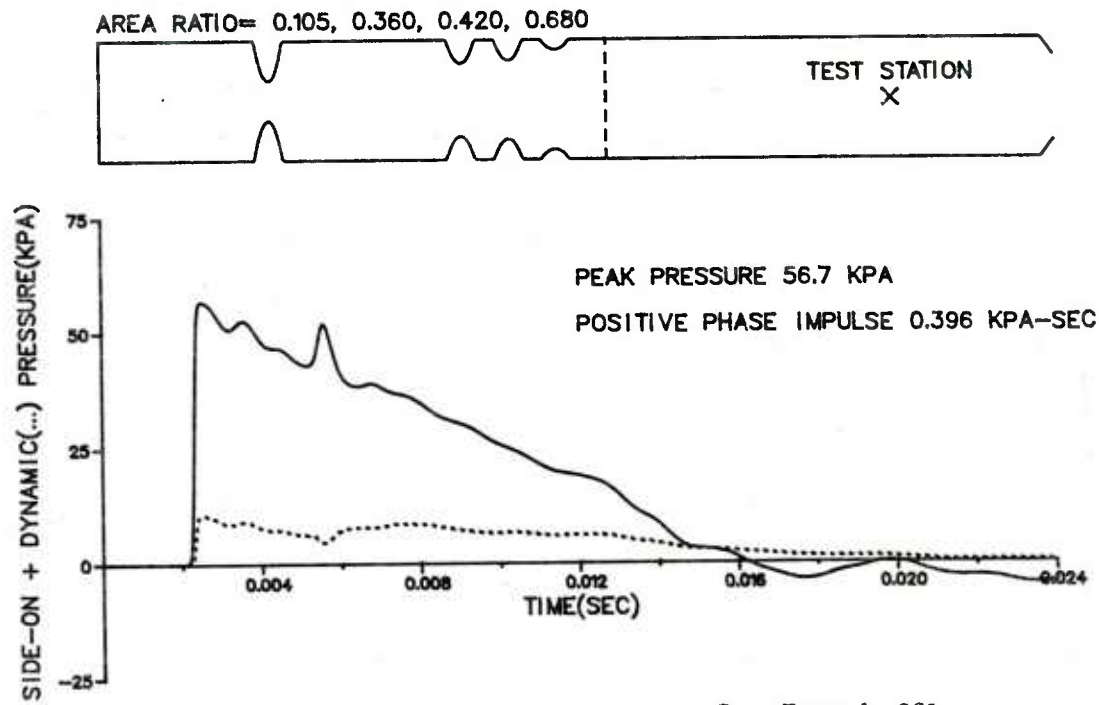

B. Four baffles.

Figure A-4. Computational Modeling of Smoothly Decaying Waves with Five Baffles and Four Baffles

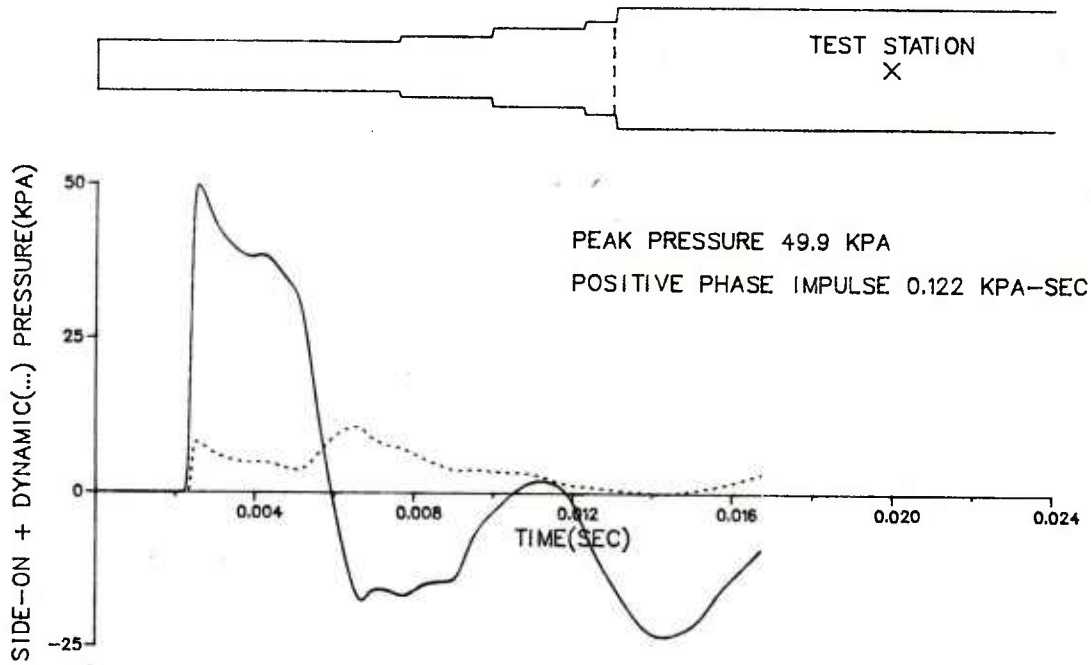

A. Without RWE.

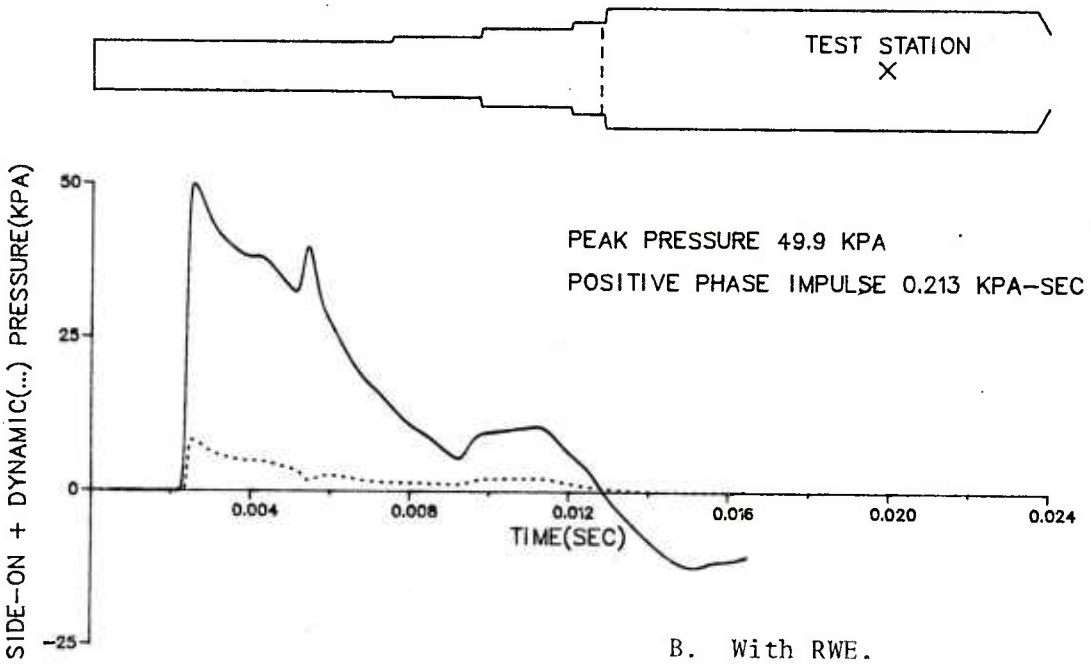

B. With RWE.

Figure A-5. Simulation of the 5.08 cm Shock Tube Experiment with Pipes for the Driver

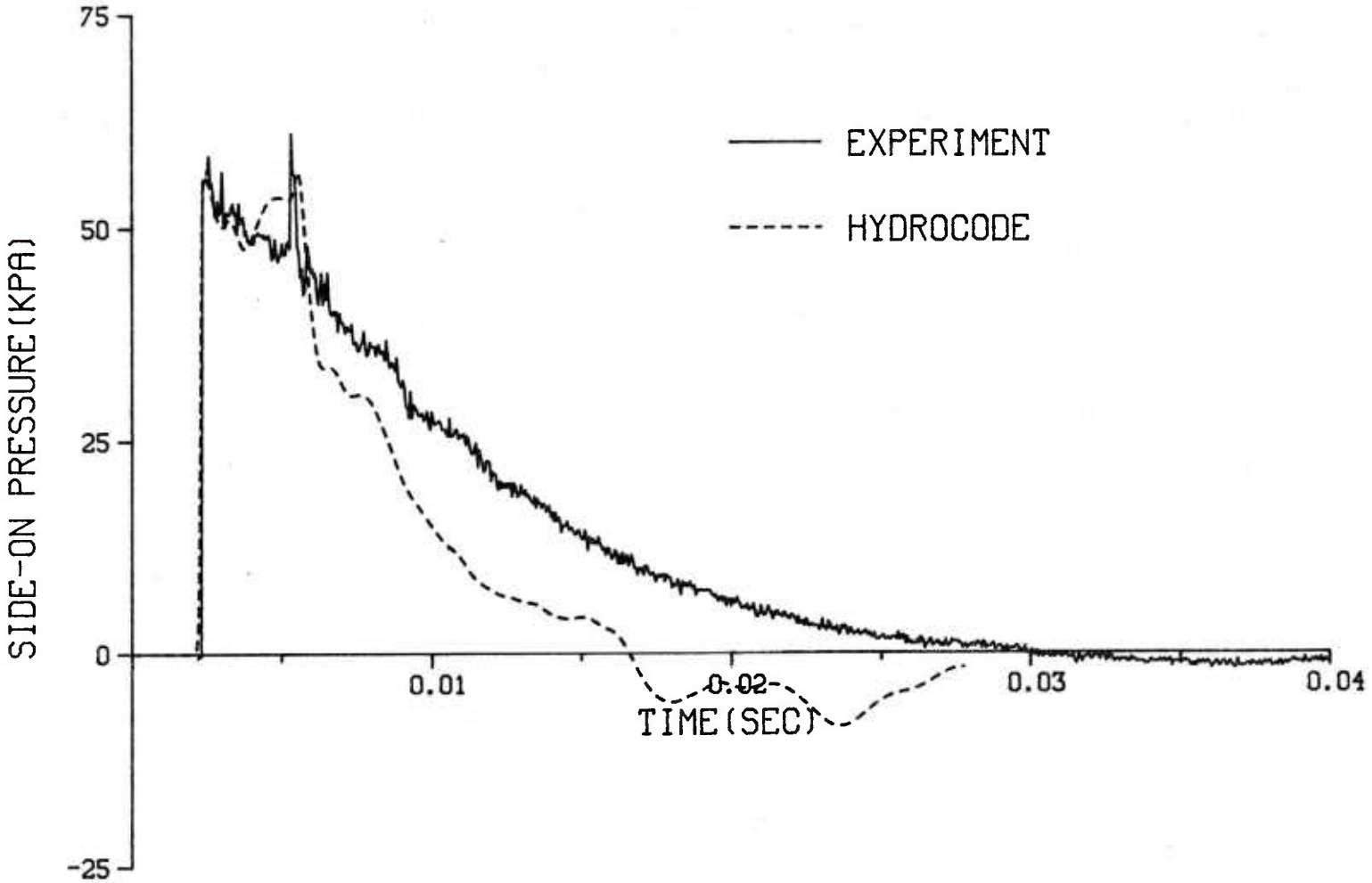

Figure A-6. Comparison Between the 5.08 cm Shock Tube Experiment and Computer Simulation with Five Baffles

LIST OF REFERENCES

A-1. Brian P. Bertrand, "BRL Dual Shock Tube Facility," BRL M-2001, August 1969 (AD 693264).

A-2. Patrick J. Roache, Computational Fluid Mechanics, Hermosa Publishers, Albuquerque, N.M., 1972, pp 1-13, 204-286.

A-3. Andrew Mark, "Computational Design of Large Scale Blast Simulators," AIAA 19th Aerospace Sciences Meeting, January 12-15, 1981, St. Louis, MO.

A-4. R. M. Beam and R. F. Warming, "An Implicit Factored Scheme for the Compressible Navier Stokes Equations," AIAA Journal, Volume 16, No. 4, April 1978, pp 393 - 402.

A-5. George A. Coulter, Gerald Bulmash, and Charles N. Kingery, "Experimental and Computational Modeling of Rarefaction Wave Eliminators Suitable for the BRL 2.44 m Shock Tube," Technical Report ARBRL-TR-02503, Ballistic Research Laboratory, Aberdeen Proving Ground, MD, June 1983 (AD A131894).

A-6. James Joseph Gottlieb and Tsutomu Saito, "Use of Perforated Plates in the Driver of the BRL 8-Foot Shock Tube to Produce Simulated Blast Waves with Decaying Overpressure Signatures," Final Progress Report, April 7, 1983, University of Toronto Institute for Aerospace Studies, Downsview, Canada.

DISTRIBUTION LIST

No. of Copies	Organization
12	Administrator Defense Technical Information Center ATTN: DTIC-DDA Cameron Station Alexandria, VA 22314
1	Office Secretary of Defense ADUSDRE (R/AT) (ET) ATTN: Mr. J. Persh, Staff Specialist, Materials and Structures Washington, DC 20301
1	Under Secretary of Defense for Research and Engineering Department of Defense Washington, DC 20301
1	Director of Defense Research and Engineering Washington, DC 20301
1	Assistant Secretary of Defense (MRA&L) ATTN: EO&SP Washington, DC 20301
1	Assistant Secretary of Defense (Atomic Energy) ATTN: Document Control Washington, DC 20301
1	Director Defense Advanced Research Projects Agency 1400 Wilson Boulevard Arlington, VA 22209
1	Director Defense Intelligence Agency ATTN: DT-1B, Dr. J. Vorona Washington, DC 20301
5	Chairman DOD Explosives Safety Board Room 856-C, Hoffman Bldg I 2461 Eisenhower Avenue Alexandria, VA 22331
1	AFWL/SUL Kirtland AFB, NM 87117
3	Director Institute for Defense Analysis ATTN: Dr. H. Menkes Dr. J. Bengston Tech Info Ofc 1801 Beauregard St. Alexandria, VA 22311
2	Chairman Joint Chiefs of Staff ATTN: J-3, Operations J-5, Plans & Policy (R&D Division) Washington, DC 20301
1	Director Defense Communications Agency ATTN: NMCSSC (Code 510) 8th St. and S. Courthouse Rd. Washington, DC 20305
4	Director Defense Nuclear Agency ATTN: SPTD, Mr. T.E. Kennedy DDST (E), Dr. E. Sevin OALG, Mr. T.P. Jeffers LEEE, Mr. J. Eddy Washington, DC 20305

DISTRIBUTION LIST

No. of Copies	Organization
1	DNA Information and Analysis Center Kaman Tempo ATTN: DASIAC 816 State Street P.O. Drawer OQ Santa Barbara, CA 93102
1	Commander Air Force Armament Laboratory ATTN: DLYV, Mr. R.L. McGuire Eglin AFB, FL 32542
1	Ogden ALC/MMWRE ATTN: (Mr. Ted E. Comins) Hill AFB, UT 84406
5	AFWL (DEO, Mr. F.H. Peterson SYT, MAJ W.A. Whitaker; SRR; WSUL, SR) Kirtland AFB, NM 87117
1	Director of Aerospace Safety HQ, USAF ATTN: JGD/AFISC (SEVV), COL J.E. McQueen Norton AFB, CA 92409
2	HQ, USAF ATTN: IDG/AFISC, (SEW)W.F. Gavitt, Jr. (SEV)Mr. K.R. Shopher Norton AFB, CA 92409
2	Director Joint Strategic Target Planning Staff ATTN: JLTW; TPTP Offutt AFB, NB 68113
1	HQ AFESC RDC Walter Buckholtz Tyndall AFB, FL 32403
1	AFCEC (DE-LTC Walkup) Tyndall AFB, FL 32403
1	AFFDL (FBE) Wright-Patterson AFB OH 45433
1	AFLC (MMWM/CPT D. Rideout) Wright-Patterson AFB, OH 45433
1	AFLC (IGYE/K. Shopker) Wright-Patterson AFB, OH 45433
1	AFML (LLN, Dr. T. Nicholas) Wright-Patterson AFB, OH 45433
1	FTD (ETD) Wright-Patterson AFB OH 45433
1	Mr. Richard W. Watson Director, Pittsburgh Mining & Safety Research Center Bureau of Mines, Dept of the Interior 4800 Forbes Avenue Pittsburgh, PA 15213
1	Headquarters Energy Research and Development Administration Department of Military Applications Washington, DC 20545
1	Director Office of Operational and Environmental Safety US Department of Energy Washington, DC 20545
1	Commander US Army Armament Materiel Readiness Command ATTN: DRSAR-LEP-L Rock Island, IL 61299
1	AFML (MAS) Wright-Patterson AFB, OH 45433

DISTRIBUTION LIST

No. of Copies	Organization
1	Albuquerque Operations Office US Department of Energy ATTN: Div of Operational Safety P.O. Box 5400 Albuquerque, NM 87115
1	Commander US Army Aviation Research and Development Command ATTN: DRDAV-E 4300 Goodfellow Blvd St. Louis, MO 63120
1	Director US Army Air Mobility Research and Development Laboratory Ames Research Center Moffett Field, CA 94035
2	Director Lewis Directorate US Army Air Mobility Research and Development Laboratory Lewis Research Center ATTN: Mail Stop 77-5 21000 Brookpark Road Cleveland, OH 44135
2	Commander US Army Communications Research and Development Command ATTN: DRDCO-PPA-SA DRSEL-ATDD Fort Monmouth, NJ 07703
1	Commander US Army Electronics Research and Development Command Technical Support Activity ATTN: DELSD-L Fort Monmouth, NJ 07703
1	Commander US Army Missile Command ATTN: DRSMI-RSS, Mr. Bob Cobb Redstone Arsenal, AL 35898
1	Commander US Army Harry Diamond Labs ATTN: DELHD-TI 2800 Powder Mill Road Adelphi, MD 20783
1	Commander US Army Missile Command ATTN: DRSMI-R Redstone Arsenal, AL 35898
1	Commander US Army Missile Command ATTN: DRSMI-YDL Redstone Arsenal, AL 35898
1	Commander US Army Mobility Equipment Research & Development Command ATTN: DRDFB-ND, Mr. R.L. Brooke Fort Belvoir, VA 22060
1	Commander US Army Natick Research and Development Laboratory ATTN: DRDNA-D, Dr. D. Seiling Natick, MA 01760
2	Commander US Army Tank Automotive Command ATTN: DRDTA-TL DRSTA-TSL Warren, MI 48090
1	Commander Dugway Proving Ground ATTN: STEDP-TO-H, Mr. Miller Dugway, UT 84022

DISTRIBUTION LIST

No. of Copies	Organization
1	Commander US Army Foreign Science and Technology Center ATTN: RSCH & Data Branch Federal Office Building 220-7th Street, NE Charlottesville, VA 22901
1	Commander US Army Materials and Mechanics Research Center ATTN: DRXMR-ATL Watertown, MA 02172
1	Director DARCOM, ITC ATTN: Dr. Chiang Red River Depot Texarkana, TX 75501
1	Commander US Army Armament Research and Development Command ATTN: DRDAR-LCM-SP Dover, NJ 07801
2	Commander US Army Armament Material Readiness Command ATTN: Joint Army-Navy-Air Force Conventional Ammunition Prof Coord GP/El Jordan Rock Island, IL 61299
3	Commander US Army Armament Research and Development Command ATTN: DRDAR-TSS DRDAR-TDC Dover, NJ 07801
1	Commander Pine Bluff Arsenal Pine Bluff, AR 71601
1	Commander US Army Rock Island Arsenal Rock Island, IL 61299
1	Director US Army ARRADCOM Benet Weapons Laboratory ATTN: DRDAR-LCB-TL Watervliet, NY 12189
2	Commandant US Army Infantry School ATTN: ATSH-CD-CSO-OR Fort Benning, GA 31905
1	Commander Cornhusker Army Ammunition Plant Grand Island, NE 68801
1	Commander Iowa Army Ammunition Plant Burlington, IA 52601
1	Commander Indiana Army Ammunition Plant Charlestown, IN 47111
1	Commander Joliet Army Ammunition Plant Joliet, IL 60436
1	Commander Kansas Army Ammunition Plant Parsons, KS 67357
1	Commander Lone Star Army Ammuntion Plant Texarkana, TX 75501
1	Commander Longhorn Army Ammuntion Plant Marshall, TX 75671
1	Commander Louisiana Army Ammunition Plant Shreveport, LA 71102

DISTRIBUTION LIST

No. of Copies	Organization
1	Commander Milan Army Ammunition Plant Milan, TN 38358
1	Commander Radford Army Ammunition Plant Radford, VA 24141
1	Commander Ravenna Army Ammuntion Plant Ravenna, OH 44266
1	Commander Field Command Defense Nuclear Agency ATTN: Tech Lib, FCWS-SC Kirtland AFB, NM 87117
1	HQDA (DAMA-CSM-CA) Washington, DC 20310
1	HQDA (DAMA-AR; NCL Div) Washington, DC 20310
1	HQDA (DAMA-NCC, COL R.D. Orton) Washington, DC 20310
1	HQDA (DAEN-RDL, Mr. Simonini) Washington, DC 20310
1	HQDA (DAEN-RDZ-A, Dr. Choromokos) Washington, DC 20310
1	Commander US Army Europe ATTN; AEAGA-BE, Mr. P. Morgan APO, NY 09801
1	HQDA (DAPE-HRS) Washington, DC 20310
1	HQDA (DAEN-MCC-D/Mr. L. Foley) Washington, DC 20310
1	HQDA (DAEN-ECE-T/Mr. R.L. Wright) Washington, DC 20310
1	Director US Army BMD Advanced Tech Ctr ATTN: M. Whitfield P.O. Box 1500 Huntsville, AL 35807
1	Commander US Army Ballistic Missile Defense Systems Command ATTN: J. Veeneman P.O. Box 1500, West Station Huntsville, AL 35807
1	Commander US Army Engineer Waterways Experiment Station ATTN: WESNP P.O. Box 631 Vicksburg, MS 39181
1	Commander US Army Materiel Development and Readiness Command ATTN: DRCSF 5001 Eisenhower Avenue Alexandria, VA 22333
1	Commander US Army Materiel Development and Readiness Command ATTN: DRCDMD-ST 5001 Eisenhower Avenue Alexandria, VA 22333
1	Director DARCOM Field Safety Activity ATTN: DRXOSOES Charlestown, IN 47111

DISTRIBUTION LIST

No. of Copies	Organization
1	Office of the Inspector General Department of the Army ATTN: DAIG-SD Washington, DC 20310
1	Commander US Army Engineer Div. Europe ATTN: EUDED, Mr. N. Howard APO, NY 09757
1	Commander US Army Research Office P.O. Box 12211 Research Triangle Park NC 27709
1	Director US Army TRADOC Systems Analysis Activity ATTN: ATTA-SL White Sands Missile Range NM 88002
1	Division Engineer US Army Engineer Division Fort Belvoir, VA 22060
1	Commander US Army Engineer Division ATTN; Mr. Char P.O. Box 1600 Huntsville, AL 35807
1	Commandant US Army Engineer School ATTN: ATSE-CD Fort Belvoir, VA 22060
1	Commander US Army Construction Engineering Research Lab P.O. Box 4005 Champaign, IL 61820
1	Commander US Army Missile Command ATTN: DRSMI-RR, Mr. L. Lively Redstone Arsenal, AL 35898
1	Chief of Research, Development, and Acquisition Department of the Army ATTN: DAMA-CSN-CA, LTC V. F. Burrell Washington, DC 20310
1	Assistant Secretary of the Navy (Rsch & Dev) Navy Development Washington, DC 20350
2	Chief of Naval Operation ATTN: OP-411, C. Ferraro, Jr. OP-41B, CAPT V.E. Strickland Washington, DC 20350
1	Commander Naval Air Systems Command ATTN: AIR-532 Washington, DC 20360
2	Commander Naval Sea Systems Command ATTN: SEA-62R SEA-62Y Washington, DC 20360
1	Commander Naval Sea Systems Command ATTN: SEA-9961 Washington, DC 20360
1	Commander Naval Facilities Engineering Command ATTN: Code 045 Washington, DC 20360
1	Commander US Army Missile Command ATTN: DRSMI-RX, Mr. W. Thomas Redstone Arsenal, AL 35898

DISTRIBUTION LIST

No. of Copies	Organization
2	Commander David W. Taylor Naval Ship Research & Development Center ATTN: Mr. A. Wilner, CODE 1747 Mr. W.W. Murray, CODE 17 Bethesda, MD 20084
3	Commander Naval Surface Weapons Center ATTN: Dr. Leon Schindel Dr. Victor Dawson Dr. P. Huang Silver Spring, MD 20910
1	Commander Naval Surface Weapons Center White Oak Laboratory ATTN: R-15, Mr. M.M. Swisdak Silver Spring, MD 20910
1	Commander Naval Surface Weapons Center Dahlgren Laboratory ATTN: E-23, Mr. J.J. Walsh Dahlgren, VA 22448
1	Commander Naval Weapons Center ATTN: Code 0632, Mr. G. Ostermann China Lake, CA 93555
1	Commander Naval Ship Research and Development Center Facility ATTN: Mr. Lowell T. Butt Underwater Explosions Research Division Portsmouth, VA 23709
1	Commanding Officer Naval Weapons Support Center Crane, IN 47522
1	Commander Naval EOD Facility ATTN: Code D, Mr. L. Dickenson Indian Head, MD 20640
1	Commander Naval Weapons Evaluation Facility ATTN: Document Control Kirtland AFB, NM 87117
1	Commander Naval Research Laboratory ATTN: Code 2027, Tech Lib Washington, DC 20375
1	Officer in Charge (Code L31) Civil Engineering Lab ATTN: Code L51, Mr. W.A. Keenan Naval Construction Battalion Center Port Hueneme, CA 93041
2	Superintendent Naval Postgraduate School ATTN: Tech Reports Sec. Code 57, Prof. R. Ball Monterey, CA 93940
1	Commander Bureau of Naval Weapons Department of the Navy Washington, DC 20360
1	HQ USAF (AFNIE-CA) Washington, DC 20331
3	HQ USAF (AFRIDQ, AFRODXM, AFRDPM) Washington, DC 20331
1	AFTAWC (OA) Eglin AFB, FL 32542

DISTRIBUTION LIST

No. of Copies	Organization
1	Air Force Systems Command/SDOA ATTN: IGFG Andrews AFB, MD 20334
1	AFRPL Edwards AFB, CA 93523
1	ADTC (DLODL, Tech Lib) Eglin, AFB, FL 32542
1	ADTC Eglin AFB, FL 32542
1	Institute of Makers of Explosives ATTN: Mr. Harry Hampton Graybar Buildings, Rm 2449 420 Lexington Avenue New York, NY 10017
1	Institute of Makers of Explosives ATTN: Mr. F.P. Smith, Jr., Executive Director 1575 Eye St., N.W. Washington, DC 20005
1	Director Lawrence Livermore Laboratory Technical Information Division P.O. Box 808 Livermore, CA 94550
1	Director Los Alamos Scientific Lab ATTN: Dr. J. Taylor P.O. Box 1663 Los Alamos, NM 87544
2	Director Sandia National Laboratory ATTN: Info Dist Div Dr. W. A. von Riesemann Albuquerque, NM 87115
1	Director National Aeronautics and Space Administration Marshall Space Flight Center Huntsville, AL 35812
2	National Aeronautics and Space Administration Aerospace Safety Research and Data Institute, Lewis Rsch Ctr ATTN: Mr. S. Weiss, Mail Stop 6-2 Mr. R. Kemp, Mail Stop 6-2 21000 Brookpark Road Cleveland, OH 44135
1	Director National Aeronautics and Space Administration Scientific and Technical Information Facility P.O. Box 8757 Baltimore/Washington International Airport, MD 21240
1	President National Academy of Science ATTN: Mr. D.G. Groves 2101 Constitution Avenue, NW Washington, DC 20418
1	Aeronautical Research Associates of Princeton, Inc. ATTN: Dr. C. Donaldson 50 Washington Road, PO Box 2229 Princeton, NJ 08540
1	Aerospace Corporation P.O. Box 92957 Los Angeles, CA 90009
1	Agbabian Associates ATTN: Dr. D. P. Reddy 250 N. Nash Street El Segundo, CA 90245

DISTRIBUTION LIST

No. of Copies	Organization
2	AVCO Corporation Structures and Mechanics Dept. ATTN: Dr. William Broding Dr. J. Gilmore 201 Lowell Street Wilmington, MA 01887
2	Battelle Memorial Institute ATTN: Dr. L.E. Hulbert Mr. J.E. Backofen, Jr. 505 King Avenue Columbus, OH 43201
1	Black & Vetach Consulting Engineers ATTN: Mr. H.L. Callahan 1500 Meadow Lake Parkway Kansas City, MO 64114
2	The Boeing Company Aerospace Group ATTN: Dr. Peter Grafton Dr. D. Strome Mail Stop 8C-68 Seattle, WA 98124
1	General American Transportation Corp. General American Research Div. ATTN: Dr. J.C. Shang 7449 N. Natchez Avenue Niles, IL 60648
1	Hercules, Inc. ATTN: Billings Brown Box 93 Magna, UT 84044
2	Kaman-AviDyne ATTN: Dr. N.P. Hobbs Mr. S. Criscione Northwest Industrial Park 83 Second Avenue Burlington, MA 01803
1	J.G. Engineering Research Associates 3831 Menlo Drive Baltimore, MD 21215
3	Kaman-Nuclear ATTN: Dr. F.H. Shelton Dr. D. Sachs Dr. R. Keffe 1500 Garden of the Gods Road Colorado Springs, CO 80907
1	Knolls Atomic Power Laboratory ATTN: Dr. R.A. Powell Schenectady, NY 12309
1	Lovelace Research Institute ATTN: Dr. E.R. Fletcher P.O. Box 5890 Albuquerque, NM 87115
2	Martin Marietta Laboratories ATTN: Dr. P.F. Jordan Mr. R. Goldman 1450 S. Rolling Road Baltimore, MD 21227
1	Mason & Hanger-Silas Mason Co., Inc. Pantex Plant ATTN: Director of Development P.O. Box 647 Amarillo, TX 79117
1	McDonnell Douglas Astronautics Western Division ATTN: Dr. Lea Cohen 5301 Bolsa Avenue Huntington Beach, CA 92647
1	Monsanto Research Corporation Mound Laboratory ATTN: Frank Neff Miamisburg, OH 45342

DISTRIBUTION LIST

No. of Copies	Organization
1	Physics International 2700 Merced Street San Leandro, CA 94577
1	R&D Associates ATTN: Mr. John Lewis P.O. Box 9695 Marina del Rey, CA 90291
1	Science Applications, Inc. 8th Floor 2361 Jefferson Davis Highway Arlington, VA 22202
1	Brown University Division of Engineering ATTN: Prof. R. Clifton Providence, RI 02912
1	Florida Atlantic University Dept. of Ocean Engineering ATTN: Prof. K.K. Stevens Boca Raton, FL 33432
1	Georgia Institute of Tech ATTN: Dr. S. Atluri 225 North Avenue, NW Atlanta, GA 30332
1	IIT Research Institute ATTN: Mrs. H. Napadensky 10 West 35 Street Chicago, IL 60616
1	Massachusetts Institute of Tech Aeroelastic & Structures Rsch Laboratory ATTN: Dr. E. A. Witmar 77 Massachusetts Avenue Cambridge, MA 02139
3	Southwest Research Institute ATTN: Dr. H.N. Abramson Dr. W.E. Baker Dr. U.S. Lindholm 8500 Culebra Road San Antonio, TX 78228
1	Ammann & Whitney ATTN: Mr. N. Dobbs Suite 1700 Two World Trade Center New York, NY 10048
1	Texas A&M University Department of Aerospace Engineering ATTN: Dr. James A. Stricklin College Station, TX 77843
1	University of Alabama ATTN: Dr. T.L. Cost P.O. Box 2908 University, AL 35486
1	University of Delaware Department of Mechanical and Aerospace Engineering ATTN: Prof J.R. Vinson Newark, DE 19711

Aberdeen Proving Ground

Dir, USAMSAA
ATTN: DRXSY-D
DRXSY-G, Mr. R. Norman
DRXSY-MP, H. Cohen
Cdr, USATECOM
ATTN: DRSTE-TO-F
Cdr, US Army Toxic and Hazardous Materials Agency
ATTN: DRXTH-TE

Dir, USACSL
ATTN: DRDAR-CLB-PA
DRDAR-CLN
DRDAR-CLJ-L

USER EVALUATION OF REPORT

Please take a few minutes to answer the questions below; tear out this sheet, fold as indicated, staple or tape closed, and place in the mail. Your comments will provide us with information for improving future reports.

1. BRL Report Number _____

2. Does this report satisfy a need? (Comment on purpose, related project, or other area of interest for which report will be used.)

_____

_____

_____

3. How, specifically, is the report being used? (Information source, design data or procedure, management procedure, source of ideas, etc.) _____

_____

_____

4. Has the information in this report led to any quantitative savings as far as man-hours/contract dollars saved, operating costs avoided, efficiencies achieved, etc.? If so, please elaborate.

_____

_____

5. General Comments (Indicate what you think should be changed to make this report and future reports of this type more responsive to your needs, more usable, improve readability, etc.) _____

_____

_____

_____

6. If you would like to be contacted by the personnel who prepared this report to raise specific questions or discuss the topic, please fill in the following information.

Name: _____

Telephone Number: _____

Organization Address: _____

_____

_____